European Journal of Taxonomy 804: 1–62
https://doi.org/10.5852/ejt.2022.804.1689
ISSN 2118-9773
www.europeanjournaloftaxonomy.eu
2022 · Guillam E. *et al.*

Monograph

urn:lsid:zoobank.org:pub:5EEDA63F-8A81-40DF-B5A4-C799498DC523

Late Devonian–early Carboniferous ostracods (Crustacea) from South China: taxonomy, diversity and implications

Elvis GUILLAM[1,*], Marie-Béatrice FOREL[2], Junjun SONG [3] & Sylvie CRASQUIN [4]

[1,2,4]Centre de Recherche en Paléontologie – Paris, MNHN – SU – CNRS; 8 rue Buffon, 75005 Paris, France.
[3]Nanjing Institute of Geology and Palaeontology and Center for Excellence in Life and Palaeoenvironment, Chinese Academy of Sciences, Nanjing, China.

[*]Corresponding author: elvis.guillam@sorbonne-universite.fr
[2]Email: marie-beatrice.forel@mnhn.fr
[3]Email:jjsong@nigpas.ac.cn
[4]Email: sylvie.crasquin@sorbonne-universite.fr

[1]urn:lsid:zoobank.org:author:66D41887-865C-4B91-861F-ADB09B801962
[2]urn:lsid:zoobank.org:author:063C1F7E-6D26-48F9-A8B1-2AFA496B5FB8
[3]urn:lsid:zoobank.org:author:5676B30E-AF63-45DE-A465-2EC8BF85ABF9
[4]urn:lsid:zoobank.org:author:6FDDD550-8522-404D-B3A2-D30BFAA86927

Abstract. The impact of the late Devonian Hangenberg Event on ostracods is quantified for the first time from newly acquired data from the Blue Snake section, Guizhou Province, South China. Ninety–eight species belonging to 31 genera are identified and figured. Four new species are described: *Clavofabella*? *lanshella* sp. nov., *Sansabella gelaohensis* sp. nov., *Cytherellina caerulea* sp. nov., *Sulcella baisuzhena* sp. nov. The ostracod associations from the Blue Snake section document a significant drop in specific diversity as well as major changes in taxonomic composition through the Hangenberg Event. We here report the reduction of the proportion of Palaeocopida and the increase in that of Podocopida between the latest Famennian and the Tournaisian. The specific extinction and renewal rates are estimated at 44% and 62%, respectively. The main factor of the post–crisis renewal of ostracod faunas in the Blue Snake section appears to be the progressive diversification of the family Bairdiidae and was probably related to palaeoenvironmental changes. The characteristics of associations point to an increase of the water depth over the studied area, from a near–shore shallow environment during the latest Famennian to a deeper and more open offshore environment during the Tournaisian.

Keywords. Ostracods, Devonian, Carboniferous, extinction, South China.

Guillam E., Forel M.-B., Song J.J. & Crasquin S. 2022. Late Denovian–early Carboniferous ostracods (Crustacea) from South China: taxononmy, diversity and implications. *European Journal of Taxonomy* 804: 1–62. https://doi.org/10.5852/ejt.2022.804.1689

Introduction

The late Devonian witnessed two particularly intense biotic events: the Kellwasser event close to the Frasnian–Famennian boundary (F–FB) and the Hangenberg Event (HE) close to the Devonian-Carboniferous boundary (D–CB). The Kellwasser event particularly affected marine ecosystems of the warm intertropical zone and caused the disappearance of 97% of shallow-water rugose corals, 60% to 70% of deeper species (Pedder 1982) and 75% of ostracods species (Lethiers & Casier 1999a). The Hangenberg Event, sometimes considered as severe as the Kellwasser event, impacted both marine and terrestrial ecosystems. It particularly impacted marine ecosystems and caused the disappearance of 85% of ammonoid genera (Becker 1993), about 30% to 50% of benthic neritic ostracod species (Kaiser *et al*. 2016 after data from Casier *et al.* 2004, 2005), about 60% (Holy Cross Mountains, estimated from data from Olempska 1997) to 66% (Thuringia, estimated from data from Blumenstengel 1993) of deeper species and about 50% of pelagic species (Walliser 1996). However, the impact of the Hangenberg Event on the Thuringian mega-assemblage is varying among the different locations in which it has been studied. For example, the specific extinction rate of these deep faunas is lesser in Puech de la Suque (Montagne Noire, France) with a value between 25% and 31.5 % (Casier *et al.* 2001) and in Avesnois (North of France) than in the Holy Cross Mountains and Thuringia (Casier *et al.* 2002). It also impacted terrestrial ecosystems such as the *Archaeopteris* forests (Kaiser *et al.* 2016) and *Retispora lepidophyta* flora (Streel *et al.* 2000).

These events were essentially controlled by anoxia, which is often indicated by the occurrence of black shales in outcrops of marine deposits. Other factors controlling the Hangenberg Event have also been debated, including the development of terrestrial plants (e.g., Algeo *et al.* 1995, 2001; Algeo & Scheckler 1998, 2010; Le Hir *et al.* 2011), volcanism (e.g., Marynowski *et al.* 2012; Kalvoda *et al.* 2015; Paschall *et al.* 2019; Pisarzowska *et al.* 2020), meteor impact (e.g., Caplan & Bustin 1999; Bond & Grasby 2017), sea–level variations (e.g., Walliser 1996; Hallam & Wignall 1999; Sandberg *et al.* 2002) with a minor regressive pulse in the middle *praesulcata* zone (Kaiser *et al.* 2011, 2016), carbon cycle perturbations (e.g., Kaiser *et al.* 2006, 2008, 2011; Marynowski *et al.* 2012; Kumpan *et al.* 2013, 2015) and glaciations (e.g., Caputo 1985; Streel *et al.* 2000; Lakin *et al.* 2016). This event has been reviewed in detail by Kaiser *et al.* (2016).

Ostracods are bivalved micro–crustaceans, which are among the most diversified arthropod taxa in marine ecosystems and are present from the intertidal zone to the deepest zones of the oceans. In benthic marine ecosystems, they are known since the early Ordovician (e.g., Salas *et al.* 2007; Siveter 2008; Williams *et al.* 2008). They subsequently conquered pelagic environments during the Silurian (e.g., Siveter *et al*. 1991; Perrier *et al.* 2011) and brackish–fresh waters during the Carboniferous (e.g., Benett 2008; Benett *et al.* 2012). Ostracods are mainly benthic and are thus strongly affected by the variations of environmental conditions such as salinity, bathymetry, oxygenation, temperature, nutrients availability and hydrodynamics (e.g., Moore 1961; Puri 1966; Whatley 1990; Boomer *et al.* 2003). Thus, the study of ostracod associations allows to determine palaeoenvironmental settings and their changes through time.

Ostracods from the Famennian and early Carboniferous (Strunian, Tournaisian and Visean) have already been documented from Australia (e.g., Jones 1968, 2011), Belgium (e.g., Lethiers 1982; Crasquin 1984a, 1986; Crasquin-Soleau 1988; Casier *et al.* 2004, 2005), Canada (e.g., Green 1963; Lethiers 1981, 1982; Dewey 1983; Crasquin 1984; Crasquin *et al.* 1986), France (e.g., Lethiers 1982 ; Crasquin 1984, 1986; Casier & Préat 2003; Casier *et al.* 2001, 2002), Germany (e.g., Kummerow 1939; Becker *et al.* 1993; Blumenstengel 1993, 1995; Blumenstengel *et al.* 1997), North–western China (e.g., Song & Gong 2015; Song *et al.* 2018), South China (e.g., Coen 1989; Olempska 1999; Song & Gong 2019), Poland (e.g., Błaszyk & Natusiewicz 1973; Olempska 1981, 1997), Russia (e.g., Jones 1901; Batalina 1924; Buschmina 1975, 1986; Kotschetkova 1980; Buschmina *et al.* 1984; Sobolev 2019, 2020; Zhuravlev &

Sobolev 2018, 2019), United Kingdom (e.g., Gooday 1983; Jones & Kirkby 1886; Williams *et al.* 2005), and USA (e.g., Morey 1935; Cooper 1941; Sohn 1969, 1975; Olempska & Chauffe 1999). Ostracods from Devonian–Carboniferous transition in South China remain poorly documented except from Lechang, Guangdong (Zhao & Zhang 1997) and Dushan, Guizhou (Song & Gong 2019).

The aim of the present contribution is to quantify and discuss the biodiversity variations and recovery of neritic ostracod faunas following the Hangenberg Event in Dushan, Guizhou, South China and to characterize the palaeoenvironmental settings at the Devonian–Carboniferous transition.

Stratigraphic and geological setting

During the late Devonian–early Carboniferous interval, the South China Block was located in the north–eastern part of the Palaeotethys, at subequatorial latitude (Fig. 1). Dushan County, Guizhou Province, was a part of the Qiangui platform on the passive margin of the South China Craton (Qie *et al.* 2016, 2021) and the palaeoenvironments were dominated by carbonate platforms separated by deeper basins (Dong 1982; Ma & Bai 2002; Hou *et al.* 2011).

The name Baihupo has been used for different sections and localities near Dushan city exposing the Zhewang, Gelaohe and Tangbagou Formations. For example, Coen (1989: 311) studied ostracods from the section at Baihupo located at 3 km northwest of Dushan. In Zhang S. *et al.* (2000), the "Baihupo section" is shown to be located in the west of Dushan (Zhang S. *et al.* 2000: fig. 1). In Qie *et al.* (2016), the locality named "Baihupo" is located at about 3 km northwest of Dushan (Qie *et al.* 2016: fig. 1; modified after Fenq *et al.* 1998). Song & Gong (2019) studied ostracods from the Baihupo section that they located at 3 km southwest of Dushan. Consequently, Baihupo became an unreliable name so we herein choose to give a new name to the studied section which corresponds to the Baihupo section sensu Song & Gong (2019).

The Blue Snake section, named in reference to a beautiful blue snake found during the fieldwork, is located about 3 km southwest of Dushan (25°50'14.14" N; 107°30'26.56" E) in Guizhou Province, along the road between Feifengjing and Bailuocun (Fig. 2). The Blue Snake section exposes a 195 m succession essentially composed of limestones and argillaceous limestones interbedded with mudstones and shales of the Zhewang, Gelaohe and Tangbagou Formations in ascending order. In the present work, we studied 67 meters corresponding to the Gelaohe and Tangbagou Formations, as shown in Fig. 3.

The upper part of the Gelaohe Formation exposes thicker beds of shales than the rest of the formation. The base of the Tangbagou Formation is composed of thick beds of massive limestones which become relatively thinner and intercalated with argillaceous beds higher up (Tournaisian). In this work, corals, crinoids, bivalves and brachiopods have been observed in the Gelaohe Formation but only the top of the Tangbagou Formation yielded some crinoids and brachiopods. The Devonian–Carboniferous faunas from the different Baihupo sections located in Dushan County have already been studied, particularly conodonts (Jiang 1994), brachiopods (Yang 1964, 1978), corals (Zhang Y.B *et al.*, 2011b), trace fossils (Wang & Wang 1996; Zhang L.J. *et al.* 2011a) and ostracods (Coen 1989; Song & Gong 2019). Here, we provide the first in–depth taxonomic treatment of these ostracod assemblages.

The Gelaohe and Tangbagou Formations exposed in the Blue Snake section have been recently dated by conodont biostratigraphy in the Qilinzhai section (Dushan, Guizhou) located at a few kilometers south of the Blue Snake section (Qie *et al.* 2015, 2016). The Gelaohe Formation was deposited during the late Famennian and is not younger than the middle *Siphonodella praesulcata* Zone (Qie *et al.* 2015). The Tangbagou Formation is dated from the upper *S. praesulcata–S. duplicata* zones and consequently deposited during the latest Famennian–Tournaisian interval (Qie *et al.* 2015, 2016). In the lowermost part of the Tangbagou Formation, Qie *et al.* (2015) recognized the *Clydagnathus gilwernensis–Clydagnathus*

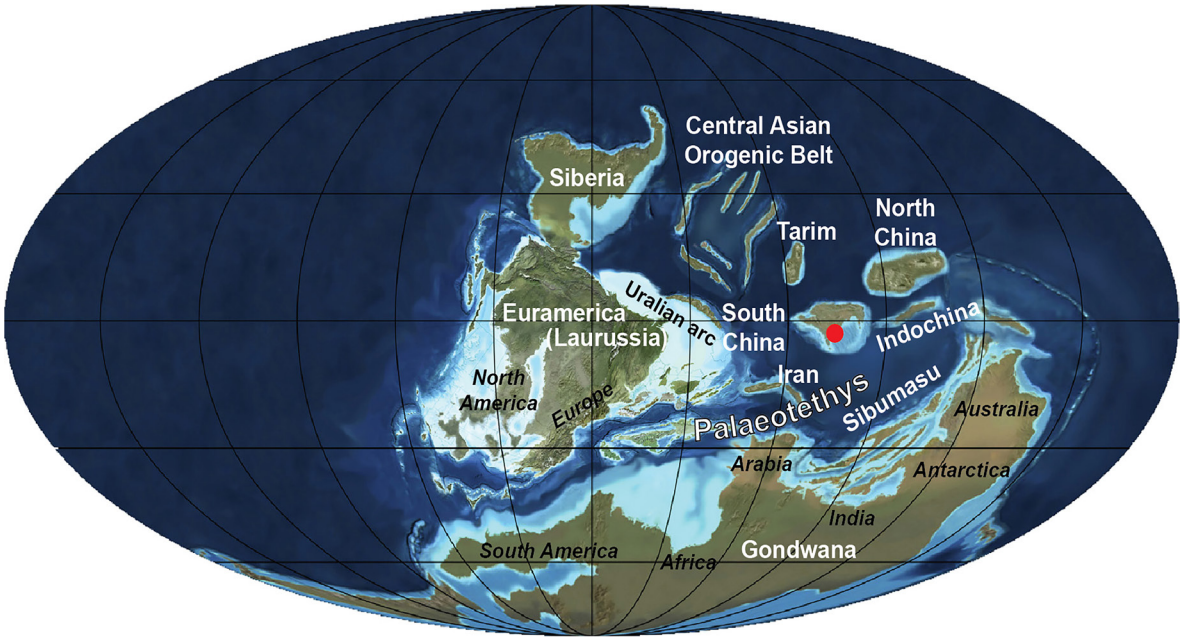

Fig. 1. Palaeogeographic map with the rough location of the Blue Snake section (red spot) during the late Devonian (modified from Carmichael *et al.* 2019).

cavusformis Assemblage Zone which is considered as equivalent to the standard upper *S. praesulcata* Zone and that has already been recognized in Central Hunan and Southern Guangdong (Ji 1987; Qin *et al.* 1988). The high $\delta^{13}C$ values documented in Qie *et al.* (2015) for this part of the Tangbagou Formation support this correlation. Consequently, the D–CB is placed in the lowermost part of the Tangbagou Formation (between units B and C, Qie *et al.* 2015: fig. 2).

Miospores (Gao 1981) and foraminifers (Wang 1987) indicate a latest Devonian age (Liao 2003) for the Zhewang and Gelaohe formations. Gao (1981) placed the D–CB within the Gelaohe Formation on the basis of miospores assemblages but others rather placed it within the lower part of the Tangbagou Formation where a maximum flooding surface occurred (Wang & Wang 1996; Feng *et al.* 2010). Song & Gong (2019) studied the faunal variations of ostracod assemblages at the Devonian–Carboniferous transition in Baihupo section (= Blue Snake section, Dushan, Guizhou) and placed the D–CB at the base of the Tangbagou Formation (Song & Gong 2019: fig. 3).

Doubts remain as to the location of the different sections named Baihupo and their datations have not been recently revised. Consequently, we choose to place the D–CB in the lowermost part of the Tangbagou Formation at the top of the succession of thick beds of massive limestones. This part of the formation may correspond to the Unit B of the Qilinzhai section in Qie *et al.* (2015) and the position of the bed of yellowish shales at the top of the Gelaohe Formation must correspond to the Hangenberg Event which occurred in the middle *S. praesulcata* Zone.

Material and methods

For the present investigation, 88 samples (labelled 19BAI xxx) spanning the Devonian–Carboniferous boundary were collected: 30 from the Gelaohe Formation and 58 from the Tangbagou Formation (Fig. 3). Ostracods were extracted by hot acetolysis technique (Lethiers & Crasquin–Soleau 1988; Crasquin–Soleau *et al.* 2005). About 2150 specimens were pictured using the Hitashi FlexSEM1000 Scanning

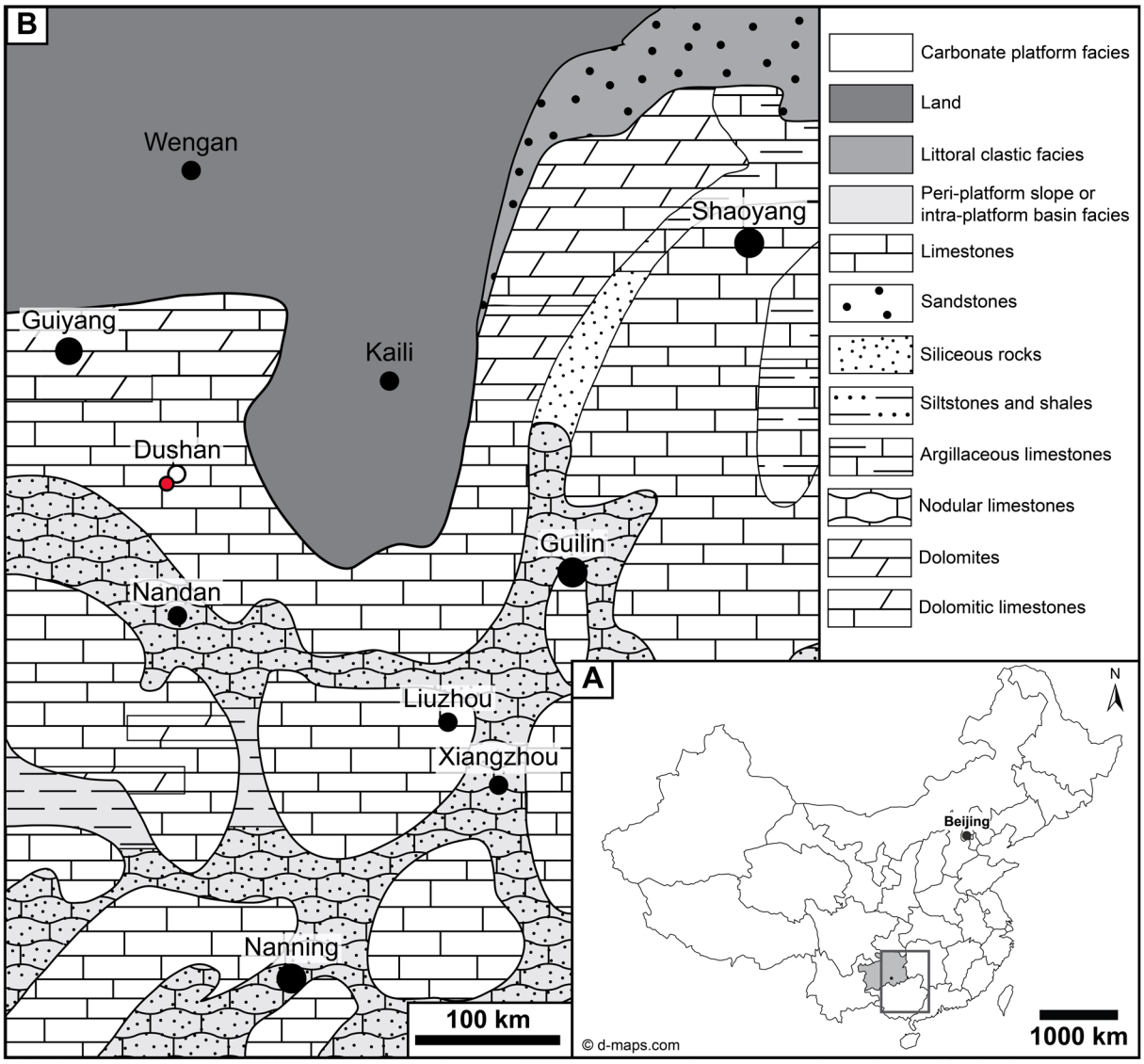

Fig. 2. A. Location map of the Guizhou Province in China. **B**. Geological map of the Blue Snake Section and its surroundings (modified after Song & Gong 2019 and Ma *et al.* 2016). The red spot indicates the location of the Blue Snake section and the black circle indicates the location of Dushan city.

Electron Microscope and the Zeiss Axio Zoom V.16 microscope of the CR2P. 98 species belonging to 31 genera are identified and figured. Most of the specimens are relatively poorly preserved (recrystallized), particularly brittle and thus difficult to move once prepared for the SEM work: most of them are only shown in lateral view. Following Fürsich & Wendt (1977), Nützel & Kaim (2014) and Haussmann & Nützel (2015), the number of specimens of each species was counted by adding articulated carapaces and higher number of left or right valves.

Many species are kept in open nomenclature because of a poor preservation and/or availability of specimens that don't allow a precise attribution. Species left in open nomenclature or referred to already known species are only discussed when necessary but the complete taxonomic list is available (Table 1) and all species are figured to allow future comparison. In order to make descriptions as objective as possible, characters are quantified as much as possible and the length convention of carapaces/valves

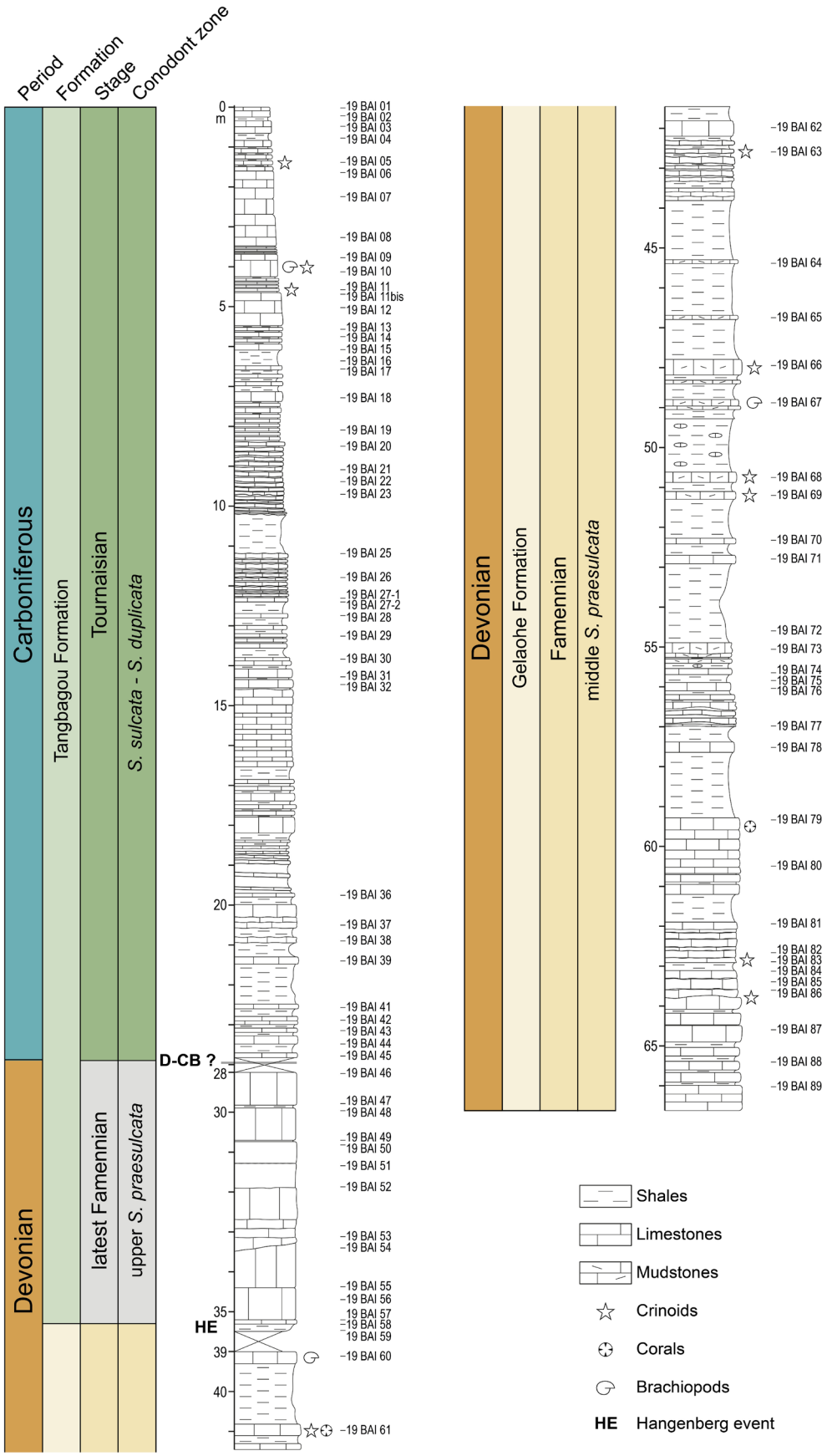
Period
Formation
Stage
Conodont zone
Carboniferous
Devonian
Tangbagou Formation
Tournaisian
latest Famennian
S. sulcata - S. duplicata
upper S. praesulcata
D-CB ?
HE
Devonian
Gelaohe Formation
Famennian
middle S. praesulcata
m
0
5
10
15
20
28
30
35
39
40
45
50
55
60
65
19 BAI 01
19 BAI 02
19 BAI 03
19 BAI 04
19 BAI 05
19 BAI 06
19 BAI 07
19 BAI 08
19 BAI 09
19 BAI 10
19 BAI 11
19 BAI 11bis
19 BAI 12
19 BAI 13
19 BAI 14
19 BAI 15
19 BAI 16
19 BAI 17
19 BAI 18
19 BAI 19
19 BAI 20
19 BAI 21
19 BAI 22
19 BAI 23
19 BAI 25
19 BAI 26
19 BAI 27-1
19 BAI 27-2
19 BAI 28
19 BAI 29
19 BAI 30
19 BAI 31
19 BAI 32
19 BAI 36
19 BAI 37
19 BAI 38
19 BAI 39
19 BAI 41
19 BAI 42
19 BAI 43
19 BAI 44
19 BAI 45
19 BAI 46
19 BAI 47
19 BAI 48
19 BAI 49
19 BAI 50
19 BAI 51
19 BAI 52
19 BAI 53
19 BAI 54
19 BAI 55
19 BAI 56
19 BAI 57
19 BAI 58
19 BAI 59
19 BAI 60
19 BAI 61
19 BAI 62
19 BAI 63
19 BAI 64
19 BAI 65
19 BAI 66
19 BAI 67
19 BAI 68
19 BAI 69
19 BAI 70
19 BAI 71
19 BAI 72
19 BAI 73
19 BAI 74
19 BAI 75
19 BAI 76
19 BAI 77
19 BAI 78
19 BAI 79
19 BAI 80
19 BAI 81
19 BAI 82
19 BAI 83
19 BAI 84
19 BAI 85
19 BAI 86
19 BAI 87
19 BAI 88
19 BAI 89
Shales
Limestones
Mudstones
Crinoids
Corals
Brachiopods
HE Hangenberg event

Fig. 3. Stratigraphic log of the Blue Snake Section and sampling points. Colours on stages and conodont zones correspond to the stratigraphic repartition of the 3 ostracod associations recognized in the present work. Orange: Association A. Grey: Association B. Green: Association C.

is as follows: < 0.40 mm: very small, 0.40–0.50 mm: small, 0.50–0.70 mm: medium, 0.70–1.00 mm large, >1.0: very large. The stratigraphic distribution of all species is available in Table 2.

Material repository

All type and figured specimens are temporarily in the collections of Sorbonne Université, Paris, France under catalogue numbers P6M 3837 to P6M 3975.

Anatomical abbreviations

AB = anterior border
ADB = antero–dorsal border
ACA = anterior cardinal angle
AVB = antero–ventral border
DB = dorsal border
H = height
Hmax = maximal height
L = length
Lmax = maximal length
LV = left valve
PB = posterior border
PCA = posterior cardinal angle
PDB = postero–dorsal border
PVB = postero–ventral border
RV = right valve
VB = ventral border
W = width
Wmax = maximal width

Results

Systematic palaeontology

(E. Guillam & M.–B. Forel)

We follow the classification of Moore (1961), Becker (2002) and Horne *et al.* (2002).

Class Ostracoda Latreille, 1806
Subclass Podocopa Müller, 1894
Order Palaeocopida Henningsmoen, 1953
Suborder Beyrichiocopina Scott, 1961
Superfamily Aparchitoidea Jones, 1901
Family Aparchitidae Jones, 1901

Genus ***Fellerites*** Gründel, 1962

Type species

Fellerites bohlenensis Gründel, 1962 by original designation.

Fellerites sp. 1
Fig. 5B

Material examined

CHINA • 1 complete carapace (Fig. 5B); Blue Snake section, Gelaohe Formation, sample 19BAI 67; P6M 3838. • 7 complete carapaces; Blue Snake section, Gelaohe Formation, samples 19BAI 67, 19BAI 68, 19BAI 74, 19BAI 80. All from the Famennian, late Devonian.

Dimensions

RV: L = 595–625 µm, H = 388–423 µm, H/L = 0.65–0.68.
LV: L = 455–753 µm, H = 286–479 µm, H/L = 0.63–0.68.

Remarks

This taxon is rare in the studied material and is represented by poorly preserved specimens that do not allow for a specific attribution. It is morphologically close to *Phlyctiscapha*? *xiangzhouensis* Wang, 1983 from the Lower Devonian of the Sipai Formation, Guangxi, South China (Wang 1983a). The specimen illustrated in Wang (1983a) lacks the small velate ridge parallel to the marginal ridge characteristic of the genus *Phlyctiscapha*. Its outline, the absence of velar structure or teeth along free margin and the carapace slightly compressed along free margin could rather pointed to the genus *Fellerites* Gründel, 1962. *Fellerites* sp. 1 differs from *Phlyctiscapha*? *xiangzhouensis* by its higher carapace, slightly stockier morphology and its smaller size (L = 1060–1360 µm, H = 660–920 µm, H/L = 0.62–0.76 for *Phlyctiscapha*? *xiangzhouensis*).

Occurrence

Samples 19BAI 67, 19BAI 68, 19BAI 74, 19BAI 80, Gelaohe Formation, Blue Snake section, Famennian, late Devonian (this work).

Superfamily Primitiopsoidea Swartz, 1936
Family Primitiopsidae Swartz, 1936

Genus ***Clavofabella*** Martinsson, 1955

Type species

Clavofabella incurvata Martinsson, 1955 by original designation.

Preliminary remark

The original diagnosis of *Clavofabella* by Martinsson (1955) is questionable because it does not include characters shared by all specimens: "Dolonate flanges do not meet posteriorly. Dolon that continues forwards in a velar ridge or a velar bend" (Martinsson 1955: 23). These structures are absent in non-dolonate specimens described or mentioned by Martinsson in the same paper in *Clavofabella multidentata* Martinsson, 1955, *Clavofabella incurvata* Martinsson, 1955 and *Clavofabella reticristata* (Jones, 1888). We follow the diagnosis of *Clavofabella* provided in Moore (1961) because it is based on characters shared by all forms: "inequivalved, RV overlapping LV; hinge consisting of median groove with corresponding ridge and lateral elongate pits and sockets; unisulcate […]; surface pitted or reticulate, marginal structure tuberculate" (Moore 1961: 174). Moore (1961) furthermore indicates that velar structures are developed as ridge but that in heteromorphs they are wider and form posterior flanges that do not meet.

Table 1 (continued on next two pages)**.** List and systematic placement of species occurring in the Blue Snake section.

Class Ostracoda Latreille, 1806
Subclass Podocopa Müller, 1894
Order Palaeocopida Henningsmoen, 1953
Suborder Beyrichiocopina Scott, 1951
Superfamily Aparchitoidea Jones, 1901
Family Aparchitidae Jones, 1901
Genus *Aparchites* Jones, 1889
Aparchites sp. Fig. 5A
Genus *Fellerites* Gründel, 1962
Fellerites sp. 1 Fig. 5B
Fellerites sp. 2 Fig. 5C

Superfamily Hollinoidea Swartz, 1936
Family Hollinellidae Bless and Jordan, 1971
Genus *Parabolbinella* Adamczak, 1968
Parabolbinella sp. Fig. 5D

Superfamily Kirkbyoidea Ulrich and Bassler, 1906
Family Amphissitidae Knight, 1928
Genus *Amphissites* Girty, 1910
Amphissites sp. Fig. 5E

Superfamily Primitiopsoidea (Swartz, 1936)
Family Primitiopsidae Swartz, 1936
Genus *Clavofabella* Martinsson, 1955
Clavofabella? *lanshella* sp. nov. Fig. 5F-G (Holotype), Fig. 5H (Paratype), Fig. 5I-J (A-1), Fig. 5K (A-2), Fig. 5L (A-3).
Clavofabella? sp. Fig. 5M (Ad), Fig. 5N (A-1), Fig. 5O (A-2), Fig. 5P (A-3), Fig. 5Q (A-4), Fig. 5R (A-5).
Genus *Coryellina* Bradfield, 1935
Coryellina grammi Olempska, 1999 Fig. 5S.
Genus *Selebratina* Polenova, 1953
Selebratina sp. Fig. 5T.

Suborder Kloedenellocopina Scott, 1961
Superfamily Kloedenelloidea Ulrich and Bassler, 1908
Family Beyrichiopsidae Henningsmoen, 1953
Genus *Beyrichiopsis* Jones & Kirkby, 1886
Beyrichiopsis sp. Fig. 5U.
Genus *Kloedenellitina* Egorov, 1950
Kloedenellitina sincera Tschigova, 1960 Fig. 6A.
Kloedenellitina spinosa Gurevitch, 1972 Fig. 6B (female), Fig. 6C (male).
Kloedenellitina sygmaeformis Egorov, 1950 Fig. 6D.

Family Geisinidae Sohn, 1961
Genus *Blessites* Tschigova, 1977
Blessites feluyensis Tschigova, 1977 Fig. 6E.
Genus *Hypotetragona* Morey, 1935
Hypotetragona angulata (Posner, 1951) Fig. 6F (Ad), Fig. 6G (A-1), Fig. 6H. (A-2), Fig. 6I (A-3).
Hypotetragona sp. Fig. 6J (Ad), Fig. 6K (A-1), Fig. 6L (A-2), Fig. 6M (A-3).
Genus *Knoxiella* Egorov, 1950
Knoxiella archedensis Tschigova, 1960 Fig. 6N.
Knoxiella complanata (Kummerow, 1939) Fig. 6O.
Knoxiella subcompressa Wang & Ma, 2007 Fig. 6P.
Knoxiella cf. *subcompressa* Wang & Ma, 2007 Fig. 6Q (Ad), Fig. 6R (A-1).
Genus *Knoxina* Coryell & Rogatz, 1932
Knoxina sp. Fig. 6S-T.
Genus *Knoxites* Egorov, 1950
Knoxites cf. argulata Zaspelova, 1959 Fig. 6U (Ad), Fig. 7A (A-1).

Superfamily Paraparchitoidea Scott, 1959
Family Paraparchitidae Scott, 1959
Genus *Paraparchites* Ulrich & Bassler, 1906
Paraparchites longmenshanensis Wei, 1983 Fig. 7B.
Paraparchites sp. 1 Fig. 7C.
Paraparchites sp. 2 Fig. 7D.
Genus *Shishaella* Sohn, 1971
Shishaella hastierensis Crasquin-Soleau, 1988 Fig. 7E.
Shishaella porrecta (Zanina, 1956) Fig. 7F.

Superfamily Sansabelloidea Sohn 1961
Family Sansabellidae Sohn, 1961
Genus *Sansabella* Roundy, 1926
Sansabella gelaohensis sp. nov. Fig. 7G (Holotype), Fig. 7H (Paratype 1), Fig. 7I (Paratype 2), Fig. 7J (A-1), Fig. 7K (A-2), Fig. 7L (A-2), Fig. 7M (A-4), Fig. 7N (A-5).

Table 1 (continued)**.** List and systematic placement of species occurring in the Blue Snake section.

Order Platycopida Sars, 1866
Suborder Platycopina Sars, 1866
Superfamily Cavellinoidea, Egorov, 1950
Family Cavellinidae Egorov, 1950
Genus *Cavellina* Coryell, 1928
Cavellina cf. *dushanenis* Shi, 1964 Fig. 7O.
Cavellina cf. *recta* (Jones, Kirkby & Brady, 1884) Fig. 7P.
Genus *Sulcella* Coryell & Sample, 1932
Sulcella baisuzhena sp. nov. Fig. 7Q (Holotype), Fig. 7R (Paratype, A-1), Fig. 7S (Paratype, A-1), Fig. 7T (A-2), Fig. 7U (A-3), Fig. 8A (A-4), Fig. 8B (A-5).

Order Podocopida Sars, 1866
Suborder Podocopina Sars, 1866
Superfamily Bairdiocypridoidea Shaver, 1961
Family Bairdiocyprididae Shaver, 1961
Genus *Bairdiocypris* Kegel, 1932
Bairdiocypris elliptica Wei, 1983 Fig. 8C.
Bairdiocypris fomikhaensis Buschmina, 1968 Fig. 8D-E.
Bairdiocypris marginifera (Geis, 1932) sensu Buschmina, 1968 Fig. 8F.
Bairdiocypris sp. Fig. 8G.
Genus *Cytherellina* Jones & Holl, 1869
Cytherellina caerulea sp. nov. Fig. 8H (Holotype), Fig. 8I (Paratype 1), Fig. 8J (Paratype 2), Fig. 8K-L.
Genus *Healdianella* Posner, 1951
Healdianella alba Lethiers, 1981 Fig. 8M.
Healdianella faseollina Rozhdestvenskaya, 1959 in Song & Gong 2019 Fig. 8N.
Healdianella lumbiformis, Lethiers & Feist, 1991 Fig. 8O.
Healdianella cf. *insolita* (Buschmina, 1977) Fig. 8P.
Healdianella cf. *subdistincta* Wang, 1983 Fig. 8Q-R.
Healdianella sp. Fig. 8S.
Genus *Praepilatina* Polenova 1970
Praepilatina adamczaki Olempska 1979 Fig. 8T.

Family Pachydomellidae Berdan and Sohn, 1961
Genus *Elliptocyprites* Swain, 1962
Elliptocyprites lorangeri Lethiers, 1981 Fig. 8U.
Elliptocyprites sp. Fig. 9A.
Genus *Microcheilinella* Geis, 1933
Microcheilinella infradominaca Rozhdestvenskaya, 1962 in Song & Gong, 2018 Fig. 9B.
Microcheilinella larionovae Polenova, 1955 Fig. 9C.
Microcheilinella sp. A, aff. *buschminae* Olempska, 1981 in Casier et al., 2004 Fig. 9D.
Microcheilinella sp. cf. *M. buschminae* Olempska, 1982 in Song & Gong, 2017 Fig. 9E.
Microcheilinella sp. sensu Olempska, 1979 Fig. 9F.
Microcheilinella subrhomboidalis Xie, 1983 Fig. 9G.
Microcheilinella cf. *decora* Shi, 1964 Fig. 9H.
Microcheilinella sp. Fig. 9I.

Superfamily Bairdioidea Sars, 1888
Family Bairdiidae Sars, 1888
Genus *Acratia* Delo, 1930
Acratia acutiangulata (Posner in Tschigova, 1960) Fig. 9J.
Acratia similaris Green, 1963 Fig. 9K.
Acratia subobtusa Lethiers, 1974 Fig. 9L.
Acratia cf. *disjuncta* Morey, 1935 Fig. 9M.
Acratia cf. *evlanensis* Egorov, 1953 Fig. 9N-O.
Acratia cf. *insolita* Buschmina, 1970 Fig. 9P.
Acratia cf. *tschudovoensis* Zaspelova, 1959 Fig. 9Q.
Acratia sp. Fig. 9R.
Genus *Acutiangulata* Buschmina, 1968
Acutiangulata acutiangulata (Tschigova, 1959) Fig. 9S.
Genus *Bairdia* McCoy, 1844
Bairdia cestriensis Ulrich, 1891 Fig. 9T.
Bairdia confragosa Samoilova & Smirnova, 1960 Fig. 9U.
Bairdia feliumgibba Becker, 1982 Fig. 10A.
Bairdia hypsela Rome, 1971 Fig. 10B.
Bairdia mnemonica Schevtsov, 1964 Fig. 10C.
Bairdia nanbiancunensis Wang, 1988 Fig. 10D-E.
Bairdia natiformis Buschmina, 1970 Fig. 10F.
Bairdia obliqua Rozhdestvenskaya, 1972 Fig. 10G (Ad), Fig. 10H (A-1), Fig. 10I (A-2).
Bairdia quasikuznecovae Buschmina, 1968 Fig. 10J.
Bairdia rustica Kotschetkova, 1983 Fig. 10K.
Bairdia semichatovae Tschigova, 1960 Fig. 10L.
Bairdia solita Buschmina, 1970 Fig. 10M.
Bairdia submongolensis Buschmina, 1968 Fig. 10N.
Bairdia cf. *altifrons* Knight, 1928 in Crasquin, 1984 Fig. 10O.
Bairdia cf. *extenuata* Nazarova, 1951 Fig. 10P.
Bairdia cf. *grahamensis* Harlton, 1928 Fig. 10Q.
Bairdia cf. *susoroides* Jiang, 1983 Fig. 10R.
Bairdia sp. 1 Fig. 10S.
Bairdia sp. 2 Fig. 10T.

Table 1 (continued)**.** List and systematic placement of species occurring in the Blue Snake section.

Bairdia sp. 3 Fig. 10U.
Bairdia sp. 4 Fig. 11A.
Bairdia sp. 5 Fig. 11B.
Bairdia sp. 6 Fig. 11C.
Bairdia sp. 7 Fig. 11D.
Bairdia (*Cryptobairdia*) *curta* McCoy, 1844 emend. Jones & Kirkby, 1878 in Crasquin, 1986 Fig. 11E.
Bairdia (*Cryptobairdia*) *laveinei* Crasquin, 1985 Fig. 11F.
Bairdia (*Rectobairdia*) *angulatiformis* Posner, 1951 Fig. 11G.
Bairdia (*Rectobairdia*) *buschminaae* Crasquin, 1985 Fig. 11H.
Bairdia (*Rectobairdia*) cf. *plebeja* Reuss, 1854 Fig. 11I.
Bairdia (*Rectobairdia*) sp. cf. *R. sinuosa* (Morey, 1936) in Crasquin, 1985 Fig. 10J-L.
Genus *Bairdiacypris* Bradfield, 1935
Bairdiacypris nanbiancunensis Wang, 1988 Fig. 10M.
Bairdiacypris quasielongata Buschmina, 1968 Fig. 10N.
Bairdiacypris subcylindrica Buschmina, 1984 Fig. 10O.
Genus *Bairdianella* Harlton, 1929
Bairdianella cuspis Buschmina, 1970 Fig. 10P.
Genus *Fabalicypris* Cooper, 1946
Fabalicypris sundarijanata Wang and Cao, 1997 in Song & Gong, 2019 Fig. 10Q.

Superfamily Bairdioidea Sars, 1888?
Family indet
Genus indet
Bairdioidea? indet. Fig. 10R.

Clavofabella*? *lanshella Guillam & Forel sp. nov.
urn:lsid:zoobank.org:act:9B24EB32-22A9-4A92-99D8-6C5F7B6744D0
Fig. 5F–L

Diagnosis

A new species questionably attributed to *Clavofabella* with elongate outline and laterally compressed spinose free margin at LV.

Etymology

The specific epithet refers to the Latinization of the Chinese '*lan she*', which means 'blue snake' in reference to the name given to the section.

Material examined

Holotype

CHINA • 1 complete carapace (Fig. 5F–G); Blue Snake section, Gelaohe Formation, sample 19BAI 68; Famennian, late Devonian; P6M 3842.

Paratype

CHINA • 1 complete carapace (Fig. 5H); Blue Snake section, Gelaohe Formation, sample 19BAI 68; Famennian, late Devonian; P6M 3843.

Other material

CHINA • 1 complete carapace (A-1, Fig. 5I); Blue Snake section, Gelaohe Formation, sample 19BAI 68; P6M 3844 • 1 complete carapace (A-2, Fig. 5J); Blue Snake section, Gelaohe Formation, sample 19BAI 68; P6M 3845 • 1 complete carapace (A-3, Fig. 5L); Blue Snake section, Gelaohe Formation, sample 19BAI 68; P6M 3846 • 20 complete carapaces; Blue Snake section, Gelaohe Formation, samples 19BAI 63, 19BAI 67, 19BAI 68, 19BAI 74. All from the Famennian, late Devonian.

Dimensions

See Fig. 4A.

Description

Carapace large, preplete, ovoid/rectangular (adults) to inverted triangular (young juveniles) in lateral view, lenticular with laterally compressed anterior and posterior margins in dorsal view. Lmax slightly above mid-H, Hmax in front of mid-L, Wmax around mid-H and slightly in front of mid-L. RV overlaps LV all around, with maximum along free margin. Hinge line slightly sinuous with gentle concavity immediately posterior to ACA, slightly invaginated all along its length. Obtuse cardinal angles, ACA about 145°, PCA about 130°. Surface coarsely reticulate with round reticulae. LV with a spinose free margin that could indicate the presence of a velar structure. Pit relatively large (H about 32% of Hmax, L about 14% of Lmax), ovoid, elongated dorso-ventrally, located slightly in front of mid-L, slightly above mid-H, at Wmax.

Remarks

This species is doubtfully attributed to the genus *Clavofabella* Martinsson, 1955 described from the Late Wenlock (Silurian) of Gotland, Sweden (Martinsson 1955) because of RV overlapping LV, surface reticulated, sulcal pit and spinose free margin that could indicate the presence of a velar structure and that points to heteromorphs after Moore (1961). However, the tubercles in all known species belonging to *Clavofabella* are short and rounded and are absent at DB where the dolon is located in heteromorphs. In our material, these structures are spines rather than tubercles and are located along the entire free margin and are larger than those described from all known species belonging to this genus. *Clavofabella*? *lanshella* sp. nov. also differs from all other species of this genus by its laterally compressed morphology, more elongate lateral outline, larger sulcal pit, coarse reticulation and straighter DB. The H/L scatter plot of *Clavofabella*? *lanshella* sp. nov. (Fig. 4A) allows to discriminate four ontogenetic stages (A-3 to Ad). The ontogenetic development of this species is marked by the elongation of the carapace, increasing compression of the free margin, enlargement of the pit and growth of spines along free margin.

Occurrence

Samples 19BAI 63, 19BAI 67, 19BAI 68, 19BAI 74, Gelaohe Formation, Blue Snake section, Famennian, late Devonian (this work).

***Clavofabella*?** sp.
Fig. 5M–R

Material examined

CHINA • 1 complete carapace (Ad, Fig. 5M); Blue Snake section, Gelaohe Formation, sample 19BAI 68; P6M 3847 • 1 complete carapace (A-1, Fig. 5N); Blue Snake section, Gelaohe Formation, sample 19BAI 69; P6M 3848 • 1 complete carapace (A-2, Fig. 5O); Blue Snake section, Gelaohe Formation, sample 19BAI 68; P6M 3849 • 1 complete carapace (A-3, Fig. 5P); Blue Snake section, Gelaohe Formation, sample 19BAI 68; P6M 3850 • 1 complete carapace (A-4, Fig. 5Q); Blue Snake section, Gelaohe Formation, sample 19BAI 68; P6M 3851 • 1 complete carapace (A-5, Fig. 5R); Blue Snake section, Gelaohe Formation, sample 19BAI 68; P6M 3852 • 10 complete carapaces; Blue Snake section, Gelaohe Formation, sample 19BAI 68. All from the Famennian, late Devonian.

Dimensions

RV: L = 204–805 µm, H = 139–554 µm, H/L = 0.68–0.74.
LV: L = 202–805 µm, H = 136–546 µm, H/L = 0.65–0.73.

Remarks

Our material is morphologically close to non-dolonate specimens of *Clavofabella multidentata* Martinsson, 1955 from the Late Wenlock, Silurian of Mulde, Parish Fröjel, Gotland, Sweden

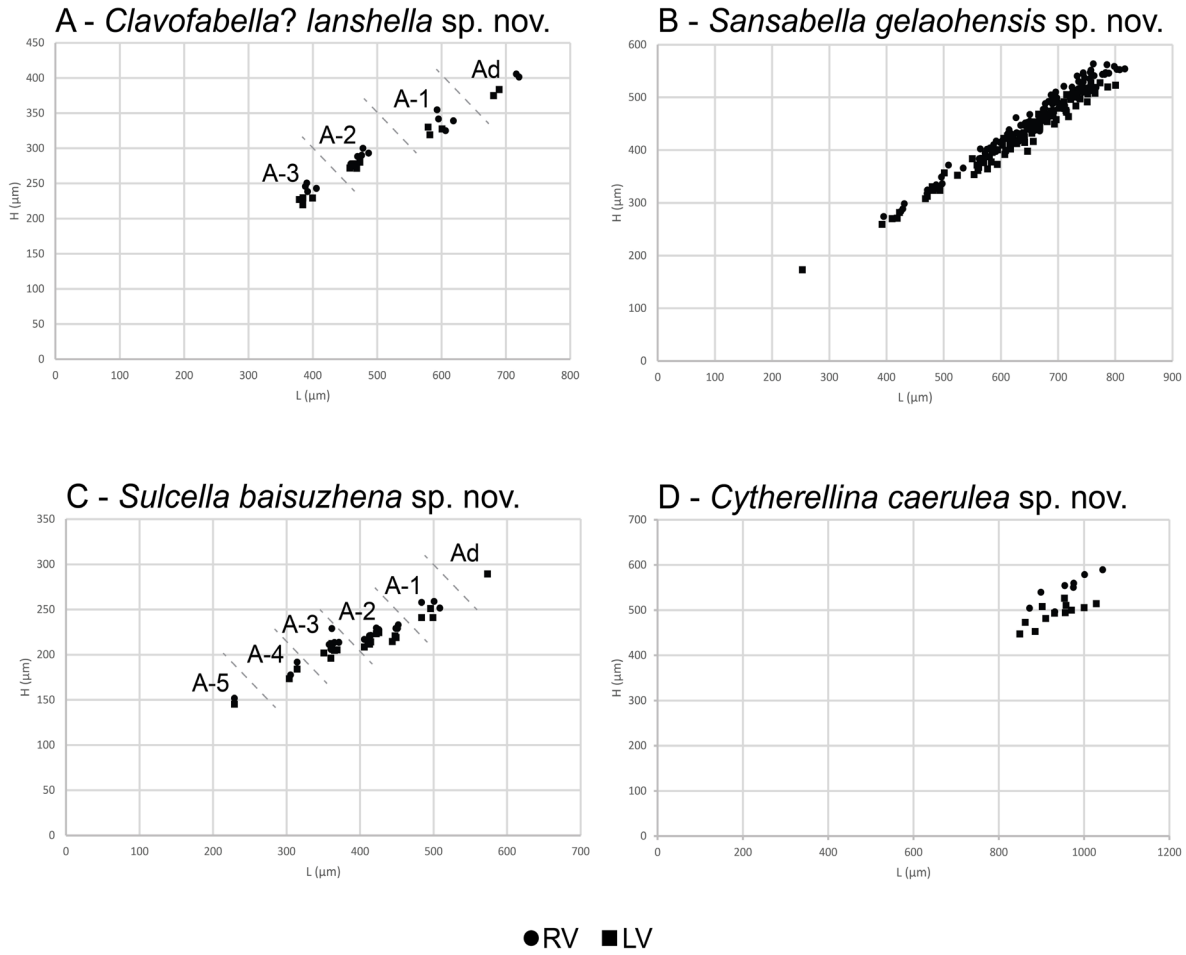

Fig. 4. H/L scatter plots of all specimens belonging to the four new species described in this contribution. **A**. *Clavofabella*? *lanshella* Guillam & Forel sp. nov. **B**. *Sansabella gelaohensis* Guillam & Forel sp. nov. **C**. *Sulcella baisuzhena* Guillam & Forel sp. nov. **D**. *Cytherellina caerulea* Guillam & Forel sp. nov.

(Martinsson 1955) but differs by its more rounded cardinal angles, deeper sulcus and larger adductorial pit. It is also close to *Libumella*? sp. from the Famennian, late Devonian of the Yjid-Kamenka River section, Pechora Uplift, Russia (Sobolev 2020) but our material differs from this species by its more laterally compressed free margin, its deeper sulcal pit and its more developed lobation. This species may be new to science but the 16 specimens discovered are not sufficient to establish its generic attribution and to reasonably describe its diagnostic characters. Six different ontogenetic stages are present in our material (from A-5 to Ad). The ontogenetic changes through development cannot be precisely observed because of preservation but it seems that the outline does not show major changes, the sulcus apparently becomes deeper and the anterior lobe more developed.

Occurrence

Samples 19BAI 68, 19BAI 69, Gelaohe Formation, Blue Snake section, Famennian, late Devonian (this work).

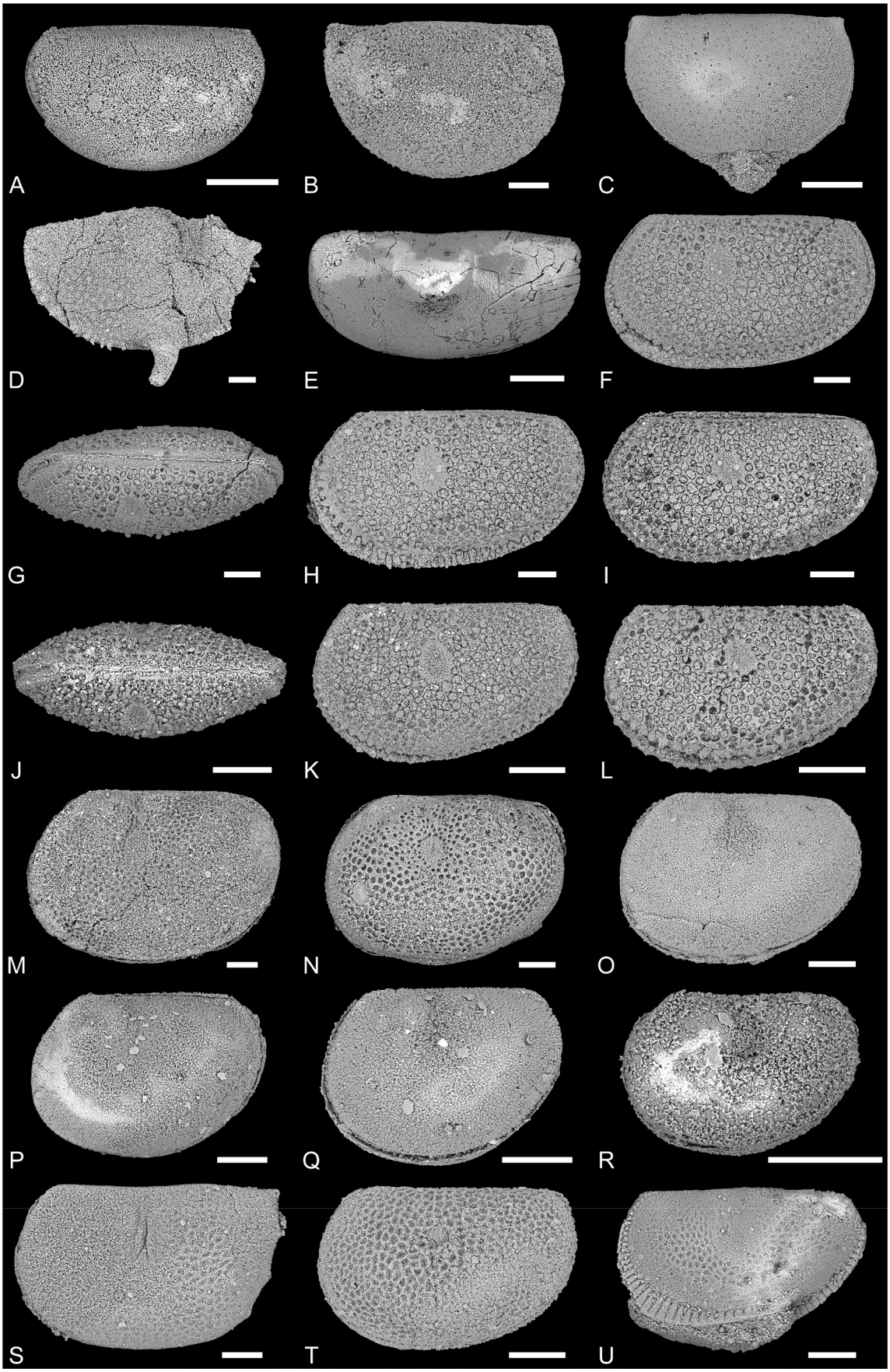
A
B
C
D
E
F
G
H
I
J
K
L
M
N
O
P
Q
R
S
T
U

Fig. 5. SEM pictures of ostracods from Blue Snake section, Dushan County, South China, late Famennian–Tournaisian, late Devonian–early Carboniferous. All specimens are temporarily housed in the collections of Sorbonne Université, Paris, France (numbers P6M****). **A**. *Aparchites* sp., left lateral view of a carapace, sample 19BAI 08 (P6M 3837). **B**. *Fellerites* sp. 1, right lateral view of a carapace, sample 19BAI 67 (P6M 3838). **C**. *Fellerites* sp. 2, right lateral view of a carapace, sample 19BAI 80 (P6M 3839). **D**. *Parabolbinella* sp., right lateral view of an anteriorly broken carapace, sample 19BAI 74 (P6M 3840). **E**. *Amphissites* sp., right lateral view of a steinkern, sample 19BAI 74 (P6M 3841). **F–L**. *Clavofabella*? *lanshella* Guillam & Forel sp. nov. **F**. Holotype, left lateral view of a carapace, sample 19BAI 68 (P6M 3842). **G**. Same specimen, dorsal view. **H**. Paratype, left lateral view of a carapace, sample 19BAI 68 (P6M 3843). **I**. A-1, left lateral view of a carapace, sample 19BAI 68 (P6M 3844). **J**. Same specimen, dorsal view. **K**. A-2, left lateral view of a carapace, sample 19BAI 68 (P6M 3845). **L**. A-3, left lateral view of a carapace, sample 19BAI 68 (P6M 3846). **M–R**. *Clavofabella*? sp. **M**. Adult, left lateral view of a carapace, sample 19BAI 68 (P6M 3847). **N**. A-1, left lateral view of a carapace, sample 19BAI 69 (P6M 3848). **O**. A-2, left lateral view of a carapace, sample 19BAI 68 (P6M 3849). **P**. A-3, left lateral view of a carapace, sample 19BAI 68 (P6M 3850). **Q**. A-4, left lateral view of a carapace, sample 19BAI 68 (P6M 3851). **R**. A-5, left lateral view of a carapace, sample 19BAI 68 (P6M 3852). **S**. *Coryellina grammi* Olempska, 1999, left lateral view of a carapace, sample 19BAI 41 (P6M 3853). **T**. *Selebratina* sp., left lateral view of a carapace, sample 19BAI 41 (P6M 3854). **U**. *Beyrichiopsis* sp., left lateral view of a carapace, sample 19BAI 41 (P6M 3855). Scale bars = 100 µm.

Suborder Kloedenellocopina Scott, 1961
Superfamily Kloedenelloidea Ulrich & Bassler, 1908
Family Beyrichiopsidae Henningsmoen, 1953

Genus ***Kloedenellitina*** Egorov, 1950

Type species

Beyrichia (?) *sygmaeformis* Batalina, 1941 subsequently designated by Egorov (1950).

Kloedenellitina sincera Tschigova, 1960
Fig. 6A

Kloedenellitina sincera Tschigova, 1960: 223, pl. 8p figs 1–3.

Knoxiella cf. *oblonga* – Song & Gong 2019: fig. 4p–q.

Material examined

CHINA • 1 complete carapace (Fig. 6A); Blue Snake section, Gelaohe Formation, sample 19BAI 69; P6M 3856 • 19 complete carapaces; Blue Snake section, Gelaohe Formation, sample 19BAI 74. All from the Famennian, late Devonian.

Dimensions

RV: L = 360–864 µm, H = 206–455 µm, H/L = 0.49–0.59.
LV: L = 360–842 µm, H = 196–435 µm, H/L = 0.47–0.56.

Remarks

Knoxiella cf. *oblonga* Wang, 1978 in Song & Gong (2019) from the Famennian, late Devonian of Baihupo section, Guizhou, South China (Song & Gong 2019) does not belong to the genus *Knoxiella* Egorov, 1950. The specimens shown in Song & Gong (2019: fig. 4p–q) has the typical *Kloedenellitina*

outline with AB and PB that are in the same plane. It is morphologically similar to *Kloedenellitina sincera* Tschigova, 1960 from our material and we consider that they are conspecific.

The adult carapace in our material is bigger than the holotype (L = 795 µm, H = 422 µm in Tschigova 1960) but the H/L ratio is similar (H/L = 0.53). The other specimens from our material are smaller and may represent juveniles of this species. The specimen shown in Song & Gong (2019: fig. 4p) is larger than our material and the holotype (L = 970 µm, H = 530 µm) but the H/L ratio is also similar (H/L = 0.55). The posterior part is inflated and shows a vertical sulcus opened ventrally which suggests that it may be a female (Ellis & Messina 1964). All our specimens are less inflated in the posterior part so they may correspond to males. The size variations clearly indicate that several stages are present in the assemblages studied but it is impossible to discriminate them.

Occurrence

Dankovo–Lebedyan Horizon, Russian platform, Famennian, late Devonian (Tschigova 1960). Blue Snake section, Guizhou, South China, Gelaohe and Tangbagou Formations, Famennian–Tournaisian, late Devonian–early Carboniferous (Song & Gong 2019). Samples 19BAI 69, 19BAI 74, Gelaohe Formation, Blue Snake section, Famennian, late Devonian (this work).

Kloedenellitina spinosa Gurevitch, 1972
Fig. 6B–C

Kloedenellitina spinosa Gurevitch, 1972: 333, pl. 11 figs 3–4.

Kloedenellitina spinosa – Tschigova 1977: 171, pl. 41 fig. 13.

Material examined

CHINA • 1 complete carapace (♀, Fig. 6B); Blue Snake section, Gelaohe Formation, sample 19BAI 60; P6M 3857 • 1 complete carapace (♂, Fig. 6C); Blue Snake section, Gelaohe Formation, sample 19BAI 69; P6M 3858 • 16 complete carapaces; Blue Snake section, Gelaohe Formation, samples 19BAI 60, 19BAI 67–69, 19BAI 74, 19BAI 80. All from the Famennian, late Devonian.

Dimensions

RV: L = 552–783 µm, H = 307–394 µm, H/L = 0.48–0.59.
LV: L = 434–761 µm, H = 210–377 µm, H/L = 0.45–0.56.

Remarks

In the genus *Kloedenellitina*, females have an inflated posterior carapace, which corresponds to a brood pouch (Ellis & Messina 1964). This character allows us to distinguish females (Fig. 6B) from males (Fig. 6C) in the studied material. The lateral surface of the specimens preserving their carapace appears as reticulate (Fig. 6C), it is rather smooth in steinkern but the reticulation remains visible in certain areas (Fig. 6B). Our material is smaller than the type material (L = 760–930 µm, H = 440–490 µm in Gurevitch 1972) with H/L between 0.53 and 0.58 while it is between 0.45 and 0.59 in our material (both valves taken together). The specimen shown in Tschigova (1977: pl. 61 fig. 13) is also larger with L = 1200 mm, H = 556 mm but the H/L ratio is similar (H/L = 0.46). In the present material, this species may mainly be represented by juvenile specimens corresponding to at least two different ontogenetic stages that we cannot discriminate because of the wide distribution of their dimensions.

Table 2 (continued on next two pages)**.** Stratigraphic distribution of species in the Blue Snake section.

Orange: Association A, Grey: Association B, Green: Association C.

	Gelaohe Formation							Tangbagou Formation																
	Famennian							latest Fa.			Tournaisian													
Species \ Sample 19BAI	80	74	69	68	67	63	60	58	55	54	44	43	41	39	37	27-2	23	16	08	05	03	02	01
Knoxina sp.	1	8																					
Bairdia nanbiancunensis	1		2	1	2																		
Fellerites sp. 1	2	1	1	1	3																		
Beyrichiopsis sp.	8		1		2	3	1																
Kloedenellitina spinosa	1	2	2	2	3	1	7																
Kloedenellitina sygmaeformis	3	2	1	6		3	3																
Knoxiella subcompressa	2	1		2	2		1																
Fellerites sp. 2	2		2				5		1	1		2											
Knoxiella complanata	2														1		4		6	2	9	17	5
Bairdia hypsela	2		6						1	1	7	1	2	14	2	2	1	9		7	16	3	6
Parabolbinella sp.		1																					
Sulcella baisuzhena sp. nov.		1	1	19																			
Clavofabella? *lanshella* sp. nov.		2	4	17	1	1																	
Kloedenellitina sincera		14	1	2		3																	
Sansabella gelaohensis sp. nov.		73	8	2	3	15	5																
Healdianella sp.		1		12		3	7																
Acratia acutiangulata		5		15		1		2			4			2									
Bairdia quasikuznecovae		1	4		1		2				7	3	1					1					
Acratia cf. *tschudovoensis*		1	1	8															1				
Bairdiacypris nanbiancunensis		1					1		1	2									3	1	1	2	2
Clavofabella? sp.			1	14																			
Selebratina sp.			1	7		2																	
Cytherellina caerulea sp. nov.			5	4		2	1																
Healdianella cf. *insolita*			1				1		1	1				1									
Hypotetragona sp.			13	12			8			1	3		1	1	1					1			
Bairdia cf. *susoroides*			2		1						2				1								1
Knoxiella cf. *subcompressa*				2																			
Cavellina cf. *dushanensis*				2		1																	
Bairdia semichatovae				1	6		1					1											
Bairdia (*R.*) *angulatiformis*				1	1							3		1	1	1					1		

Table 2 (continued)**.** Stratigraphic distribution of species in the Blue Snake section.

Microcheilinella cf. *decora*				8						1			1			2			1	1		1	
Praepilatina adamszaki				1												1			1	2	4	2	2
Bairdia obliqua				2	1	2	4	3		6		1	4		1		3		9	2	2	12	10
Paraparchites sp. 2					1																		
Cavellina cf. *recta*					2																		
Bairdiocypris marginifera					1																		
Fabalicypris sundarijanata					4				2														
Acratia cf. *evlanensis*					1								1				1			3			
Knoxiella archedensis					1				1			2		1	4		2		2		8	1	2
Elliptocyprites sp.					1	2														1			1
Bairdia sp. 3					2															2			2
Bairdioidea? indet						1	1																
Acratia subobtusa						2											1				2		
Elliptocyprites lorangeri							1																
Bairdia cf. *extenuata*							1																
Bairdia (*C.*) *curta* McCoy, 1844 emend. Jones & Kirkby, 1878 in Crasquin, 1986							1																
Healdianella faseollina							2					1											
Bairdia sp. 5							5		1					1	1						1	2	
Healdianella alba							1		1	3		2	3	3					2		9	9	9
Microcheilinella larionovae							1						1			1				1	1	3	1
Microcheilinella sp.							4		1				4			3					1	1	3
Microcheilinella sp. sensu Olempska, 1979							1														1	1	3
Bairdia (*R.*) sp. cf. *R. sinuosa* (Morey, 1936) in Crasquin, 1985							1					5		1	2							1	2
Healdianella lumbiformis								16	2	1							1						
Bairdiacypris subcylindrica								33	12	7			1		1	1					2		
Shishaella hastierensis								8	2		6	5		5	7	1	7	1	3			2	1
Bairdia cestriensis								1															1
Shishaella porrecta									2						1								
Bairdia submongoliensis									1										1				
Bairdia (*C.*) *laveinei*									1								1			1	1	1	
Acratia cf. *insolita*									1			1	1		1	1	2					1	2
Acutiangulata acutiangulata									1							1			3		3	3	2
Bairdia mnemonica									4	2							4				3	2	1
Bairdia sp.1										2												1	
Bairdia natiformis										1	1	2	2				1					1	2
Bairdiacypris quasielongata										1		1					1		1	1	3	3	5
Amphissites sp.											2	1	2					5					1

Table 2 (continued)**.** Stratigraphic distribution of species in the Blue Snake section.

Blessites feluyensis											8		1	8	1								
Bairdia sp. 6											1							1			1		
Hypotetragona angulata											3	4	2	2		1			2	3	7	8	5
Paraparchites longmenshanensis											22	1		2		1	1						1
Bairdiocypris fomikhaensis											1	2	1	1			1			1	2	2	5
Bairdianella cuspis											1			1	2		1			3	5	7	6
Bairdia sp. 2												2											
Bairdia solita												1	4			1							
Microcheilinella sp. cf. *M. buschminae* Olempska, 1982 in Song & Gong, 2017												1								1	3		
Coryellina grammi												1	4	1	1	2							1
Acratia similaris												1					2		4		2	4	3
Acratia sp.												1							3	3	1	1	1
Bairdia cf. *altifrons*												1				1							2
Bairdia confragosa												3	5	3		2			1	3	10	2	6
Bairdia feliumgibba												2								6	5	2	7
Microcheilinella sp. A, aff. *buschminae* Olempska, 1981 in Casier et al., 2004													1			1					2		
Paraparchites sp. 1														1									
Bairdia (*R.*) *buschminaae*														2					2				
Bairdia (*R.*) cf. *plebeja*														14		1				1	3	2	
Bairdia sp. 4															1				1		4	6	1
Bairdia sp. 7																	1		1				
Healdianella cf. *subdistincta*																	2		5		2	1	
Bairdia cf. *grahamensis*																			1				
Bairdia rustica																			26				
Bairdiocypris elliptica																			3				2
Aparchites sp.																			5	2	1	1	
Acratia cf. *disjuncta*																			1				3
Bairdiocypris sp.																				1	2	1	2
Microcheilinella subrhomboidalis																					1		
Microcheilinella infradominica in Song & Gong, 2019																					2	2	
Knoxites cf. *argulata*																						1	1

Occurrence

Torchinsk Formation, Volyn region, Russian platform, Tournaisian, early Carboniferous (Gurevitch 1972). Lebedyan horizon, Torchinsk Formation, Central regions of the Russian platform, Famennian, late Devonian (Tschigova 1977). Samples 19BAI 60, 19BAI 67–69, 19BAI 74, 19BAI 80, Gelaohe Formation, Blue Snake section, Famennian, late Devonian (this work).

Family **Geisinidae** Sohn, 1961

Preliminary remark

This family has been revised by Adamczak (2006). Following these recommendations, the family name Knoxitidae Egorov, 1951 is here not adopted because "no generotype was explicitly designated" (Adamczak 2006: 277) and we chose to use Geisinidae Sohn, 1961.

Several genera belonging to this family have very similar morphologies (Adamczak 2006): *Geisina* Johnson, 1936, *Hypotetragona* Morey, 1935, *Jonesina* Ulrich & Bassler, 1908, and *Knoxiella* Egorov, 1950. This observation has led some authors to consider these genera as synonyms (e.g., Sohn in Moore 1961; Adamczak 2006; Jones 2011). Pollard (1966) considered that *Geisina* and *Jonesina* are both valid genera and indicated that *Jonesina* differed from *Geisina* by valves strongly and deeply bisulcate, S2 deep and ending by a pit, hinge not depressed in the posterior half and overlap absent along the hinge except at cardinal angles. Lethiers (1981) distinguished *Knoxiella* from *Hypotetragona* essentially by the invagination of the hinge and weak variations of the reticulation (Lethiers 1981: fig. 17). Here, we consider that these characters are not sufficient for generic discrimination, more specifically owing that the weak reticulation variations may be related to the preservation state. Thus, the morphologic differences observed by Lethiers (1981) could rather be differences at specific level.

Adamczak considered *Knoxiella* and *Jonesina* as "waste-basket taxon(s)" (Adamczak 2006: 299) and indicated that *Hypotetragonais* is preferred over *Knoxiella* in recent work. For *Jonesina*, it seems that "most of the species referred to this genus belong to *Geisina* and *Hypotetragona*" (Moore 1961: 413). However, *Hypotetragona* and *Knoxiella* are still being used (e.g., Casier 2017 for *Knoxiella*; Nazik *et al.* 2021 for *Hypotetragona*; Olempska 1999 used both genera) and an in–depth revision of all species is necessary to clarify their generic status.

As this revision is out of the scope of the present contribution and material:
– We here consider *Knoxiella* and *Hypotetragona* as synonyms, *Knoxiella* being a junior synonym of *Hypotetragona*. We therefore attribute all the present species to *Hypotetragona*, for which we can fully appreciate the morphological characters;
– We keep the genus name *Knoxiella* for the species that have already been attributed to this genus until they are thoroughly revised (Table 1).

Genus ***Hypotetragona*** Morey, 1935

Type species

Hypotetragona impolita Morey, 1935 by original designation.

Hypotetragona sp.
Fig. 6J–M

Indivisia minata – Song & Gong, 2019: fig. 4t.

Material examined

CHINA • 1 complete carapace (Ad, Fig. 6J); Blue Snake section, Tangbagou Formation, sample 19BAI 39; Tournaisian, early Carboniferous; P6M 3865 • 1 complete carapace (A-1, Fig. 6K); Blue Snake section, Tangbagou Formation, sample 19BAI 05; Tournaisian, early Carboniferous; P6M 3866 • 1 complete carapace (A-2, Fig. 6L); Blue Snake section, Gelaohe Formation, sample 19BAI 60; Famennian, late Devonian; P6M 3867 • 1 complete carapace (A-3, Fig. 6M); Blue Snake section, Gelaohe Formation, sample 19BAI 69; Famennian, late Devonian; P6M 3868 • 37 complete carapaces; Blue Snake section, Gelaohe and Tangbagou Formations, samples 19BAI 37, 19BAI 41, 19BAI 44, 19BAI 54, 19BAI 60, 19BAI 68, 19BAI 69; Famennian–Tournaisian, late Devonian–early Carboniferous.

Dimensions

RV: L = 302–846 µm, H = 198–519 µm, H/L = 0.57–0.7.
LV: L = 299–834 µm, H = 195–509 µm, H/L = 0.56–0.65.

Remarks

The adults of this species are represented by poorly preserved specimens that do not allow for a precise specific attribution. *Indivisia minata* Wei, 1988 in Song & Gong (2019) from the Famennian, late Devonian, of Blue Snake section, Guizhou, South China (Song & Gong 2019) differs from *Indivisia minata* which is stockier, has a more rounded outline, an ADB which is not truncated and a less compressed laterally posterior part in LV. *Indivisia minata* in Song & Gong (2019) furthermore does not belong to the genus *Indivisia* Zaspelova, 1954 as shown by the deep sulcus and prominent lobe in the antero–dorsal part of the carapace. It has the typical outline of the family Geisinidae and displays the diagnostic lobes and sulcus of the genus *Hypotetragona*. It is morphologically similar to *Hypotetragona* sp. and is considered as conspecific. The specimen shown in Song & Gong (2019) is a steinkern which would explain the absence of ornamentation which is visible in well–preserved juveniles in our material. The size and the H/L ratio of the specimens shown in Song & Gong (2019) are similar to our material. At least 4 ontogenetic stages are present in our material. The ontogenetic development of this species is marked by the outline becoming more rectangular, the sulcus becoming deeper and lobes more developed.

Occurrence

Gelaohe Formation, Blue Snake section, Guizhou, South China, Famennian, late Devonian, (Song & Gong 2019). Samples 19BAI 05, 19BAI 37, 19BAI 39, 19BAI 41, 19BAI 44, 19BAI 54, 19BAI 60, 19BAI 68, 19BAI 69, Gelaohe and Tangbagou Formations, Blue Snake section, Guizhou, South China, Famennian–Tournaisian, late Devonian–early Carboniferous (this work).

Genus ***Knoxina*** Coryell & Rogatz, 1932

Preliminary remark

Adamczak (2006) revised the family Geisinidae and considered that *Knoxina* Coryell & Rogatz, 1932 and *Chesterella* Croneis & Gutke, 1939 are synonyms, the latter being junior synonym of the former. Thus, both have typical Geisinidae outline, deep adductorial sulcus, prominent costa along ventral margin and one or two longitudinal costae. He also considered *Knoxina* as an "unclear [genus] to be investigated in details" (Adamczak 2006: 294–295). As this revision is out of the scope of the present contribution and material, we choose to keep the genus *Knoxina* in Geisinidae until its family position is thoroughly revised.

Type species

Knoxina lecta Coryell & Rogatz, 1932, by original designation.


A
B
C
D
E
F
G
H
I
J
K
L
M
N
O
P
Q
R
S
T
U

Fig. 6. SEM pictures of ostracods from Blue Snake section, Dushan County, South China, late Famennian–Tournaisian, late Devonian–early Carboniferous. All specimens are temporarily housed in the collections of Sorbonne Université, Paris, France (SU). **A**. *Kloedenellitina sincera* Tschigova, 1960, left lateral view of a carapace, sample 19BAI 69 (P6M 3856). **B–C**. *Kloedenellitina spinosa* Gurevitch, 1972. **B**. ♀, right lateral view of a carapace, sample 19BAI 60 (P6M 3857). **C**. ♂, right lateral view of a carapace, sample 19BAI 69 (P6M 3858). **D**. *Kloedenellitina sygmaeformis* Egorov, 1950, right lateral view of a carapace, sample 19BAI 80 (P6M 3859). **E**. *Blessites feluyensis* Tschigova, 1977, right lateral view of a carapace, sample 19BAI 39 (P6M 3860). **F–I**. *Hypotetragona angulata* (Posner, 1951). **F**. Adult, left lateral view of a carapace, sample 19BAI 44 (P6M 3861). **G**. A-1, left lateral view of a carapace, sample 19BAI 02 (P6M 3862). **H**. A-2, left lateral view of a carapace, sample 19BAI 02 (P6M 3863). **I**. A-3, left lateral view of a carapace, sample 19BAI 03 (P6M 3864). **J–M**. *Hypotetragona* sp. **J**. Adult, left lateral view of a carapace, sample 19BAI 39 (P6M 3865). **K**. A-1, left lateral view of a carapace, sample 19BAI 05 (P6M 3866). **L**. A-2, left lateral view of a carapace, sample 19BAI 60 (P6M 3867). **M**. A-3, left lateral view of a carapace, sample 19BAI 69 (P6M 3868). **N**. *Knoxiella archedensis* Tschigova, 1960, left lateral view of a carapace, sample 19BAI 03 (P6M 3869). **O**. *Knoxiella complanata* (Kummerow, 1939), left lateral view of a carapace, sample 19BAI 80 (P6M 3870). **P**. *Knoxiella subcompressa*, Wang & Ma, 2007, left lateral view of a carapace, sample 19BAI 68 (P6M 3871). **Q–R**. *Knoxiella* cf. *subcompressa*, Wang & Ma, 2007. **Q**. Adult, left lateral view of a carapace, sample 19BAI 68 (P6M 3871). **R**. A-1, left lateral view of a carapace, sample 19BAI 68 (P6M 3872). **S–T**. *Knoxina* sp. **S**. Left lateral view of a carapace, sample 19BAI 80 (P6M 3873). **T**. Left lateral view of a carapace, sample 19BAI 74 (P6M 3874). **U**. *Knoxites* cf. *argulata* Zaspelova, 1959, adult, left lateral view of a carapace, sample 19BAI 02 (P6M 3875). Scale bars = 100 µm.

Knoxina sp.
Fig. 6S–T

Knoxiella subreticulata Wang, 1983 – Song & Gong 2019: fig. 4o.

Material examined

CHINA • 1 complete carapace (Fig. 6S); Blue Snake section, Gelaohe Formation, sample 19BAI 74; P6M 3873 • 1 complete carapace (Fig. 6T); Blue Snake section, Gelaohe Formation, sample 19BAI 74; P6M 3874 • 7 complete carapaces; Blue Snake section, Gelaohe Formation, samples 19BAI 74, 19BAI 80. All from the Famennian, late Devonian.

Dimensions

RV: L = 536–585 µm, H = 309–343 µm, H/L = 0.57–0.6.
LV: L = 484–558 µm, H = 263–311 µm, H/L = 0.5–0.6.

Remarks

The present species is rare in the studied material and is represented by poorly preserved specimens that do not allow for a specific attribution. It is attributed to the genus *Knoxina* because it has a sulcus opened dorsally just anterior to mid-L, a node in antero-dorsal part of the carapace and longitudinal ridges, which are diagnostic of the genus. It is morphologically close to *Knoxina costata* (Zaspelova, 1959) from the Frasnian of the Russian Platform by its rectangular outline, presence and location of anterior, ventral and dorsal ridges and node located in front of sulcus. However, the specimens found here have a more rounded morphology, a strong overlap all around free margin and are smaller (based on the dimension of the figured holotype of *Knoxina costata* shown in Zaspelova (1959: pl. 8 fig. 9): L = 700 µm, H = 400 µm and H/L around 0.57). The presence of pit and ornamentation cannot be verified because of the poorly preservation of our material. The specimen attributed to *Knoxiella subreticulata* Wang, 1983 shown in

Song & Gong (2019: fig. 4o) does not belong to *Knoxiella* because it has ridges located dorsally and along ventral margin that point to the genus *Knoxina*. It is close to *Knoxina* sp. but the figured carapace is less stocky, has a slightly more concave VB and does not have a strong overlap as our material. The specimen shown in Song & Gong (2019) is a steinkern which would explain these differences so that we still consider it as conspecific.

Occurrence

Samples 19BAI 74, 19BAI 80, Gelaohe Formation, Blue Snake section, Famennian, late Devonian (this work).

Superfamily Paraparchitoidea Scott, 1959
Family Paraparchitidae Scott, 1959

Genus ***Shishaella*** Sohn, 1971

Type species

Paraparchites nicklesi var. *cyclopea* Girty, 1910 subsequently designated by Sohn (1971).

Shishaella hastierensis Crasquin-Soleau, 1988
Fig. 7E

Shishaella hastierensis Crasquin-Soleau, 1988: 312, pl 1 figs 1–4.

? *Paraparchites* sp. – Song & Gong 2019: fig. 4k.

Material examined

CHINA • 1 complete carapace (Fig. 7E); Blue Snake section, Tangbagou Formation, sample 19BAI 39; Tournaisian, early Carboniferous; P6M 3880 • 48 complete carapaces; Blue Snake section, Tangbagou Formation, samples 19BAI 01, 19BAI 02, 19BAI 08, 19BAI 16, 19BAI 23, 19BAI 27-2, 19BAI 37, 19BAI 39, 19BAI 43, 19BAI 44, 19BAI 55, 19BAI 58; latest Famennian–Tournaisian, late Devonian–early Carboniferous.

Dimensions

RV: L = 380–1176 µm, H = 271–886 µm, H/L = 0.71–0.79.
LV: L = 380–1193 µm, H = 276–918 µm, H/L = 0.68–0.77.

Remarks

Paraparchites sp. in Song & Gong (2019) from the Famennian, late Devonian, of Blue Snake section, Guizhou, South China (Song & Gong 2019) does not belong to the genus *Paraparchites* Ulrich & Bassler 1906 as indicated by the postero-dorsal spine on the illustrated right valve. The specimen shown in Song & Gong (2019) is only questionably attributed to *Shishaella hastierenesis* Crasquin-Soleau, 1988 because the occurrence of a postero-dorsal spine at left valve, which would point to the genus *Shivaella* Sohn, 1971, cannot be verified.

Occurrence

Hastière Formation, Quarry "de l'ancien four à chaux", northwest of Landelies, Massif de la Tombe, Namur Synclinorium, Belgium, Tournaisian, early Carboniferous (Crasquin-Soleau 1988). Gelaohe and Tangbagou Formations, Blue Snake section, Guizhou, South China, Famennian–Tournaisian, late Devonian–early Carboniferous (Song & Gong 2019). Samples 19BAI 01, 19BAI 02, 19BAI 08, 19BAI

16, 19BAI 23, 19BAI 27-2, 19BAI 37, 19BAI 39, 19BAI 43, 19BAI 44, 19BAI 55, 19BAI 58, Tangbagou Formation, Blue Snake section, latest Famennian–Tournaisian, late Devonian–early Carboniferous (this work).

Superfamily Sansabelloidea Sohn 1961
Family Sansabellidae Sohn, 1961

Genus ***Sansabella*** Roundy, 1926

Type species

Sansabella amplectans Roundy, 1926 by original designation.

Remarks

The genus *Reversabella* Coryell & Johnson, 1939 (type species: *Reversabella njorthi* Coryell & Johnson, 1939) was originally erected "to receive form which have reversed overlap" (Coryell & Johnson 1939: 221) compared to *Sansabella* Roundy, 1936. Later, reversed overlap appears to be common in the genus *Sansabella* (Moore 1961; Sohn 1988: 187) and *Reversabella* has subsequently been considered as a junior synonym of *Sansabella* (Sohn 1988).

Sansabella gelaohensis Guillam & Forel sp. nov.
urn:lsid:zoobank.org:act:7626056B-A0B0-41BE-AC1D-308F2A935888
Fig. 7G–N

Sansabella sp. Coen, 1989: pl. 2 fig. 11.

Diagnosis

Smooth *Sansabella* species with a convex free margin, strong ventral overlap, a postero-ventral spine at LV, hinge line straight, occupying entire dorsal margin.

Etymology

The specific epithet refers to the Gelaohe Formation in which all the specimens were found.

Material examined

Holotype

CHINA • 1 complete carapace (Fig. 7G); Blue Snake section, Gelaohe Formation, sample 19BAI 74; Famennian, late Devonian; P6M 3882.

Paratypes

CHINA • 1 complete carapace (Fig. 7H); Blue Snake section, Gelaohe Formation, sample 19BAI 74; P6M 3883 • 1 complete carapace (Fig. 7I); Blue Snake section, Gelaohe Formation, sample 19BAI 74; P6M 3884. All from the Famennian, late Devonian.

Other material

CHINA • 1 complete carapace (A-1, Fig. 7J); Blue Snake section, Gelaohe Formation, sample 19BAI 74; P6M 3884 • 1 complete carapace (A-2, Fig. 7K); Blue Snake section, Gelaohe Formation, sample 19BAI 74; P6M 3885 • 1 complete carapace (A-3, Fig. 7L); Blue Snake section, Gelaohe Formation, sample 19BAI 74; P6M 3886 • 1 complete carapace (A-4, Fig. 7M); Blue Snake section, Gelaohe Formation, sample 19BAI 63; P6M 3887 • 1 complete carapace (A-5, Fig. 7N); Blue Snake section, Gelaohe Formation, sample 19BAI 63; P6M 3888 • 98 carapaces; Blue Snake section, Gelaohe Formation, samples 19BAI 60, 19BAI 63, 19BAI 67–69, 19BAI 74. All from the Famennian, late Devonian.

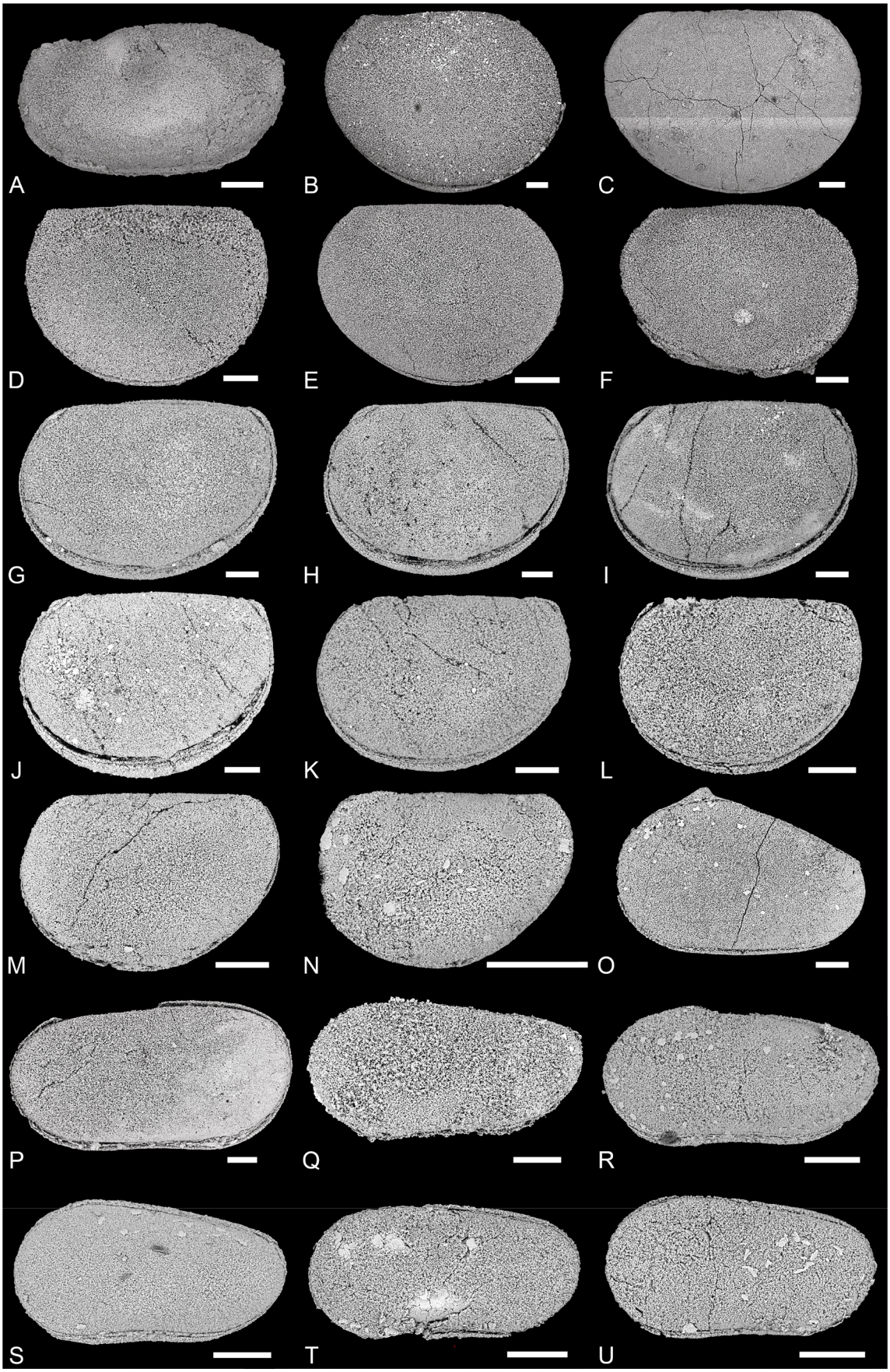
A
B
C
D
E
F
G
H
I
J
K
L
M
N
O
P
Q
R
S
T
U

Fig. 7. SEM pictures of ostracods from Blue Snake section, Dushan County, South China, late Famennian–Tournaisian, late Devonian–early Carboniferous. All specimens are temporarily housed in the collections of Sorbonne Université, Paris, France (SU). **A**. *Knoxites* cf. *argulata* Zaspelova, 1959, left lateral view of a carapace, sample 19BAI 02 (P6M 3876). **B**. *Paraparchites longmenshanensis* Wei, 1983, right lateral view of a carapace, sample 19BAI 43 (P6M 3877). **C**. *Paraparchites* sp. 1, right lateral view of a carapace, sample 19BAI 39 (P6M 3878). **D**. *Paraparchites* sp. 2, right lateral view of a carapace, sample 19BAI 67 (P6M 3879). **E**. *Shishaella hastierensis* Crasquin-Soleau, 1988, right lateral view of a carapace, sample 19BAI 39 (P6M 3880). **F**. *Shishaella porrecta* (Zanina, 1956), left lateral view of a carapace, sample 19BAI 55 (P6M 3881). **G–N**. *Sansabella gelaohensis* Guillam & Forel sp. nov. **G**. Holotype, left lateral view of a carapace, sample 19BAI 74 (P6M 3882). **H**. Paratype 1, left lateral view of a carapace, sample 19BAI 74 (P6M 3883). **I**. Paratype 2, left lateral view of a carapace, sample 19BAI 74 (P6M 3884). **J**. A-1, left lateral view of a carapace, sample 19BAI 74 (P6M 3884). **K**. A-2, left lateral view of a carapace, sample 19BAI 74 (P6M 3885). **L**. A-3, left lateral view of a carapace, sample 19BAI 74 (P6M 3886). **M**. A-4, left lateral view of a carapace, sample 19BAI 63 (P6M 3887). **N**. A-5, left lateral view of a carapace, sample 19BAI 63 (P6M 3888). **O**. *Cavellina* cf. *dushanensis* Shi, 1964, left lateral view of a carapace, sample 19BAI 63 (P6M 3889). **P**. *Cavellina* cf. *recta* (Jones, Kirby & Brady, 1884), left lateral view of a carapace, sample 19BAI 67 (P6M 3890). **Q–U**. *Sulcella baisuzhena* Guillam & Forel sp. nov. **Q**. Holotype, left lateral view of a carapace, sample 19BAI 74 (P6M 3991). **R**. Paratype 1, A-1, left lateral view of a carapace, sample 19BAI 68 (P6M 3992). **S**. A-1, left lateral view of a carapace, sample 19BAI 68 (P6M 3893). **T**. A-2, left lateral view of a carapace, sample 19BAI 68 (P6M 3894). **U**. A-3, left lateral view of a carapace, sample 19BAI 68 (P6M 3895). Scale bars = 100 µm.

Dimensions

See Fig. 4B.

Description

Carapace large, subcircular in lateral view, slightly preplete, with Lmax above mid-H. RV larger than LV, overlapping it all around with maximum along VB and interruption at DB directly posterior to ACA. Hinge line straight, invaginated, occupying entire dorsal margin and equivalent to about 70% of the Lmax. Dorsal margin straight. Cardinal angles blunt, ACA about 135°, PCA about 130°. Ventral margin largely convex at both valves. Left valve with a short latero-ventral spine, slightly posterior to mid-L. AB largely convex with maximum of convexity around mid-H. PB from narrowly rounded in juveniles to close to vertical in adults, with maximum of convexity around the upper ⅓rd of H. Shallow sulcus opened dorsally sometimes visible, located in front of mid-L, never extending below mid-H. Node sometimes visible, located in the antero-dorsal part of carapace, just in front of the sulcus. Juveniles morphologically similar to adults except for the size, morphology of PB and less developed ventral spine. Carapace smooth.

Remarks

This species, identified as *Sansabella* sp., was only briefly described by Coen (1989) from a sample from the Famennian, late Devonian, Gelaohe Formation of Baihupo section, Dushan County. *Sansabella gelaohensis* sp. nov. differs from the majority of species belonging to *Sansabella* Roundy, 1926 by its subcircular lateral outline. More precisely, it differs from *Sansabella amplectans* Roundy, 1926 from the Mississippian of Texas (Roundy 1926) in which the larger valve is the left one and has a parallelogram lateral outline. *Sansabella gelaohensis* sp. nov. also differs from *Sansabella polonica* Błaszyk & Natusiewicz, 1973 from the Tournaisian of Poland (Błaszyk & Natusiewicz 1973) which has a longer trapezoidal carapace, a reticulate surface with a more distinct sulcus at both valves which begins in the medial part of the DB. *Sansabella sinuoventralis* Lethiers, 1981 from the Famennian of

Western Canada (Lethiers 1981) has a more convex VB. *Sansabella*? *curiosa* Stewart & Hendrix, 1945 from the Upper Devonian of Ohio (Stewart & Hendrix 1945) has LV larger than RV, H practically uniform throughout its L, a less convex VB, a granulate or reticulate ornamentation. The H/L scatter plot (Fig. 4B) does not allow to discriminate different ontogenetic stages but the wide distribution of the dimensions of the specimens clearly indicates that several stages are present in the assemblages studied.

Occurrence

Gelaohe Formation, Baihupo section, Dushan, Guizhou, South China, Famennian, late Devonian (Coen 1989). Samples 19BAI 60, 19BAI 63, 19BAI 67-69, 19BAI 74, Gelaohe Formation, Blue Snake section, Famennian, late Devonian (this work).

Order Platycopida Sars, 1866
Suborder Platycopina Sars, 1866
Superfamily Cavellinoidea Egorov, 1950
Family Cavellinidae Egorov, 1950

Genus ***Sulcella*** Coryell & Rogatz, 1932

Type species

Sulcella sulcata Coryell & Rogatz, 1932 by original designation.

Sulcella baisuzhena Guillam & Forel sp. nov.
urn:lsid:zoobank.org:act:5E0110EC-49F8-4F34-BC57-C46B3232DAAA
Figs 7Q–U, 8A–B

Diagnosis

A species belonging to the genus *Sulcella* with elongate outline, VB concave, very long and slightly arched DB. Stragulum absent.

Etymology

The specific epithet refers to the latinization of the Chinese *Bai Suzhen* (also known as Baishe Niangniang which means White Snake Empress), which is a snake spirit in the Chinese "Legend of the white snake".

Material examined

Holotype

CHINA • 1 complete carapace (Fig. 7Q); Blue Snake section, Gelaohe Formation, sample 19BAI 74; Famennian, late Devonian; P6M 3991.

Paratype

CHINA • 1 complete carapace (A–1, Fig. 7R); Blue Snake section, Gelaohe Formation, sample 19BAI 68; Famennian, late Devonian; P6M 3892.

Other material

CHINA • 1 complete carapace (A-1, Fig. 7S); Blue Snake section, Gelaohe Formation, sample 19BAI 68; P6M 3993 • 1 complete carapace (A-2, Fig. 7T); Blue Snake section, Gelaohe Formation, sample 19BAI 68; P6M 3894 • 1 complete carapace (A-3, Fig. 7U); Blue Snake section, Gelaohe Formation, sample 19BAI 68; P6M 8395 • 1 complete carapace (A-4, Fig. 8A); Blue Snake section, Gelaohe Formation, sample 19BAI 68; P6M 3996 • 1 complete carapace (A-5, Fig. 8B); Blue Snake section, Gelaohe Formation, sample 19BAI 68; P6M 3897 • 15 complete carapaces; Blue Snake section, Gelaohe Formation, samples 19BAI 67, 19BAI 68. All from the Famennian, late Devonian.

Dimensions

See Fig. 4C.

Description

Carapace of medium size, elongate with Hmax around to slightly anterior to the ⅓rd of Lmax, at the junction between DB and ADB; Lmax at mid-H. RV larger than LV, overlapping it all around, sometimes absent or reduced at PVB and AB, stronger along dorsal margin and VB. Dorsal margin with a very long and straight to slightly arched DB, short PDB and uniformly convex ADB. VB concave; AB largely rounded with maximum around mid–H at both valves; PB weakly rounded, PVB slightly truncated. ACA about 155°, PCA close to 90°. Stragulum absent. Surface smooth.

Remarks

The present species is morphologically close to *Sulcella kotchoensis* Lethiers, 1981 from the Famennian of the Kotcho Formation, Imperial Island River 1, Western Canada (Lethiers 1981) but it has a less stocky morphology, a less convex PVB, a more concave VB and Lmax located higher. *Sulcella kotchoensis* Lethiers, 1981 is also larger, with L ranging from 580 to 860 µm and H from 300 to 420 µm. The H/L scatter plot of *Sulcella baisuzhena* sp. nov. (Fig. 4C) allows to discriminate six ontogenetic stages (A-5 to Ad). The ontogenetic development of this species is marked by the elongation of outline and the VB becoming more concave.

Occurrence

Samples 19BAI 63, 19BAI 67, 19BAI 68, 19BAI 74, Gelaohe Formation, Blue Snake section, Famennian, late Devonian (this work).

Order Podocopida Sars, 1866
Suborder Podocopina Sars, 1866
Superfamily Bairdiocypridoidea Shaver, 1961
Family Bairdiocyprididae Shaver, 1961

Genus ***Cytherellina*** Jones & Holl, 1869

Type species

Beyrichia siliqua Jones, 1855 subsequently designated by Jones & Holl (1869)

Cytherellina caerulea Guillam & Forel sp. nov.
urn:lsid:zoobank.org:act:094CDF1E-56D9-4459-8A8C-367F44755F7B
Fig. 8H–L

Cavellina sp. Coen, 1989: 312, pl. 2 fig. 10.

Cavellina prona Wei, 1988 – Song & Gong 2019: fig. 4s.
Cytherellina subclara Wang, 1983 – Song & Gong 2019: fig. 5o.

non *Cavellina prona* Wei, 1988: 304, pl. 112, fig. 14-15.
non *Cytherellina subclara* Wang, 1983: 190, pl. 5, fig. 20-24.

Diagnosis

A new species of *Cytherellina* with carapace compressed along AB and PB, more or less pointed anterior end, RV with bipartite DB and a strong angulation, ADB straight and more inclined than PDB.

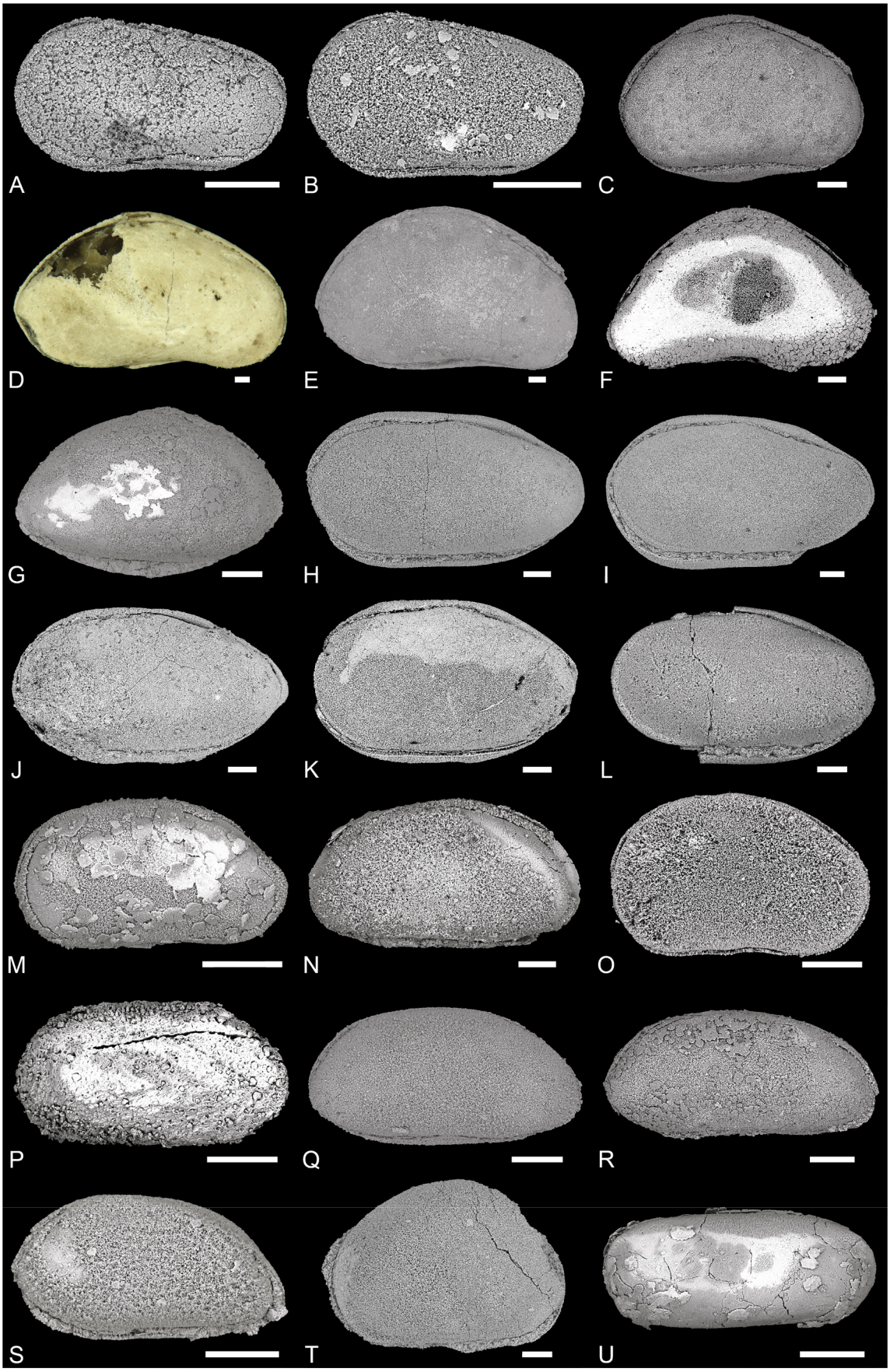
A
B
C
D
E
F
G
H
I
J
K
L
M
N
O
P
Q
R
S
T
U

Fig. 8. SEM pictures and focus stacking method pictures (with an *) of ostracods from Blue Snake section, Dushan County, South China, late Famennian–Tournaisian, late Devonian–early Carboniferous. All specimens are temporarily housed in the collections of Sorbonne Université, Paris, France (SU). **A–B**. *Sulcella baisuzhena* Guillam & Forel sp. nov. **A**. A-4, left lateral view of a carapace, sample 19BAI 68 (P6M 3996). **B**. A-5, left lateral view of a carapace, sample 19BAI 68 (P6M 3897). **C**. *Bairdiocypris elliptica* Wei, 1983, right lateral view of a carapace, sample 19BAI 08 (P6M 3898). **D–E**. *Bairdiocypris fomikhaensis* Buschmina, 1968. **D**. Left lateral view of a carapace*, sample 19BAI 41 (P6M 3899). **E**. Left lateral view of a carapace, sample 19BAI 44 (P6M 3900). **F**. *Bairdiocypris marginifera* (Geis, 1932) sensu Buschmina, 1968, left lateral view of a carapace, sample 19BAI 67 (P6M 3901). **G**. *Bairdiocypris* sp., left lateral view of a carapace, sample 19BAI 01 (P6M 3902). **H–L**. *Cytherellina caerulea* Guillam & Forel sp. nov. **H**. Holotype, right lateral view of a carapace, sample 19BAI 68 (P6M 3903). **I**. Paratype 1, right lateral view of a carapace, sample 19BAI 68 (P6M 3904). **J**. Paratype 2, right lateral view of a carapace, sample 19BAI 63 (P6M 3905). **K**. Right lateral view of a carapace, sample 19BAI 63 (P6M 3906). **L**. Right lateral view of a carapace, sample 19BAI 69 (P6M 3907). **M**. *Healdianella alba* Lethiers, 1981, right lateral view of a carapace, sample 19BAI 60 (P6M 3908). **N**. *Healdianella faseolina* Rozhdestvenskaya in Song & Gong, 2019, right lateral view of a carapace, sample 19BAI 43 (P6M 3909). **O**. *Healdianella lumbiformis* Lethiers & Feist, 1991, right lateral view of a carapace, sample 19BAI 58 (P6M 3910). **P**. *Healdianella* cf. *insolita* (Buschmina, 1977), right lateral view of a carapace, sample 19BAI 55 (P6M 3911). **Q–R**. *Healdianella* cf. *subdistincta* Wang, 1983. **Q**. right lateral view of a carapace, sample 19BAI 02 (P6M 3912). **R**. right lateral view of a carapace, sample 19BAI 03 (P6M 3913). **S**. *Healdianella* sp., right lateral view of a carapace, sample 19BAI 60 (P6M 3914). **T**. *Praepilatina adamczaki* Olempska, 1979, left lateral view of a carapace, sample 19BAI 68 (P6M 3915). **U**. *Elliptocyprites lorangeri* Lethiers, 1981, right lateral view of a carapace, sample 19BAI 60 (P6M 3916). Scale bars = 100 µm.

Etymology

By apposition, in reference to the blue colour (Latin: *caeruleus*) of the snake found during the fieldwork which gave its name to the studied section.

Material examined

Holotype

CHINA • 1 complete carapace (Fig. 8H); Blue Snake section, Gelaohe Formation, sample 19BAI 68; Famennian, late Devonian; P6M 3903.

Paratypes

CHINA • 1 complete carapace (Fig. 8I); Blue Snake section, Gelaohe Formation, sample 19BAI 68; P6M 3904 • 1 complete carapace (Fig. 8J); Blue Snake section, Gelaohe Formation, sample 63; P6M 3905 • 1 complete carapace (Song & Gong 2019: fig. 5o); Blue Snake section, Gelaohe Formation, bed 17 (Song & Gong 2019: fig. 3); GBL2014007 (palaeontological collections of the Museum of the China University of Geosciences, Wuhan, China). All from the Famennian, late Devonian.

Other material

CHINA • 1 complete carapace (Fig. 8K); Blue Snake section, Gelaohe Formation, sample 19BAI 63; P6M 3907 • 1 complete carapace (Fig. 8L); Blue Snake section, Gelaohe Formation, sample 19BAI 69; P6M 3907 • 7 complete carapaces; Blue Snake section, Gelaohe Formation, samples 19BAI 60, 19BAI 63, 19BAI 68, 19BAI 69. All from the Famennian, late Devonian.

Dimensions

See Fig. 4D.

Description

Carapace large, subreniform and elongate. Hmax around to slightly posterior to mid-L; Lmax slightly below mid-H; dorsal margin arched on both valves. LV larger than RV, overlapping it all around, sometimes absent or reduced at PVB, stronger along dorsal margin and VB. DB tripartite on LV, bipartite and with a strong obtuse angle at mid-L on RV. VB very gently convex at LV, with a tenuous oral concavity around mid-L at RV. RV with very straight ADB which is longer and more inclined than PDB. The anterior extremity is more or less rounded, particularly on LV. Maximum curvature slightly under mid-H at AB and about mid–H at PB. Wmax in the posterior part of the carapace, slightly after mid-L. Laterally compressed anterior and posterior margins. Carapace smooth.

Remarks

This species was only briefly described, identified as *Cavellina* sp., from an assemblage from the latest Famennian Gelaohe Formation, Baihupo section, Dushan County (Coen 1989). The specimen shown in Coen (1989: pl. 2 fig. 10) is smaller than our material with L = 850 µm, H = 533 but H/L = 0.62 while it is between 0.5 and 0.6 in our material. It has a more rounded outline and could be a juvenile of *Cytherellina caerulea* sp. nov. *Cavellina prona* Wei, 1988 shown in Song & Gong (2019: fig. 4s) is removed from *Cavellina prona*, which has a less elongated outline and an overlap less developed along free margin, and absent at PDB. The specimen shown in Song & Gong (2019) is slightly tilted anteriorly and the posterior extremity is broken. This specimen is considered as *Cytherellina caerulea* sp. nov. because it is morphologically very close to our materiel which has a rounded extremity at RV and its size is consistent with our material with L = 916 µm, H = 596 µm, while H/L is greater with 0.65.

Cytherellina subclara Wang, 1983 in Song & Gong 2019 is morphologically similar and its size is consistent with our material with L = 1157 µm, H = 673 µm, H/L = 0.58. Although, this species was originally described from the Ertang Formation, early Devonian of Guangxi (Wang 1983b). Raup (1978) showed that the mean species duration among invertebrates is about 11 Ma. For the ostracod genus *Puriana* Coryell & Fields 1953, common in Cenozoic shallow marine fossil assemblages from the Americas and many Caribbean islands, the mean species duration of most species is between 5 and 8 Ma (Cronin 1987). Consequently, it is unlikely to find *Cytherellina subclara* in the late Famennian because the duration of this species would then be at least 30 Ma. The taxa duration of ostracod species is out of the scope of this paper: the reader is refered to Forel *et al.* (2021) for further discussion. It is here considered as *Cytherellina caerulea* sp. nov.

The new species differs from *Cytherellina obusa* Lethiers, 1976 in Casier (1989) from the Frasnian of Belgium by its smaller size (holotype: L = 1.19 mm, H = 0.80 mm, W = 0.40 mm), the absence of overlap at PVB and PDB, its more arched DB with a stronger angle at mid-L and its pointed posterior end. *Cytherellina caerulea* sp. nov. is also different from *Cytherellina* sp. 3 in Olempska & Chauffe 1999 from the Famennian of Iowa (Olempska & Chauffe 1999) by its smaller size (figured specimen in Olempska & Chauffe 1999: L = 960 µm, H = 480 µm), its straighter PDB, its stockier morphology and the overlap which is really weak in *Cytherellina* sp. 3 in Olempska & Chauffe 1999. It is morphologically close to *Sulcella* cf. *altifrons* Jones, 1968 in Lethiers (1981) from the Upper Frasnian-Lower Famennian of Western Canada (Lethiers 1981) but this species has a shorter and less convex AVB, a shorter ADB, a more rounded anterior extremity and the overlap stronger at AVB and along dorsal margin. The H/L scatter plot of all *Cytherellina caerulea* sp. nov. specimens from this work (Fig. 4D) documents a relatively narrow dispersion of the specimens as regard to their size, with the impossibility to discriminate ontogenetic stages.

Occurrence

Gelaohe Formation, Baihupo section, Dushan, Guizhou, South China, Famennian, late Devonian (Coen 1989). Gelaohe and Tangbagou Formations, Blue Snake section, Guizhou, South China, Famennian–Tournaisian, late Devonian–early Carboniferous (Song & Gong 2019). Samples 19BAI 60, 19BAI 63, 19BAI 68, 19BAI 69, Gelaohe Formation, Blue Snake section, Famennian, late Devonian (this work).

Genus ***Healdianella*** Posner, 1951

Type species

Healdianella darwinuloides Posner, 1951 by original designation.

Healdianella cf. ***subdistincta*** Wang, 1983
Fig. 8Q–R

Material examined

CHINA • 1 complete carapace (Fig. 8Q); Blue Snake section, Tangbagou Formation, sample 19BAI 02; P6M 3912 • 1 complete carapace (Fig. 8R); Blue Snake section, Tangbagou Formation, sample 19BAI 02; P6M 3913 • 8 complete carapaces; Blue Snake section, Tangbagou Formation, samples 19BAI 03, 19BAI 08, 19BAI 23. All from the Tournaisian, early Carboniferous.

Dimensions

RV: L = 359–697 µm, H = 189–300 µm, H/L = 0.42–0.52.
LV: L = 359–688 µm, H = 200–291 µm, H/L = 0.42–0.56.

Remarks

This species is rare in the studied material. The specimens are morphologically close to *Healdianella subdistincta* Wang, 1983 from the Emsian, early Devonian of Guangxi, South China (Wang 1983a) but they have a more elongated morphology, a straight DB with Hmax developed all along DB and a straight PDB with distinct AD angulation. *Healdianella subdistincta* is larger, with L ranging from 1440 to 1760 µm, H from 880 to 1000 µm and H/L between 0.57 and 0.61, while it is between 0.47 and 0.56 here. Our material has a small size and may correspond to juveniles so that we only compare them to *Healdianella subdistincta* until more material is found to clarify this issue.

Occurrence

Samples 19BAI 02, 19BAI 03, 19BAI 08, 19BAI 23, Tangbagou Formation, Blue Snake section, Tournaisian, early Carboniferous (this work).

Superfamily Bairdioidea Sars, 1888
Family Bairdiidae Sars, 1888

Genus ***Bairdia*** McCoy, 1844

Preliminary remark

Sohn (1960) erected 2 genera from the study of specimens previously attributed to *Bairdia* McCoy, 1844: *Cryptobairdia* Sohn, 1960 and *Rectobairdia* Sohn, 1960. The first differs from *Bairdia* by the "dorso–anterior margin being not distinct" (Sohn 1960: 47) and the second by "a straight to very gently curved dorsal margin" (Sohn 1960: 52). However, Becker (1965) demonstrated that the morphology of the dorsal outline is "rather variable (even partly superficial) and, therefore only useful to described subgenera"

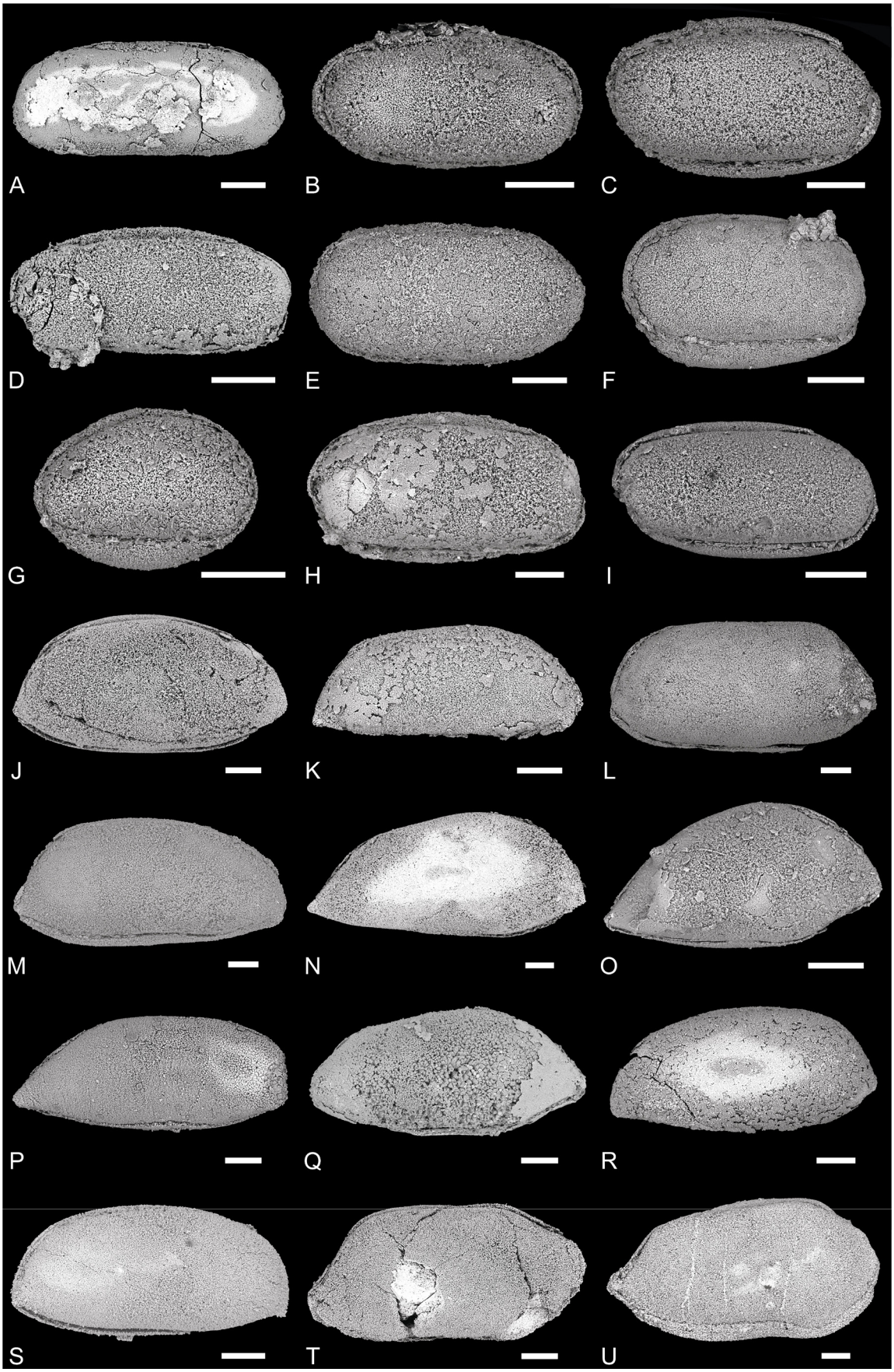
A
B
C
D
E
F
G
H
I
J
K
L
M
N
O
P
Q
R
S
T
U

Fig. 9. SEM pictures of ostracods from Blue Snake section, Dushan County, South China, late Famennian–Tournaisian, late Devonian–early Carboniferous. All specimens are temporarily housed in the collections of Sorbonne Université, Paris, France (SU). **A**. *Elliptocyprites* sp., right lateral view of a carapace, sample 19BAI 63 (P6M 3917). **B**. *Microcheilinella infradominica* Rozhdestvenskaya in Song & Gong, 2019, right lateral view of a carapace, sample 19BAI 02 (P6M 3918a). **C**. *Microcheilinella larionovae* Polenova, 1955, right lateral view of a carapace, sample 19BAI 01 (P6M 3918b). **D**. *Microcheilinella.* sp. A, aff. *buschminae* in Casier *et al.*, 2004, right lateral view of a carapace, sample 19BAI 27-2 (P6M 3919). **E**. *Microcheilinella* sp. cf. *M. buschminae* Olempska, 1981 in Song & Gong, 2019, right lateral view of a carapace, sample 19BAI 03 (P6M 3920). **F**. *Microcheilinella* sp. sensu Olempska, 1979, right lateral view of a carapace, sample 19BAI 03 (P6M 3921). **G**. *Microcheilinella subrhomboidalis* Xie, 1983, right lateral view of a carapace, sample 19BAI 03 (P6M 3922). **H**. *Microcheilinella* cf. *decora* Shi, 1964, right lateral view of a carapace, sample 19BAI 03 (P6M 3923). **I**. *Microcheilinella* sp., right lateral view of a carapace, sample 19BAI 41 (P6M 3924). **J**. *Acratia acutiangulata* (Posner in Tschigova, 1960), right lateral view of a carapace, sample 19BAI 58 (P6M 3925). **K**. *Acratia similaris* Green, 1963, right lateral view of a carapace, sample 19BAI 03 (P6M 3926). **L**. *Acratia subobtusa* Lethiers, 1974, right lateral view of a carapace, sample 19BAI 03 (P6M 3927). **M**. *Acratia* cf. *disjuncta* Morey, 1935, right lateral view of a carapace, sample 19BAI 01 (P6M 3928). **N–O**. *Acratia cf. evlanensis* Egorov, 1953. **N**. Adult, right lateral view of a carapace, sample 19BAI 67 (P6M 3929). **O**. Juveniles, right lateral view of a carapace, sample 19BAI 41 (P6M 3930). **P**. *Acratia* cf. *insolita* Buschmina, 1970, right lateral view of a carapace, sample 19BAI 41 (P6M 3931). **Q**. *Acratia* cf. *tschudovoensis* Zaspelova, 1959, right lateral view of a carapace, sample 19BAI 68 (P6M 3932). **R**. *Acratia* sp., right lateral view of a carapace, sample 19BAI 05 (P6M 3933). **S**. *Acutiangulata acutiangulata* (Tschigova, 1959), right lateral view of a carapace, sample 19BAI 01 (P6M 3934). **T**. *Bairdia cestriensis* Ulrich, 1891, right lateral view of a carapace, sample 19BAI 68 (P6M 3935). **U**. *Bairdia confragosa* Samoilova & Smirnova, 1960, right lateral view of a carapace, sample 19BAI 01 (P6M 3936). Scale bars = 100 µm.

(Becker 2001: 288). We consider that these differences are not sufficient to consider them as valid genera and we choose to follow Becker (1965) and use *Cryptobairdia* and *Rectobairdia* as subgenera.

Type species

Bairdia curta McCoy, 1844 subsequently designated by Ulrich & Bassler (1923).

Bairdia nanbiancunensis Wang, 1988
Fig. 10D–E

Bairdia nanbiancunensis Wang, 1988b: 239, pl. 60 figs 9–12.

Bairdia nanbiancunensis – Olempska 1999: 428, fig. 29h. — Jones: unpublished data, fide Olempska 1999.

Bairdia sp. – Coen 1989: 317, pl. 2 figs 2–3.

non *Bairdia beichuanensis* Wei, 1983 – Song & Gong 2019: Song & Gong 2019: fig. 5a.

Material examined

CHINA • 1 complete carapace (Fig. 10D); Blue Snake section, Gelaohe Formation, sample 19BAI 69; P6M 3940 • 1 complete carapace (Fig. 10E); Blue Snake section, Gelaohe Formation, sample 19BAI 68; P6M 3941 • 4 complete carapaces; Blue Snake section, Gelaohe Formation, samples 19BAI 67, 19BAI 69, 19BAI 80. All from the Famennian, late Devonian.

Dimensions

RV: L = 941–2112 µm, H = 516–1050 µm, H/L = 0.48–0.56.
LV: L = 941–2136 µm, H = 536–1332 µm, H/L = 0.57–0.65.

Remarks

This species is rare in the studied material. *Bairdia beichuanensis* Wei, 1983 in Song & Gong (2019) from the Famennian and the Tournaisian of the Baihupo section, Guizhou, South China (Song & Gong 2019) does not belong to *Bairdia beichuanensis* as shown by the strong ventral and dorsal overlap and stocky morphology. Based on these characters, it is here reattributed to *Bairdia nanbiancunensis* Wang, 1988. Coen (1989) reported *Bairdia* sp. from the Gelaohe Formation, Baihupo section, Guizhou, South China, Famennian. Following Olempska (1999), we consider that it belongs to *Bairdia nanbiancunensis*. The specimens shown in Coen (1989: pl. 2 gigs 2b, 3b) and in Song & Gong (2019: fig. 5a) have a size similar to our material with respectively L = 1000–1100 µm, H = 650–675 µm, H/L = 0.59–0.67 and L = 1120 µm, H = 706 µm, H/L = 0.63. The specimen shown in Olempska (1999: fig. 29h) is as long as our biggest specimen and higher (L = 2310 µm, H = 1540 µm, H/L = 0.67) but we consider that these differences are intraspecific variability. Three ontogenetic stages (A-2 to Ad) are present in our material; they only differ by the size without major changes throught ontogeny.

Occurrence

Nanbiancun, Guilin, South China, middle Tournaisian, (Wang 1988b). Gelaohe Formation, Baihupo section, Guizhou, South China, Famennian, late Devonian (Coen 1989). Muhua Formation, Guizhou, South China, early Carboniferous (Olempska 1999). Laurel Formation, Canning Basin, Western Australia, Tournaisian, early Carboniferous (Jones, unpublished data, fide Olempska 1999). Gelaohe and Tangbagou Formation, Blue Snake section, Guizhou, South China, Famennian–Tournaisian, late Devonian–early Carboniferous (Song & Gong 2019). Samples 19BAI 67, 19BAI 69, 19BAI 80, Blue Snake section, Gelaohe Formation, Famennian, late Devonian (this work).

Genus ***Bairdianella*** Harlton, 1929

Type species

Bairdianella elegans Harlton, 1929 by original designation.

Bairdianella cuspis Buschmina, 1970
Fig. 11P

Bairdianella cuspis Buschmina, 1970: 73, pl. V fig. 2.

Bairdianella cuspis – Kotschetkova & Janbulatova 1987: pl. 24 fig. 1. — Zhuravlev & Sobolev 2019: figs 4i–j. – Sobolev 2020: figs 5–10.

Material examined

CHINA • 1 complete carapace (Fig. 11P); Blue Snake section, Tangbagou Formation, sample 19BAI 03; P6M 3973 • 25 complete carapaces; Blue Snake section, Tangbagou Formation, samples 19BAI 01-03, 19BAI 05, 19BAI 37, 19BAI 39, 19BAI 44. All from the Tournaisian, early Carboniferous.

Dimensions

RV: L = 460–575 µm, H = 188–247 µm, H/L = 0.37–0.45.
LV: L = 460–587 µm, H = 201–255 µm, H/L = 0.38–0.48.

Remarks

Our material is smaller than the holotype shown in Buschmina (1970: pl: 5 fig. 2) with L = 625 µm, H = 325 µm, H/L = 0.52. Specimens shown in Kotschetkova & Janbulatova (1987: pl. 24 fig. 1) from Mugodzhary, Western Kazakhstan and Sobolev (2020: figs 5, 9–10)) from Pechora Uplift, Russia, have a similar size to our material with respectively L = 532 µm, H = 250 µm and H/L = 0.47 and L = 580 µm, H = 280 µm, H/L = 0.48. However, the specimen shown in Zhuravlev & Sobolev (2019) from North Ural is slightly larger than the present material with L = 580 µm, H = 275 µm and H/L = 0.47 but still smaller than the holotype in Buschmina (1970). The size variations in our material indicate that at least two stages are present and may correspond to juveniles, compare to the holotype in Buschmina (1970), but the wide distribution of the dimensions of the specimens does not allow to clearly discriminate them.

Five species have been mentioned as *Bairdianella* aff. *cuspis* in papers discussing Devonian–Carboniferous ostracod faunas, they are summarized in Table 3.
Based on specimens shown in these different contributions, the main differences between these species and *Bairdianella cuspis* Buschmina, 1970 seem to be weak variations of the length of the carapace, concavity at VB, degree of postero-dorsal angulation, posterior end more or less rounded and AVB sometimes truncated (visible only on *Bairdianella* sp. A, aff. *cuspis* Buschmina, 1970 in Casier *et al.* 2004). Specimens of *Bairdianella* aff. *cuspis* Buschmina, 1970 sensu Kotschetkova & Janbulatova 1987 in Casier *et al.* (2002), *Bairdianella* sp. A, aff. *cuspis* Buschmina, 1970 in Casier & Préat (2003) and *Bairdianella* sp. B, aff. *cuspis* Buschmina, 1970 in Casier *et al.* (2004) are also larger than the holotype but others had sizes similar to our material so may also correspond to juveniles. These differences do not seem sufficient to reasonably distinguish these forms from the species described by Buschmina (1970). However, only one specimen is shown in each of these papers with no discussion on possible other specimens, ontogenetic and intraspecific variations within the material or comparisons between these different species. Only a complete review of these taxa, based on close observations of all these specimens, can clarify this major issue. For this reason, they are kept as distinct species.

Occurrence

Gengis horizon, Yeltsov synclinorium, South of Occidental Siberia, early Carboniferous (Buschmina 1970). Berchogur section, Mugodzhary, Western Kazakhstan, Devonian–Carboniferous transition (Kotschetkova & Janbulatova 1987). Kamenka River section, North Urals, Russia, Famennian–Tournaisian, late Devonian–early Carboniferous (Zhuravlev & Sobolev 2019). Yjid-Kamenka river section, Pechora Uplift, Russia, Famennian–Tournaisian, late Devonian–early Carboniferous (Sobolev 2020). Samples 19BAI 01-03, 19BAI 05, 19BAI 37, 19BAI 39, 19BAI 44, Tangbagou Formation, Blue Snake section, Tournaisian, early Carboniferous (this work).

Superfamily Bairdioidea Sars, 1888?
Family Indet.
Genus Indet.

Bairdioidea? indet.
Fig. 11R

Material examined

CHINA • 1 complete carapace (Fig. 11R); Blue Snake section, Gelaohe Formation, sample 19BAI 63; P6M 3975 • 1 complete carapace; Blue Snake section, Gelaohe Formation, sample 19BAI 60. All from the Famennian, late Devonian.

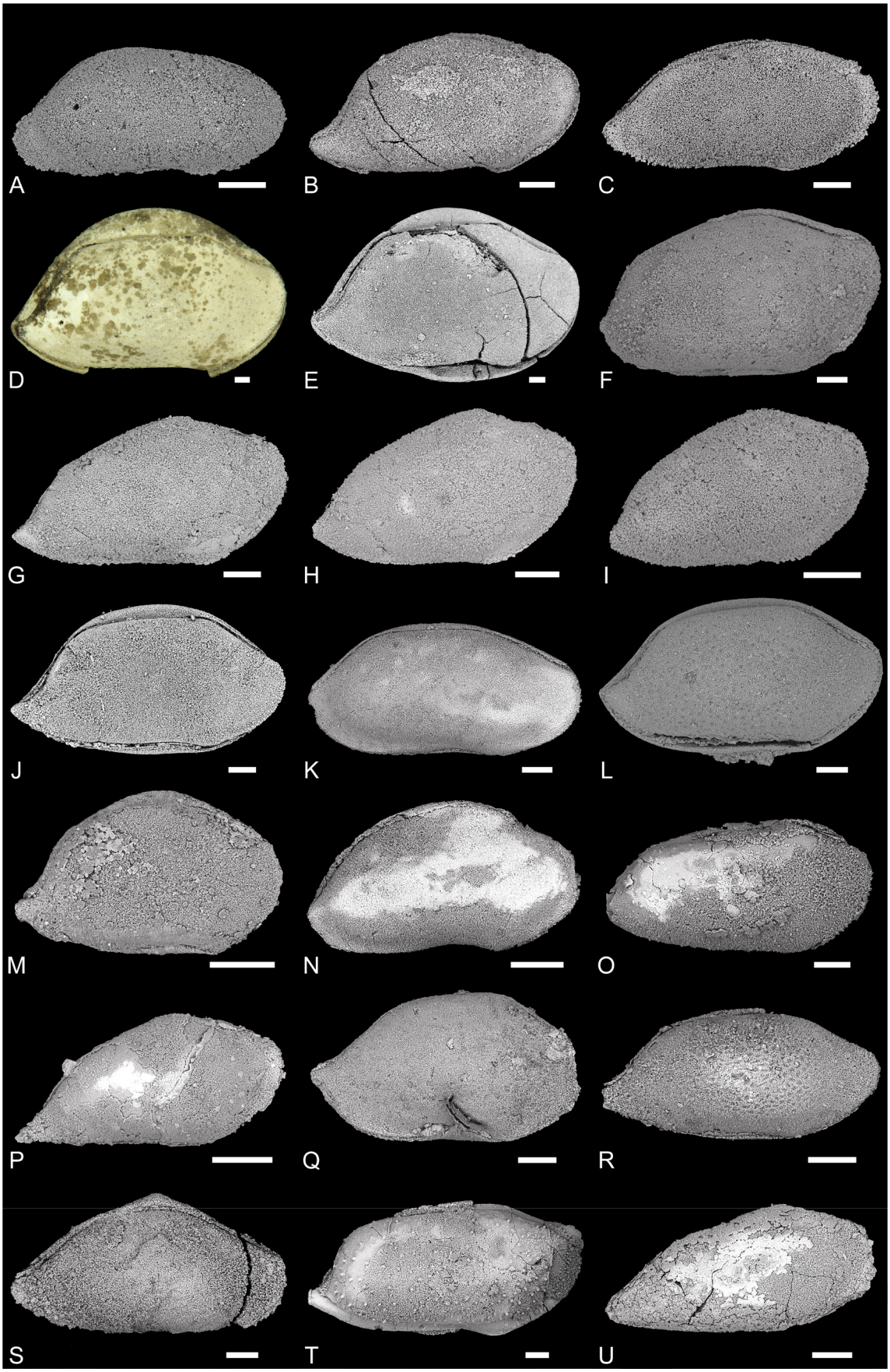
A
B
C
D
E
F
G
H
I
J
K
L
M
N
O
P
Q
R
S
T
U

Fig. 10. SEM pictures and focus stacking method pictures (with an *) of ostracods from Blue Snake section, Dushan County, South China, late Famennian–Tournaisian, late Devonian–early Carboniferous. All specimens are temporarily housed in the collections of Sorbonne Université, Paris, France (SU). **A**. *Bairdia feliumgibba* Becker, 1982, right lateral view of a carapace, sample 19BAI 01 (P6M 3937). **B**. *Bairdia hypsela* Rome, 1971, right lateral view of a carapace, sample 19BAI 03 (P6M 3938). **C**. *Bairdia mnemonica* Schevtsov, 1964 in Crasquin, 1986, right lateral view of a carapace, sample 19BAI 03 (P6M 3939). **D–E**. *Bairdia nanbiancunensis* Wang, 1988. **D**. Right lateral view of a carapace*, sample 19BAI 69 (P6M 3940). **E**. Right lateral view of a carapace, sample 19BAI 68 (P6M 3941). **F**. *Bairdia natiformis* Buschmina, 1970, right lateral view of a carapace, sample 19BAI 01 (P6M 3942). **G–I**. *Bairdia obliqua* Rozhdestvenskaya, 1972. **G**. Adult, right lateral view of a carapace, sample 19BAI 01 (P6M 3943). **H**. A-1, right lateral view of a carapace, sample 19BAI 01 (P6M 3944). **I**. A-2, right lateral view of a carapace, sample 19BAI 01 (P6M 3945). **J**. *Bairdia quasikuznecovae* Buschmina, 1968, right lateral view of a carapace, sample 19BAI 74 (P6M 3946). **K**. *Bairdia rustica* Kotchetkova, 1983, right lateral view of a carapace, sample 19BAI 08 (P6M 3947). **L**. *Bairdia semichatovae* Tschigova, 1960, right lateral view of a carapace, sample 19BAI 68 (P6M 3948). **M**. *Bairdia solita* Buschmina, 1970, right lateral view of a carapace, sample 19BAI 41 (P6M 3949). **N**. *Bairdia submongolensis* Buschmina, 1968, right lateral view of a carapace, sample 19BAI 08 (P6M 3950). **O**. *Bairdia* cf. *altifrons* Knight, 1928 in Crasquin, 1984, right lateral view of a carapace, sample 19BAI 43 (P6M 3951). **P**. *Bairdia* cf. *extenuata* Nazarova, 1951, right lateral view of a carapace, sample 19BAI 60 (P6M 3952). **Q**. *Bairdia* cf. *grahamensis* Harlton, 1928, right lateral view of a carapace, sample 19BAI 08 (P6M 3953). **R**. *Bairdia* cf. *susoroides* Jiang, 1983, right lateral view of a carapace, sample 19BAI 69 (P6M 3954). **S**. *Bairdia* sp. 1, right lateral view of a carapace, sample 19BAI 54 (P6M 3955). **T**. *Bairdia* sp. 2, right lateral view of a carapace, sample 19BAI 43 (P6M 3956). **U**. *Bairdia* sp. 3, right lateral view of a carapace, sample 19BAI 05 (P6M 3957). Scale bars = 100 µm.

Dimensions

RV: L = 375–419 µm, H = 228–237 µm
LV: L = 388–432 µm, H = 236–247 µm.

Remarks

This species is rare in the studied material. Its outline is typical of Podocopida and its lateral surface is characterized by 4 large nodes along the free margin and 3 other large nodes along the dorsal margin. This species is morphologically close to some ornamented Bairdiidae like the Triassic genus *Nodobairdia* Kollmann, 1963 which has large nodes in the dorsal part on the carapace but these forms of Bairdiidae are unknown from the Devonian and Carboniferous. Moreover, the overlap is reversed compared to most of genera among Bairdiidae, which is rare in this family. We cannot discuss further the systematic position of these specimens, even at family level, until more material will be available.

Occurrence

Samples 19BAI 60, 19BAI 63, Gelaohe Formation, Blue Snake section, Famennian, late Devonian (this work).

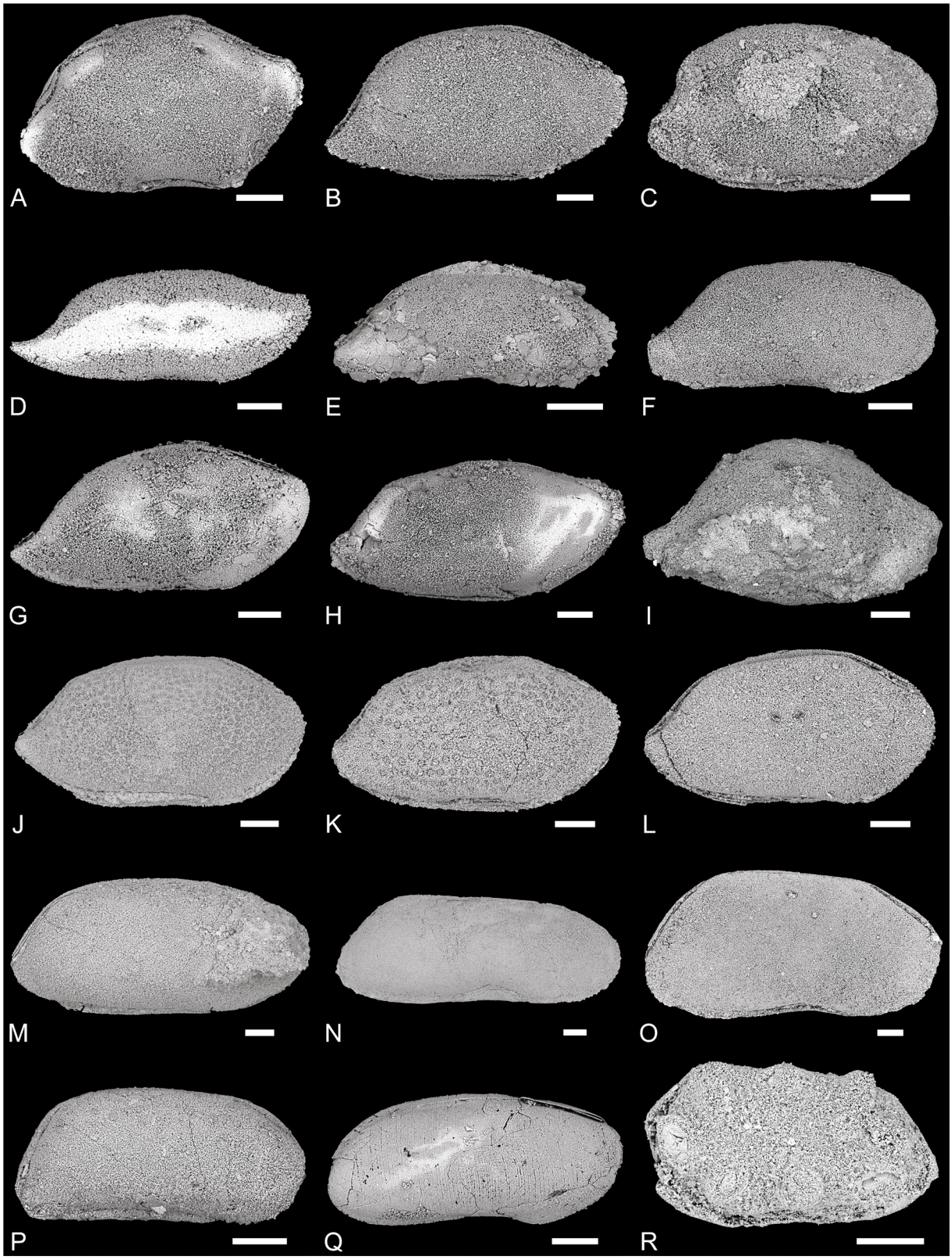
A
B
C
D
E
F
G
H
I
J
K
L
M
N
O
P
Q
R

Fig. 11. SEM pictures of ostracods from Blue Snake section, Dushan County, South China, late Famennian–Tournaisian, late Devonian–early Carboniferous. All specimens are temporarily housed in the collections of Sorbonne Université, Paris, France (SU). **A**. *Bairdia* sp. 4, right lateral view of a carapace, sample 19BAI 08 (P6M 3958). **B**. *Bairdia* sp. 5, right lateral view of a carapace, sample 19BAI 03 (P6M 3859). **C**. *Bairdia* sp. 6, right lateral view of a carapace, sample 19BAI 03 (P6M 3960). **D**. *Bairdia* sp. 7, right lateral view of a carapace, sample 19BAI 23 (P6M 3961). **E**. *Bairdia* (*Cryptobairdia*) cf. *curta* McCoy, 1844 emend. Jones & Kirkby, 1878 in Crasquin, 1986, right lateral view of a carapace, sample 19BAI 60 (P6M 3962). **F**. *Bairdia* (*Cryptobairdia*) *lavenei* Crasquin, 1985, right lateral view of a carapace, sample 19BAI 03 (P6M 3963). **G**. *Bairdia* (*Rectobairdia*) *angulatiformis* Posner, 1951, right lateral view of a carapace, sample 19BAI 67 (P6M 3964). **H**. *Bairdia* (*Rectobairdia*) *buschminae* Crasquin, 1985, right lateral view of a carapace, sample 19BAI 08 (P6M 3965). **I**. *Bairdia* (*Rectobairdia*) cf. *plebeja* Reuss, 1854, right lateral view of a carapace, sample 19BAI 03 (P6M 3966). **J–L**. *Bairdia* (*Rectobairdia*) sp. cf. *R. sinuosa* (Morey, 1936) in Crasquin, 1985. **J**. Right lateral view of a carapace, sample 19BAI 01 (P6M 3967). **K**. Right lateral view of a carapace, sample 19BAI 02 (P6M 3968). **L**. Right lateral view of a carapace, sample 19BAI 60 (P6M 3969). **M**. *Bairdiacypris nanbiancunensis* Wang, 1988, right lateral view of a carapace, sample 19BAI 60 (P6M 3970). **N**. *Bairdiacypris quasielongata* Buschimna, 1968, right lateral view of a carapace, sample 19BAI 01 (P6M 3971). **O**. *Bairdiacypris subcylindrica* Buschimna, 1984, right lateral view of a carapace, sample 19BAI 58 (P6M 3972). **P**. *Bairdianella cuspis* Buschmina, 1970, right lateral view of a carapace, sample 19BAI 03 (P6M 3973). **Q**. *Fabalicypris sundarijanata* Wang & Cao, 1997 in Song & Gong, 2019, right lateral view of a carapace, sample 19BAI 67 (P6M 3974). **R**. Bairdiodea? indet. Left lateral view of a carapace, sample 19BAI 63 (P6M 3975). Scale bars = 100 µm.

Table 3. Occurrences of species attributed to *Bairdianella* aff. *cuspis* Buschmina, 1970.

Species	Location	Reference	Figured specimen
Bairdianella aff. *cuspis* Buschmina, 1970 sensu Kotschetkova & Janbulatova, 1987	Western Kazahstan	Kotschetkova & Janbultova in Maslov 1987	pl. 24 fig. 2
	Montagne Noire, France	Casier *et al.* 2002	pl. 4 fig. 10
Bairdianella sp. A aff. *cuspis* Buschmina, 1970	Avesnois, North of France	Casier & Préat 2003	pl. 54 fig. 7
Bairdianella sp. A, aff. *cuspis* Buschmina, 1970	Dinant Basin, Belgium	Casier *et al.* 2004	pl. 4 fig. 9
Bairdianella sp. B, aff. *cuspis* Buschmina, 1970			pl. 4 fig. 10
Bairdianella sp. A, aff. *cuspis* Buschmina, 1970	Dinant Basin, Belgium	Casier *et al.* 2005	pl. 4 fig. 10

Discussion

Diversity and taxonomic composition of ostracod assemblages

On the 88 samples collected from the Blue Snake section, Dushan County, Guizhou province, South China, 23 yielded identifiable ostracods. In total, 98 species have been identified, belonging to 31 genera and 13 families. 50 species are already known from the Devonian and/or early Carboniferous, 4 are new and 44 are kept in open nomenclature due to poor preservation and/or paucity of material. The generic diversity in Blue Snake section ranges from 3 in sample 19BAI 16 to 17 in sample 19BAI 01 and the species diversity from 5 in sample 19BAI 16 to 36 in sample 19BAI 03. Species and genera both document comparable diversity variations with an important increase in the lowermost part of the section followed by a plateau throughout the Gelaohe Formation and an important drop at the top of the

Gelaohe Formation. It is followed by an increase and a plateau at the base of the Tangbagou Formation and then a progressive increase towards the top of the Tangbagou Formation.

Individual rarefaction and Shannon-Wiener and Simpson diversity indices were calculated with PAST (Hammer *et al.* 2001). Rarefaction curves (Fig. 12A) show the expected number of taxa as a function of the number of specimens in each sample from the Blue Snake section. Rarefaction curves from samples 19BAI 01-03, 19BAI 08, 19BAI 39, 19BAI 44, 19BAI 54, 19BAI 58, 19BAI 60, 19BAI 63, 19BAI 67-69, 19BAI 74 and 19BAI 80 reach a plateau, indicating that they provided assemblages representative of the original faunal diversity. On the opposite, rarefaction curves for samples 19BAI 05, 19BAI 16, 19BAI 23, 19BAI 27-2, 19BAI 37, 19BAI 41, 19BAI 43 and 19BAI 55 show that assemblages from these samples are not representative and that a more complete sampling would be useful to have a better idea of the original faunal diversity. In particular, samples 19BAI 16, 19BAI 23, 19BAI 27-2 and 19BAI 37 display only few identifiable specimens compared to other samples. Samples 19BAI 01-03 recorded the maximum of diversity with 35 to 36 species belonging to 12 to 17 genera and 5 to 7 families. Sample 19BAI 58 recorded the minimum of diversity among representative assemblages, with 6 species belonging to 5 genera and 3 families.

Diversity for each sample was calculated (Fig. 12B–C) using Shannon-Wiener (Shannon & Weaver 1949) and Simpson indices (Simpson 1949). The first is weakly affected by the sample size and allows to analyse species richness considering the number of specimens of each species. The second allows to estimate the dominance in the assemblages: it is close to 1 if species are uniformly distributed and close to 0 if the assemblage is dominated by one or few species (Forel *et al.* 2020). Diversity indices in the Blue Snake section show patterns comparable to the generic and specific variations described above (Fig. 12B–C). A decrease in diversity paralleled by an increase in dominance between samples 19BAI 80 to 19BAI 74. Both indices have low value in sample 19BAI 74 with Simpson index which reach its lowest value throughout the section with D-1 = 0.57 and Shannon-Wiener index reach one of its lowest values with H = 1.5.

The general trend across the Gelaohe Formation (samples 19BAI 80 to 19BAI 60) shows an increase in specific diversity and dominance with 1 major decrease in sample 19BAI 74 (H = 1.5, D-1 = 0.57) and a weaker at sample 19BAI 63 (H = 2.5, D-1 = 0.86). In this formation, assemblages are dominated by *Sansabella gelaohensis* sp. nov. that represents 64% of collected specimens in sample 19BAI 74. A strong reduction of diversity and increase of dominance occur between samples 19BAI 60 and 19BAI 58 at the contact between the Gelaohe and Tangbagou Formations, and the value for both indices is low in sample 19BAI 58 (H = 1.3, D-1 = 0.65). This assemblage is dominated by *Bairdiacypris subcylindrica* Buschmina, 1984 that represents half of the collected specimens. This drop is followed by an increase of both indices between samples 19BAI 58 and 19BAI 55 and an interval between samples 19BAI 55 and 19BAI 44 at the base of the Tangbagou Formation with more stable value in both indices (H = 2.3–2.7, D-1 = 0.86–0.9). Between samples 19BAI 43 and 19BAI 44, the value of both indices increases to reach 3.4 for H and 0.97 for D-1 and slightly decreases between sample 19BAI 43 and 19BAI 41 (H = 3 and D-1 = 0.95). Between sample 19BAI 41 and 19BAI 01, both indices fluctuate in this interval: H between 2.6 and 3.5 and D-1 between 0.89 and 0.97 with the lowest value for sample 39.

In the Blue Snake section, 3 different associations are recognized based on their composition, diversity (H), and dominance (D-1): their number of species, genera and families are summarized in Table 4 and the relative abundance and diversity of each family are shown on Fig. 13. The association A is characteristic of the Gelaohe Formation and corresponds to pre-Hangenberg Event assemblages (samples 19BAI 60 to 19BAI 80). It is composed of 53 species that belong to 24 genera and 12 families and is the most diversified in the Blue Snake section at genus and family levels. It is dominated by Palaeocopida (62% of collected specimens), with the family Sansabellidae represented by the single

Table 4. Summary of the diversity of each assemblage in the Blue Snake section.

	Association A Gelaohe Formation	**Association B** Lowermost Tangbagou Formation	**Association C** Middle–upper Tangbagou Formation
Species	53	26	72
Genera	24	11	20
Families	12	6	8

species *Sansabella gelaohensis* Guillam & Forel sp. nov. which accounts for 22% of the collected specimens, Beyrichiopsidae (15%), Geisinidae (11%), Primitiopsidae (10%), Aparchitidae (4%) and Hollinellidae (less than 1%). Podocopida represent less than one-third of the collected specimens (32%), Bairdiidae being the most abundant (20%) and essentially represented by *Bairdia* and *Acratia*. The families Bairdiocyprididae (9%) and Pachydomellidae (4%) are also part of this association, essentially represented by *Healdianella* and *Microcheilinella* respectively. Platycopida (5%) all belong to the family Cavellinidae with *Sulcella* (4%) and *Cavellina* (1%). They are represented only in this association.

In terms of species, Podocopida are the most diversified in this association (60%), being essentially represented by Bairdiidae (35%) with *Bairdia* and *Acratia*. Among Podocopida, this association also includes Bairdiocyprididae (12%) and Pachydomellidae (12%). Palaeocopida are less diversified and represents 34% of the specific diversity and most of species belongs to Geisinidae (12%) and Beyrichiopsidae (8%). This order is also represented by the following families: Primitiopsidae (6%), Aparchitidae (4%), Hollinellidae (2%), Paraparchitidae (2%) and Sansabellidae (2%). Platycopina represents 6% of the species diversity with *Cavellina* (4%) and *Sulcella* (2%).

The association B occurs in the lowermost Tangbagou Formation (sample 19BAI 58 to 19BAI 54) and corresponds to the assemblages in the direct aftermath of the HE. It is composed of 26 species belonging to 11 genera and 6 families and is the less diversified in this section. It is dominated by Podocopida (88% of the collected specimens), Bairdiidae being the most abundant (67%) with *Bairdiacypris* (44%) and *Bairdia* (19%) being the most representative genera. Bairdiocyprididae are well represented but only with the single genus *Healdianella* (19%). Pachydomellidae (2%) are also represented. Palaeocopida are poorly represented (12%), Paraparchitidae being the most abundant (9%) but only represented by the genus *Shishaella*. Geisinidae (2%), represented by *Hypotetragona* and *Knoxiella*, and Aparchitidae (1%), represented by the single genus *Fellerites*, are also part of this association. The family Primitiopsidae is absent only in this association. In terms of species, this association is the less diversified in the Blue Snake section.

Podocopida are the most diversified (81%), being represented by Bairdiidae (62%), with *Bairdia* (35%) that counts for more than half of the specific diversity of this family; Bairdiocyprididae (12%) and Pachydomellidae (8%). Palaeocopida are less diversified (19% of species) and represented by 3 families: Geisinidae (7.5%), Paraparchitidae (7.5%) and Aparchitidae (4%).

The association C occurs in the middle and upper Tangbagou Formation (samples 19BAI 01 to 19BAI 44) and corresponds to early Tournaisian assemblages. It is composed of 72 species belonging to 20 genera and 8 families and is the most diversified at the species level. It is dominated by Podocopida (72% of the collected specimens), in particular Bairdiidae (55%), mostly represented by *Bairdia* (40%). Bairdiocyprididae (12%) and Pachydomellidae (6%) are also represented. Palaeocopida represent 28% of species. Among them, Geisinidae is most the diversified family (16%), followed by Paraparchitidae (9%), Amphissitidae, Aparchitidae and Primitiopsidae each only correspond to about 1%. Amphissitidae is represented only in this association.

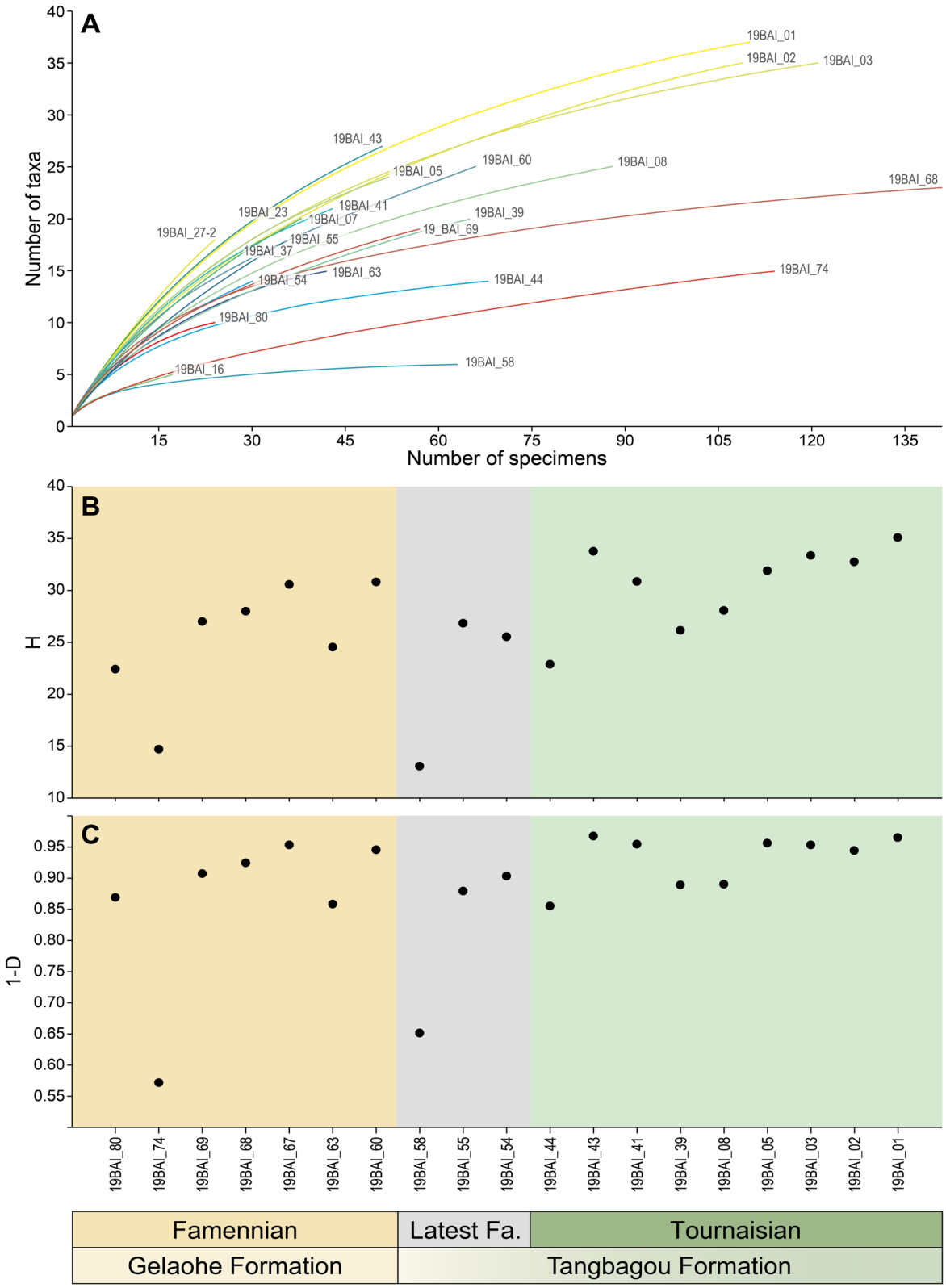

Fig. 12. Individual rarefaction curves (A) and evolution of the Shannon-Wiener (B) and Simpson indices across the Blue Snake section. Orange: Association A. Grey: Association B. Green: Association C.

Podocopida are also the most diversified (82%) and are dominated by Bairdiidae (54%) particularly by *Bairdia* (38% of the total specific diversity) and *Acratia* (10%). Bairdiocyprididae and Pachydomellidae both account for 14%. Palaeocopida are poorly diversified (18% of species) with Geisinidae (8%), Paraparchitidae (5%), Aparchitidae (3%), Amphissitidae and Primitiopsidae both represent 1.5%.

Diversity dynamics and stratigraphic implications

Impact of the Hangenberg Event on ostracod faunas

In the upper Famennian Gelaohe Formation, before the shally bed corresponding to the Hangenberg Event, 53 species belonging to 24 genera and 12 families are present. The lowermost Tangbagou Formation yielded only 26 species belonging to 11 genera and 6 families, and record the lowest value in the Blue Snake section. Moreover, the assemblage from sample 19BAI 58 is very poor with only 6 species belonging to 5 genera and 3 families: Bairdiidae represents 61% of the species and *Bairdiacypris subcylindrica* accounts for half of specimens. The Shannon-Wiener and Simpson indices are also very low in the assemblage from sample 19BAI 58 which confirms a very low diversity (H = 1.3) and the dominance of the species *Bairdiacypris subcylindrica* in this assemblage (D-1 = 0.65). Based on these data, the bed of yellowish shales (sample 19BAI 59) that yielded no ostracods certainly corresponds to the Hangenberg Event as hypothesized above. Twenty-eight of the 53 species found in our material from the Gelaohe Formation actually cross the Hangenberg Event and are present in the Tangbagou Formation. *Kloedenellitina sincera*, *Cytherellina caerulea* Guillam & Forel sp. nov, and *Bairdia nanbiancunensis* are not represented in our post-Hangenberg Event assemblages but they were found by Song & Gong (2019) in the Tournaisian Tangbagou Formation from the Blue Snake section. *Cytherellina caerulea* sp. nov is only represented in the first half of the Tangbagou Formation (Song & Gong 2019: fig. 3). Two species that are represented only in our post-event associations (Tangbagou Formation) was also found in the Gelaohe Formation by Song & Gong (2019): *Microcheilinella infradominica* in Song & Gong (2019) and *Fabalicypris sundarijanata* Wang & Cao, 1997. Consequently, 31 species of the 55 cross the Hangenberg Event and record a specific extinction rate of 44% but it is worth noting that in our material only 13 species are represented in the lowermost Tangbagou Formation (association B). The others are present only in the rest of this formation (association C). These lasts could have either temporarily disappeared from the Blue Snake section, survived at another yet unidentified location and recolonized this area when the conditions became better or their presence in the latest Famennian (lowermost Tangbagou Formation) has not been recorded here, perhaps because of low abundance (i.e., lazarus taxa). The value of specific extinction rate is slightly lower than that estimated from the data from Song & Gong (2019). In this study, 17 species among the 35 species present in the Gelaohe Formation became extant, that correspond to a specific extinction rate of about 49%. Kaiser *et al.* (2016) estimated that 30 to 50% of neritic benthic ostracod species disappeared at the Hangenberg Event from data published by Casier *et al.* (2004, 2005) from the Dinant Basin. The values in the present work and Song & Gong (2019) are consistent with this estimation. Crasquin *et al.* (1986) documented a more severe impact of the Hangenberg Event on neritic benthic ostracod faunas from Western Canada with only 5 surviving species among 148 which correspond to a specific extinction of about 96%. This discrepancy may relate to different environmental conditions.

Among species that disppeared in the Blue Snake section with the Hangenberg Event, 2 have been documented elsewhere in the Tournaisian: *Kloedenellitina spinosa* in the Russian platform (Gurevitch 1972), and *Bairdia nanbiancunensis* in Guilin (Wang 1988b) and Guizhou, China (Olempska 1999) and Canning Basin, Australia (Jones, unpublished data, fide Olempska 1999). At the genus level, the extinction rate is about 46% with the disappearance of 11 genera among the 24 represented in the pre-event assemblages.

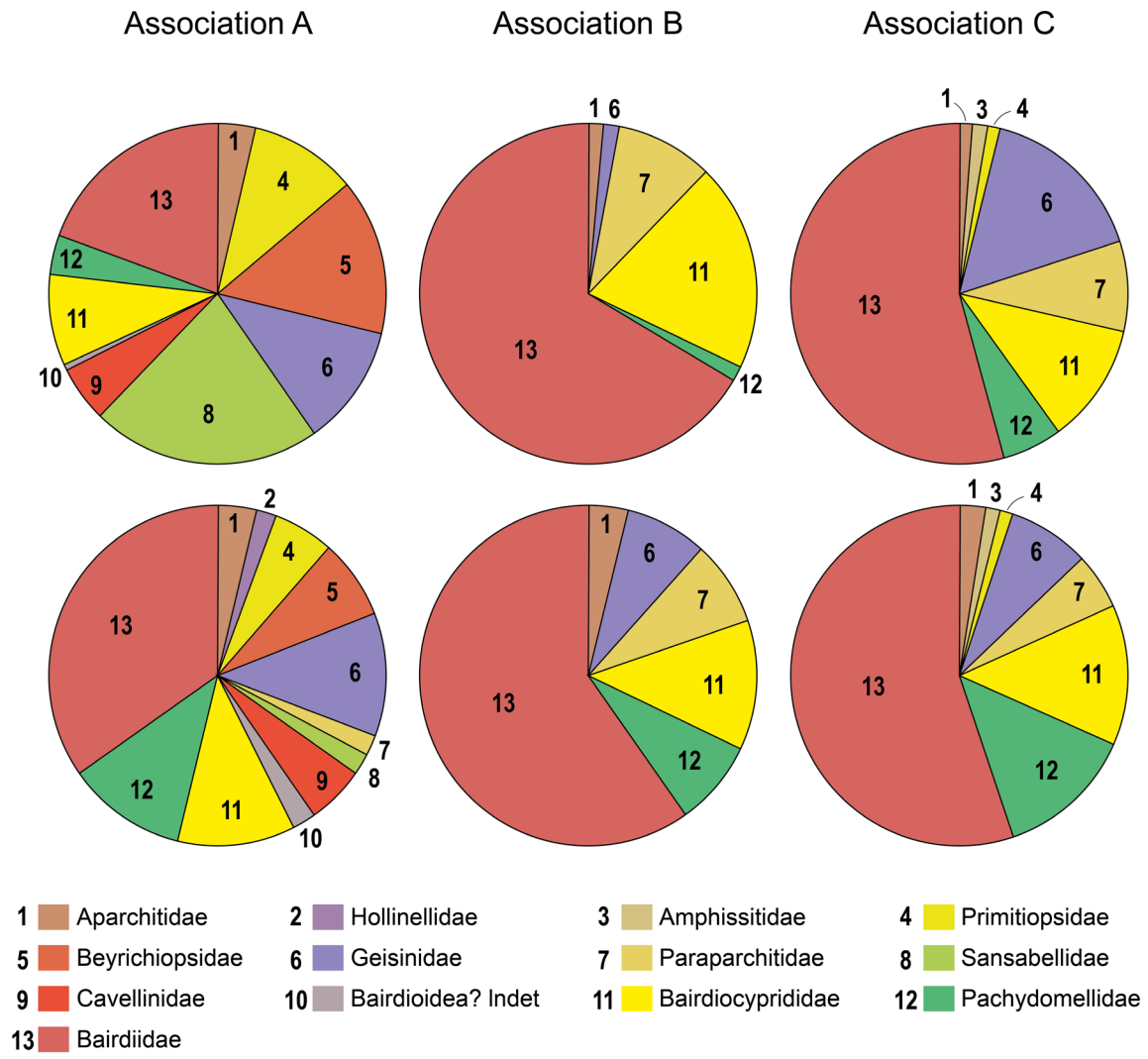

Fig. 13. Circular diagrams of relative abundance (upper = number of specimens per family) and faunal composition (lower = number of species per family) of the assemblages in the Blue Snake section.

Palaeocopida have been more impacted by the Hangenberg Event in the Blue Snake section with a specific extinction rate of about 76% while it is about 25% in Podocopida. All species of Platycopina disappeared so this order is not present in post-event associations (B and C).

Recovery of ostracod faunas after the Hangenberg Event

In the lowermost Tangbagou Formation (association B), 13 species among the 26 recorded are new, corresponding to a specific turnover rate of 50%. When considering the whole Tangbagou Formation (association B and C), 45 species among the 72 that are present after the HE are new which correspond to a specific turnover rate of about 62%. This value is for example higher than in the Yjid-Kamenka river section, Pechora Uplift in which it is only of 20% (data from Sobolev 2020). However, Crasquin *et al.* (1986) documented a severe and almost complete renewal of neritic benthic ostracod faunas from Western Canada with only 5 species that survived from the Famennian and 205 new species in the Lower Carboniferous Banff Formation. This is a sharp renewal which is unique in Palaeozoic ostracods; in most of the case the recovery is more gradual with species represented in pre-event and post-event

Table 5. Species absent in the Famennian of the Blue Snake section but represented in other localities

Species	Location	Reference
Blessites feluyensis	Dinant Basin, Belgium	Casier *et al.* 2005
	Pechora Uplift, Russia	Zhuravlev & Sobolev 2019
Healdianella lumbiformis	Montagne Noire, France	Lethiers & Feist 1991
	Avesnois, France	Casier & Préat 2003
	Dinant Basin, Belgium	Casier *et al.* 2005
Acratia insolita	South-Western Siberia	Buschmina 1970
	Hunan, South China	Hance *et al.* 1993
Bairdia confragosa	Dinant Basin, Belgium	Casier *et al.* 2005
Bairdia feliumgibba	Montagne Noire, France	Lethiers & Casier 1999b
	North-Western Turkey	Nazik *et al.* 2012
	Holy Cross Mountains, Poland	Olempska 1997; Schraut 1996
	Thuringia and Harz, Germany; Austria; Western Pyrenees and South-Eastern Cantabrian Mountains, Spain; Algeria; Morocco; Guangxi, China	Schraut 1996
Bairdianella cuspis	Western Kazakhstan	Kotschetkova & Janbulatova 1987
	Northern Urals	Zhuravlev & Sobolev 2019
	Pechora Uplift, Russia	Sobolev 2020

assemblages (Crasquin *et al.* 1986). *Acutiangulata* Buschmina, 1968, represented by the single species *Acutiangulata acutiangulata* (Tschigova, 1959) and *Shishaella*, represented by *Shishaella hastierensis* Crasquin-Soleau, 1988 and *Shishaella porrecta* (Zanina, 1956), are the only genera that appeared in the lowermost Tangbagou Formation of the Blue Snake section. No new family has been found in this part of the Tangbagou Formation.

In the rest of the Tangbagou Formation (association C), 32 of the 72 species are new. Six genera appeared, all represented by a single species (Table 1): *Blessites*, *Amphissites*, *Bairdianella*, *Coryellina*, *Aparchites* and *Knoxites*. Of species only represented after the HE in the Blue Snake section, 6 have been recorded elsewhere before the Hangenberg Event (Table 5). Most of the families represented in the association C count for between 1 and 14 % of the specific diversity except Bairdiidae which represent 54.5% of the species, in particular the genus *Bairdia* which counts for 38% of the total number of species all families included. This family recorded the greatest diversification among all families throughout the Tournaisian with 16 species in the lowermost Tangbagou Formation (associations B) and 40 species in the rest of this Formation (association C). After the HE, Podocopida became more numerous and diversified and dominate the assemblages, in particular the family Bairdiidae. The abundance of Palaeocopida did not change between lowermost Tangbagou Formation (association B) and the rest of this Formation (association C) but they became slightly more diversified at genus level with the appearance of *Aparchites* in Aparchitidae, *Knoxites* in Geisinidae, and *Paraparchites* in Paraparchitidae. At the family level, the association C from the Tournaisian of the Tangbagou Formation is also more diversified with the appearance of Amphissitidae and Primitiopsidae. All palaeocopid genera represented in the lowermost Tangbagou Formation are also represented in the Tournaisian. However, at specific level, Geisinidae and Paraparchitidae are the only families among Palaeocopida which become more diversified with both 2 species in the lowermost Tangbagou Formation (association B) and respectively 6 and 4 species in the rest of this Formation (association C).

Consequently, the recovery of ostracod faunas after the HE in the Blue Snake section is here linked essentially to the diversification of Podocopida, more particularly Bairdiidae with the genus *Bairdia*, and a turnover between Palaeocopida and Podocopida, these latter becoming dominant in post-event assemblages.

Palaeoenvironmental implications

Before discussing palaeoenvironmental interpretations, the autochthonous or allochthonous nature of ostracod assemblages must be discussed. It is generally determined by studying the ratio between complete carapaces with both articulated valves and isolated valves and the demographic structures of populations (e.g., Oertli 1971; Boomer *et al.* 2003). In all assemblages from the Blue Snake section, complete and articulated valves are dominant. Moreover, most of species are represented by adults and juvenile stages, although adults and last ontogenetic stages are often more represented in our material than the earlier stages (*Coryellina grammi*, *Paraparchites longmenshanensis*, *Sansabella gelaohensis* sp. nov., *Cytherellina caerulea* sp. nov., *Acratia* cf. *tschudovoensis*, *Bairdia confragosa*, *Bairdia nanbiancunensis*, *Bairdia quasikuznecovae*, *Bairdia rustica*, *Bairdia semichatovae*, *Bairdia* (*R.*) *angulatiformis*). A few species are represented mostly by juveniles (*Selebratina* sp., *Sulcella* (*P.*) *baisuzhena* sp. nov. *Kloedenellitina sygmaeformis*, *Hypotetragona* sp., *Healdianella* cf. *subdistincta*, *Acratia* cf. *evlanensis*, *Bairdia hypsela*, and *Bairdianella cuspis*). Our assemblages correspond to low-moderate energy autochthonous thanatocoenosis sensu Boomer *et al.* 2003. Consequently, transportation may have been limited and the assemblages from the Blue Snake section are good palaeoenvironmental indicators.

In the Palaeozoic, 3 ostracod mega-assemblages (Fig. 14) are classically recognized (recently summarized in Casier 2017):

1. Eifelian Mega-assemblage (= "sandigkalkiger Fazies Typ" from Blumenstengel 1973 and Eifelian ecotype from Becker in Bandel & Becker 1975) that indicate benthic neritic marine environments (0 to III on Fig. 14).
2. Thuringian Mega-assemblage (= "Thüringischer Typus" from Zagora 1968 and the "kalkig–toniger Fazies Typ" from Blumenstengel 1973 and Thuringian ecotype from Becker in Bandel & Becker 1975) that indicates deeper benthic environments (IV on Fig. 14).
3. Myodocopida Mega-assemblage (= "toniger, hemipelagischer Fazies Typ" from Blumenstengel 1973 and Entomozoacean ecotype from Becker in Bandel & Becker 1975) indicates poorly oxygenated marine environments, V on Fig. 14).

For the Palaeozoic of China, Wang (1988a) defined 5 ostracod associations that could be compared with the mega-assemblages as follow: leperditiid association (nearshore lagoonal environments, 0 on Fig. 14), palaeocopid association (more open shallow nearshore environments, I and II on Fig. 14), smooth-podocopid association (slightly deeper and more distal offshore environments, III on Fig. 14), spinose-podocopid association (deep environments at the base of the slope, IV on Fig. 14), and entomozoacean association, (poorly oxygenated marine environment, V on Fig. 14).

The regressive pulse that occurred in the middle *praesulcata* zone (late Famennian), interpreted as a minor sea-level fall associated with a minor glacial phase (Kaiser *et al.* 2011, 2016) and often considered as one of the possible causes of the HE (e.g., Walliser 1996) is here difficult to highlight. The study of ostracod faunas from the Famennian Zhewang Formation which was deposited before the Gelaohe Formation could bring more information about this regression trend during the late Famennian.

In the Blue Snake section, the association A is dominated by Palaeocopida (62% of collected specimens) and is the only one from the Blue Snake section that contains Platycopida. These characteristics point to the Assemblage II of the Eifelian Mega-assemblage, pointing to a nearshore shallow water environment. The presence and dominance of the genus *Sansabella* that occurred in shallow-waters and is rather

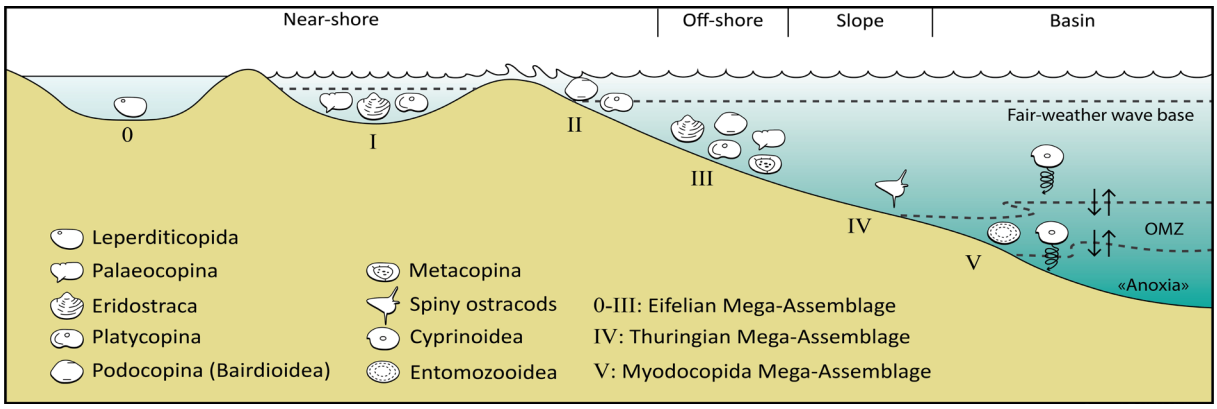

Fig. 14. Location of the different ostracod mega-assemblages along the platform (modified from Crasquin & Horne 2018; redrawn, with minor modifications, from Casier 2008).

typical of nearshore conditions (Coen 1989) also support these interpretations. However, Podocopida are more diversified (60% of species), in particular the family Bairdiidae which indicate a relatively strong marine influence and an open environment. The association B of the Blue Snake section is dominated by Podocopida, particularly Bairdiidae with the genus *Bairdiacypris*: it therefore corresponds to the Assemblage III of the Eifelian Mega-assemblage and the Smooth-Podocopid Association of Wang (1988a). However, contrary to the Assemblage III, the association B is poorly diversified which is probably linked to the HE that occurred slightly earlier. Consequently, the environmental signal is here weak and unclear but seem to correspond to a slightly deeper and opened marine environment but we cannot be sure that this corresponds to the beginning of a transgressive phase as the extinction signal may be overprinting. The association C is largely dominated by Podocopida, particularly Bairdiidae and the genus *Bairdia*. It totally corresponds to the Assemblage III of the Eifelian Mega-assemblage and the Smooth-Podocopid Association of Wang (1988a). Both indicate a shallow and open offshore marine environment. The high diversity and abundance of ostracods in the Tangbagou Formation, in particular in the top of the section, indicate an offshore environment between fair–weather and storm wave base (Casier *et al.* 2005).

Thus, the study of ostracod assemblages from the Blue Snake section documents the increasing water-depth from the late Famennian–Tournaisian interval, in line with the transgressive trends that have already been reported from the study of ostracod faunas from France (e.g., Lethiers & Feist 1991; Casier *et al.* 2002), Belgium (e.g., Casier *et al.* 2004, 2005), Canada (e.g., Lethiers *et al.* 1986), Urals (e.g., Zhuravlev & Sobolev 2019; Sobolev 2020) and South China (e.g., Song & Gong 2019). Blessites feluyensis, Knoxiella complanata, Praepilatina adamczalki and Bairdianella cuspis were also reported together from a succession recording a transgressive trend through the Devonian–Carboniferous transition from North Urals (Sobolev 2020). *Blessites feluyensis* and *Bairdia feliumgibba*, were represented together in the Devonian–Carboniferous of the Vangyr River section from the east of the Pechora plate in Russia (Zhuravlev & Sobolev 2019). *Bairdia feliumgibba*, only present in the Tournaisian in our section, were represented in lagoonal environment in the late Famennian but became extinct a little after the Hangenberg event. *Blessites feluyensis*, which is also only present in the Tournaisian in our section, was represented in shoal in marine open context and in transgressive trends in the Tournaisian (Zhuravlev & Sobolev 2019). This species seems to be represented in the same palaeoenvironmental settings in the Tournaisian of the Blue Snake section in South China. The increasing number of species and specimens belonging to Bairdiidae, in particular the genus *Bairdia*, throughout the Tangbagou Formation indicates a progressively opening and deepening of the environment during the Tournaisian. Because the renewal

of ostracod faunas in the Blue Snake section was mainly linked to this diversification, we propose that the recovery was depending on the palaeoenvironmental changes.

Conclusion

Ninety-eight species belonging to 31 genera have been retrieved from the Blue Snake section spanning the Famennian–Tournaisian transition in Dushan County, Guizhou Province, South China. Four species are newly described: *Clavofabella*? *lanshella* Guillam & Forel sp. nov., *Sansabella gelaohensis* Guillam & Forel sp. nov., *Cytherellina caerulea* Guillam & Forel sp. nov., *Sulcella baisuzhena* Guillam & Forel sp. nov. The analysis of the diversity of ostracod assemblages shows that in the studied area, the Hangenberg Event caused a significant diversity fall with the disappearance of 44% of the species. This event also influenced the taxonomic composition of the assemblages, with the reduction of the proportion of Palaeocopida and the increase in that of Podocopida between the latest Famennian and the Tournaisian. The main factor of the renewal of ostracod faunas in the Blue Snake section appears as the progressive diversification of the family Bairdiidae during the early Tournaisian, in particular the genus *Bairdia*, and was probably constrained by the palaeoenvironmental changes at the Devonian–Carboniferous transition. Thus, the study of the composition and characteristics of assemblages indicates that the Tangbagou Formation was deposited in a transgression trend, with a marine shallow environment that become deeper and more open during the Tournaisian.

Acknowledgements

We thank Atike Nazik (Cukurova University, Adana, Turkey) and Claudia Dojen (State Museum of Carinthia, Klagenfurt, Austria) for their helpful comments. We also thank Professor Yue Li (NIGPAS) and Professor Yue Wang (University of Guizhou) for their helpful support during the fieldwork, Frank Sénégas (CR2P, Paris) for processing samples and preparation of ostracods and Alexandre Lethiers (CR2P, Paris) for drawing some figures. This work was partly supported by the Strategic Priority Research Program (B) of Chinese Academy of Sciences (Grant No. XDB26000000), National Natural Science Foundation of China (Grant No. 41802002).

References

Adamczak F.J. 2006. Contributions to Palaeozoic Ostracod Classification [POC], N° 41. "Non-kloedenellacean" ostracods 1. Family Geisinidae Sohn, 1961. Assured podocopines. *Neues Jahrbuch für Geologie und Paläontologie, Abhandlungen* 240: 271–311. https://doi.org/10.1127/njgpa/240/2006/271

Algeo T.J. & Scheckler S.E. 1998. Terrestrial-marine teleconnections in the Devonian: links between the evolution of land plants, weathering processes, and marine anoxic events. *Philosophical Transactions of the Royal Society B: Biological Sciences* 353: 113–130. https://doi.org/10.1098/rstb.1998.0195

Algeo T.J. & Scheckler S.E. 2010. Land plant evolution and weathering rate changes in the Devonian. *Journal of Earth Science* 21: 75–78, Special Issue. https://doi.org/10.1007/s12583-010-0173-2

Algeo T.J., Berner R.A., Maynard J.B. & Scheckler S.E. 1995. Late Devonian oceanic anoxic events and biotic crises: "rooted" in the evolution of vascular land plants? *Geological Society of America, GSAToday* 5 (45): 64–66.

Algeo T.J., Scheckler S.E. & Maynard J.B. 2001. Effects of the middle to late Devonian spread of vascular land plants on weathering regimes, marine biotas, and global climate. *In*: Gensel P.G. & Edwards D. (eds) Plants invade the land: evolutionary and environmental. *Perspectives*, *Columbia University Press, New York*: 213–236. https://doi.org/10.7312/gens11160-013

Bandel K. & Becker G. 1975. Ostracoden aus paläozoischen pelagischen Kalken der Kärnischen Alpen (Shurium bis Unterkarbon). *Senckenbergiana Lethaea* 56 (1): 1–83.

Batalina M.A. 1924. On the Lower Carboniferous Ostracoda from the Borovichi District of the Department of Novgorod. *Bulletin of the Geologocal Commission, Leningrad.* 10 (43): 1315–1338.

Batalina M.A. 1941. Ostracods of the Main Devonian Field. *In*: Hecker R.F. (ed.) Fauna Glavnogo devonskogo polâ, *Izdatel'stvo Akademii Nauk SSSR, Moskva* 1: 285–314. [In Russian.]

Becker G. 1965. Podocopida (Ostracoda) aus dem Mitteldevon der Sötenicher Mulde (N-Eifel). *Senckenbergiana Lethaea* 46 (4–6): 367–44.

Becker G. 2001. Contributions to Palaeozoic Ostracod Classification [POC], N° 18. The Superfamily Bairdiacea Sars, 1888. 1. Family Bairdiidae Sars, 1888 (Palaeozoic members only). *Neues Jahrbuch für Geologie und Paläontologie, Abhandlungen* 220 (2): 267–294. https://doi.org/10.1127/njgpa/220/2001/267

Becker G. 2002. Contributions to Palaeozoic Ostracod Classification [POC], N° 24, Palaeozoic Ostracoda: the standard classification scheme. *Neues Jahrbuch für Geologie und Paläontologie, Abhandlungen* 226: 165–228. https://doi.org/10.1127/njgpa/226/2002/165

Becker G., Clausen C.D. & Leuteritz K. 1993. Verkieselte Ostracoden vom Thüringer Ökotyp aus dem Grenzbereich Devon/Karbon des Steinbruchs Drewer (Rheinisches Schiefergebirge). *Courier Forschungsinstitut Senckenberg* 160: 1–130.

Becker R.T. 1993. Anoxia, eustatic changes, and Upper Devonian to lowermost Carboniferous global ammonoid diversity. *In*: House M.R. (ed.) The Ammonoidea: environment, ecology, and evolutionary Change. *Systematics Association, Special Volume 47*: 115–163.

Bennett C.E. 2008. A review of the Carboniferous colonisation of non-marine environments by ostracods. *Senckenbergiana Lethaea* 88: 37–46. https://doi.org/10.1007/BF03043976

Bennett C., Siveter D.J., Davies S., Williams M., Wilkinson I.P., Browne M. & Miller C.G. 2012. Ostracods from freshwater and brackish environments of the Mississippian of the Midland Valley of Scotland: the early colonisation of terrestrial water bodies. *Geological Magazine* 149: 366–396. https://doi.org/10.1017/S0016756811000719

Błaszyk J. & Natusiewicz D. 1973. Carboniferous ostracods from the borings in North-western Poland. *Acta Palaeontologica Polonica* 18 (1): 117–151.

Blumenstengel H. 1973. Zur stratigraphischen und faziellen Bedeutung der Ostracoden im Unter- und Mittel Harz. *Zeitschrift für Geologische Wissenschaften, Themenhefte* 1: 67–79.

Blumenstengel H. 1993. Ostracodes from the Devonian-Carboniferous boundary beds in Thuringia (Germany). *Annales de la Société géologique de Belgique* 115: 483–489.

Blumenstengel H. 1995. Zur Ostracodenfauna der Oberen Clymenien-Schichten von Saalfeld (höchstes Famennium, Thüringer Schiefergebirge). *Beiträge zur Geologie von Thüringen, Neue Folge* 2: 3–27.

Blumenstengel H., Bender P. & Herbig H.G. 1997. Ostracoden aus der Gladenbach-Formation (Unterkarbon, Lahn-Dill-Mulde, Rheinisches Schiefergebirge). *Sonderveröffentlichungen, Geologisches Institut der Universität zu Köln* 114: 91–121.

Bond D.P.G., & Grasby S.E. 2017. On the causes of mass extinctions. *Palaeogeography, Palaeoclimatology, Palaeoecology* 478: 3–29. https://doi.org/10.1016/j.palaeo.2016.11.005

Boomer I., Horne D.J. & Slipper I.J. 2003. The use of ostracods in palaeoenvironmental studies, or what can you do with an ostracod shell? *Palaeontological Society Papers* 9: 153–180. https://doi.org/10.1017/S1089332600002199

Buschmina L.S. 1970. Ostracodes from the boundary layers of the Devonian and Carboniferous of the Yeltsov synclinorium (south of Western Siberia). *In*: General questions of researches of microphauna of Siberia, Far East and other areas. *Moscow: Nauka*: 60–76. [In Russian.]

Buschmina L.S. 1975. Early Carboniferous ostracodes of Kolymian Massifs. *Trudy Istituta Geologii I Geofizikki, Akademiya Nauk SSSR, Sibirskoi Otdeleniye* 219: 5–103. [In Russian.]

Buschmina L.S. 1986. Lower Carboniferous Paraparchitidae in the south of western Siberia. *Trudy Istituta Geologii I Geofizikki, Akademiya Nauk SSSR, Sibirskoi Otdeleniye* 651: 111–135. [In Russian.]

Buschmina L.S., Bogush O.J. & Kononova L.J. 1984. Microfauna and Biostratigraphy of the Lower Carboniferous of SE Siberia. *Trudy Istituta Geologii I Geofizikki, Akademiya Nauk SSSR, Sibirskoi Otdeleniye* 599: 1–127. [In Russian.]

Caplan M.L. & Bustin R.M. 1999. Devonian–Carboniferous Hangenberg mass extinction event, widespread organic-rich mudrock, anoxia, and causes and consequences. *Palaeogeography, Palaeoclimatology, Palaeoecology* 148: 187–207. https://doi.org/10.1016/S0031-0182(98)00218-1

Caputo M.V. 1985. Late Devonian glaciation in South America. *Palaeogeography, Palaeoclimatology, Palaeoecology* 205: 337–357.

Carmichael S.K., Waters J.A., Königsof P., Suttner T.J. & Kido E. 2019. Paleogeography and paleoenvironments of the Late Devonian Kellwasser event: a review of its sedimentological and geochemicalexpression. *Global and Planetary Change* 183: 102984. https://doi.org/10.1016/j.gloplacha.2019.102984

Casier J.-G. 1989. Paléoécologie des ostracodes au niveau de la limite des étages Frasnien et Famennien, à Senzeilles. *Bulletin de l'Institut royal des Sciences naturelles de Belgique, Sciences de la Terre* 59: 79–93.

Casier J.-G. 2008. Guide de l'excursion: Les Ostracodes du Dévonien moyen et supérieur du Synclinorium de Dinant. *In*: Casier J.-G. (ed.) *Résumé des communications et guide de l'excursion de la 22ième Réunion des ostracodologistes de langue française*: 25–79.

Casier J.-G. 2017. Ecology of Devonian ostracods: application to the Frasnian / Famennian boundary bioevent in the type region (Dinant Synclinorium, Belgium). *Palaeobiodiversity and Palaeoenvironments*, 97: 553–564. https://doi.org/10.1007/s12549-017-0278-z

Casier J.-G. & Préat A. 2003. Ostracods and lithofacies of the Devonian–Carboniferous boundary beds in the Avesnois, North of France. *Bulletin de l'Institut royal des Sciences naturelles de Belgique, Sciences de la Terre* 73: 83–107.

Casier J.-G., Lethiers F. & Préat A. 2001. Ostracods and rock facies associated with the Devonian/Carboniferous boundary in the Puech de la Suque section, Montagne Noire, France. *Bulletin de l'Institut royal des Sciences naturelles de Belgique, Sciences de la Terre* 71: 31–52.

Casier J.-G., Lethiers F. & Préat A. 2002. Ostracods and sedimentology of the Devonian–Carboniferous stratotype section (La Serre, Montagne Noire, France). *Bulletin de l'Institut royal des Sciences naturelles de Belgique, Sciences de la Terre* 72: 43–68.

Casier J.-G., Mamet, B., Préat, A. & Sandberg C. A. 2004. Sedimentology, conodonts and ostracods of the Devonian–Carboniferous strata of the Anseremme railway bridge section, Dinant Basin, Belgium. *Bulletin de l'Institut royal des Sciences naturelles de Belgique*, *Sciences de la Terre* 74: 45–68.

Casier J.-G., Lebon A., Mamet B. & Préat A. 2005. Ostracods and lithofacies close to the Devonian–Carboniferous boundary in the Chanxhe and Rivage sections, northeastern part of the Dinant Basin, Belgium. *Bulletin de l'Institut royal des Sciences naturelles de Belgique*, *Sciences de la Terre* 75: 95–126.

Coen M. 1989. Ostracodes of the Devonian Carboniferous transition beds of South China. *Bulletin de la Société belge de Géologie* 98: 311–317.

Cooper C.L. 1941. Chester Ostracodes of Illinois. *State Geological Survey, Report Investigation* 11 (77): 5–99. https://doi.org/10.5962/bhl.title.61675

Coryell H.N. & Johnson S.C. 1939. Ostracoda of the Clore Limestone, Upper Mississipian of Illinois. *Journal of Paleontology* 13 (2): 214–224. https://www.jstor.org/stable/1298771

Coryell H.N. & Rogatz H. 1932. A study of the ostracode fauna of the Arroyo Formation, Clearfork Group of the Permian in Tom Green County, Texas. *American Midland Naturalist* 13 (6): 378–395. https://doi.org/10.2307/2419859

Crasquin S. 1984. Ostracodes du Dinantien, Systématique-Biostratigraphie-Paléoécologie (France, Belgique, Canada). *Thèse de 3ème cycle de Université de Lille* 1: 1–238; 2: 1–68.

Crasquin S. 1986. Les Ostracodes dinantiens du Synclinal de Laval et du Synclinorium de Namur (Systématique–Biostratigraphie–Paléoécologie). *Thèse de l'Université de Lille* 1:1–169; 2: 1–71.

Crasquin S. & Horne D.J. 2018. The palaeopsychrosphere in the Devonian. *Lethaia* 51 (4): 547–563. https://doi.org/10.1111/let.12277.

Crasquin S., Lethiers F. & Mansy J.L. 1986. Modification du cortège ostracodique à la limite Dévono–Carbonifère dans l'Ouest canadien : une conséquence de l'orogenèse Antler ? *Bulletin de la Société géologique de France* (8) 2, 5: 55–60. https://doi.org/10.2113/gssgfbull.II.5.735

Crasquin-Soleau S. 1988. Ostracodes tournaisiens du Massif de la Tombe (Synclinorium de Namur – Belgique). *Annales de la Société géologique de Belgique* 110: 309–318.

Crasquin-Soleau S., Vaslet D. & Le Nindre Y.M. 2005. Ostracods as markers of the Permian/Triassic boundary in the Khuff Formation of Saudi Arabia. *Palaeontology* 48 (4): 853–868. https://doi.org/10.1111/j.1475-4983.2005.00476.x

Croneis C. & Gutke L. 1939. New Ostracodes from the Renault formation. *Denison University Bulletin, Journal of the Scientific Laboratories* 34: 33–63.

Cronin T.M. 1987. Evolution, biogeography, and Systematics of *Puriana*: evolution and speciation in Ostracoda, III. *Memoir of The Paleontological Society* 21: 1–71. https://doi.org/10.1017/S0022336000060856

Dewey C.P. 1983. The taxonomy and palaeoecology of Lower Carboniferous ostracodes and peracarids (Crustacea) from southwestern Newfoundland and central Nova Scotia. *Thesis Memorial University, St. John's, Newfoundland*.

Dong R.S. 1982. Geotectonic evolution and Devonian palaeotectonic framework in South China. *Journal of Chengdu College of Geology* 19: 58–64. [In Chinese with English abstract.]

Egorov V.G. 1950. *Frasnian Ostracods from Russian Platform. I. Kloedenellitidae*. VNIGRI (All Russia Petroleum Research Exploration Institut) [In Russian.]

Ellis B.F. & Messina A.R. 1964. *Catalogue of Ostracoda*, *Supplement 1*. American Museum of Natural History, New York.

Feng Q., Gong Y.-M. & Riding R. 2010. Mid–Late Devonian calcified marine algae and cyanobacteria, South China. *Journal of Paleontology* 84: 569–587. https://doi.org/10.1666/09-108.1

Feng Z.Z., Yang Y.Q., Bao Z.D., Jin Z.K., Zhang H.Q., Wu X.H. & Qi D.L. 1998. Lithofacies Paleogeography of the Carboniferous in South China. *Geological Publishing House: Beijing* [in Chinese.]

Forel M.-B., Kolar-Jurkovšek T. & Jurkovšek B. 2020. Ostracods from the "Raibl Beds" (Carnian, Late Triassic) of Belca section in Karavanke Mountains, northwestern Slovenia. *Geodiversitas* 42 (21): 377–407. https://doi.org/10.5252/geodiversitas2020v42a21

Forel M.-B., Kershaw S., Lord A. & Crasquin S. 2021. Applications of fossil taxonomy in palaeoenvironmental reconstruction: a case study of ostracod identification and diversity in Permian–Triassic boundary microbialites. *Facies* 67 (23) https://doi.org/10.1007/s10347-021-00632-1

Fürsich F.T. & Wendt J. 1977. Biostratinomy and Palaeoecology of the Cassian Formation (Triassic) of the Southern Alps. *Palaeogeography, Palaeoclimatology, Palaeoecology* 22: 257–323. https://doi.org/10.1016/0031-0182(77)90005-0

Gao L.D. 1981. Late Devonian and early Carboniferous miospore zones from southeastern Guizhou and the boundary of the Devonian. *Geology of Guizhou, Guiyang* 8: 59–69. [In Chinese with English abstract.]

Geis H.L. 1932. Some ostracodes from the Salem Limestone, Mississippian of Indiana. *Journal of Paleontology* 6: 149–188. https://www.jstor.org/stable/1298173

Girty G.H. 1910. The Fauna of the Phosphate Beds of the Park City Formation in Idaho, Wyoming, and Utah. *United States Geological Survey Bulletin* 436: 1–82. https://doi.org/10.3133/b436

Gooday A.J. 1983. Entomozoacean ostracod from the Lower Carboniferous of south–western England. *Palaeontology* 26 (4): 755–788.

Green R. 1963. Lower Mississippian Ostracodes from the Banff Formation, Alberta. *Research Council of Alberta, Bulletin* 11: 1–237.

Gründel J. 1962. Zur Taxonomie der Ostracoden der Gattendorfia-Stufe Thüringens. *Freiberger Forschungshefte* 151: 51–105.

Gurevich K.Y. 1972. Ostrakody Devona i Rannego Karbona Volyno–Podolskoi Okrainy Russkoy Platformy i ikh stratigraficheskoe znachenie. *Trudy Ukrainskiy Nauchno-Issledovateskiy Geologorazvedochnyy Institut* 27: 284–351.

Hallam A. & Wignall P.B. 1999. Mass extinctions and sea-level changes. *Earth-Science Reviews* 48: 217–250. https://doi.org/10.1016/S0012-8252(99)00055-0

Hammer Ø., Harper D.A.T. & Ryan P.D. 2001. PAST: paleontological statistics software package for education and data analysis. *Palaeontologia Electronica* 4: 1–9.

Hance L., Muchez P., Coen M., Fang X.-S., Groessens E., Hou H., Poty E., Steemans P.H., Streel M. Tan Z., Tourneur F., Van Steenwinkel M. & Xu S.-C. 1993. Biostratigraphy and sequence stratigraphy at the Devonian–Carboniferous transition in southern China (Hunan Province). Comparison with southern Belgium. *Annales de la Société géologique de Belgique* 116: 359–378.

Harlton B.H. 1929. Some Upper Mississippian (Fayetteville) and Lower Pennsylvanian (Wapanucka-Morrow) Ostracoda of Oklahoma and Arkansas. *American Journal of Sciences* 18 (105): 254–270. https://doi.org/10.2475/ajs.s5-18.105.254

Haussmann I.M. & Nützel A. 2015. Diversity and palaeoecology of a highly diverse Late Triassic marine biota from the Cassian Formation of north Italy. *Lethaia* 48: 235–255. https://doi.org/10.1111/let.12102

Henningsmoen G. 1953. Classification of Paleozoic straight hinged Ostracoda. *Norsk Geologisk Tidsskrift* 31: 185–288.

Horne D.J., Cohen A. & Martens K. 2002. Taxonomy, morphology and biology of Quaternary and living Ostracoda. *American Geophysical Union, Washington (Geophysical Monograph Series)* 131: 5–36. https://doi.org/10.1029/131gm02

Hou H.F., Zhou H.L. & Liu J.B. 2011. Microbial sediments occurring after the end-Devonian extinction event on the Hunan platform. *Acta Geologica Sinica* 85(1) : 145–156.

Ji W. 1987. Early Carboniferous conodonts from Jianghua County of Hunan Province, and their stratigraphic value – with a discussion on the mid-Aikuanian Event. *Bulletin of the Institute of Geology, Chinese Academy of Geological Sciences* 16: 115–141. [In Chinese with English summary.]

Jiang J.J. 1994. The Devonian-Carboniferous boundary based on Lower Carboniferous conodonts in Guizhou. *Regional Geology of China* 1: 21–27. [In Chinese with English summary.]

Jones P.J. 1968. Upper Devonian Ostracoda and Eridostraca from the Bonaparte Gulf Basin, northwestern Australia. *Bureau of Mineral Resources, Geology and Geophysics, Bulletin* 99: 1–93.

Jones P.J. 2011. Latest Devonian (Strunian) Ostracoda from the Buttons Formation, Bonaparte Basin, northwestern Australia: biostratigraphy, palaeoecology and palaeozoogeography. *Memoirs of the Association of Australasian Palaeontologists* 39: 261–322.

Jones T.R. 1901. On some Carboniferous shale from Siberia. *Geological Magazine* 8: 433–436. https://doi.org/10.1017/S0016756800179749

Jones T.R. & Kirkby J.W. 1886. On some fringed and other Ostracoda from the Carboniferous Series. *Geological Magazine, Decade* 3 (3): 433–439. https://doi.org/10.1017/S0016756800467294

Jones T.R. & Holl H.B. 1869. Notes on the Palaeozoic bivalve Entomostraca–9: some Silurian species. *Annals and Magazine of Natural History Series* 4 (3): 211–229. https://doi.org/10.1080/00222936908695920

Kaiser S.I., Steuber T. & Becker R. T. 2008. Environmental change during the Late Famennian and Early Tournaisian (Late Devonian – Early Carboniferous) – implications from stable isotopes and conodont biofacies in southern Europe. *In*: Aretz M., Herbig H.-G. & Somerville I.D. (eds) Carboniferous Platforms and Basins. *Geological Journal* 43: 241–260. https://doi.org/10.1002/gj.1111

Kaiser S.I., Aretz M. & Becker R.T. 2016. The global Hangenberg Crisis (Devonian-Carboniferous transition): review of a first-order mass extinction. *Geological Society*, *London, Special Publications* 423: 387–437. https://doi.org/10.1144/SP423.9

Kaiser S.I., Steuber T., Becker B. & Joachimski M.M. 2006. Geochemical evidence for major environmental change at the Devonian–Carboniferous boundary in the Carnic Alps and the Rhenish Massif. *Palaeogeography, Palaeoclimatology, Palaeoecology* 240: 146–160. https://doi.org/10.1016/j.palaeo.2006.03.048

Kaiser S.I., Becker R.T., Steuber T. & Aboussalam Z.S. 2011. Climate-controlled mass extinctions, facies, and sea-level changes around the Devonian–Carboniferous boundary in the eastern Anti-Atlas (SE Morocco). *Palaeogeography, Palaeoclimatology, Palaeoecology* 310: 340–364. https://doi.org/10.1016/j.palaeo.2011.07.026

Kalvoda J., Kumpan T. & Babek O. 2015. Upper Famennian and Lower Tournaisian sections of the Moravian Karst (Moravio–Silesian Zone, Czech Republic): a proposed key area for correlation of the conodont and foraminiferal zonations. *Geological Journal* 50: 17–38. https://doi.org/10.1002/gj.2523

Kollmann K. 1963. Ostracoden aus der Trias. II.–Weitere Bairdiidae. *Jahrbuch der Geologischen Bundesanstalt Wien* 106: 121–203.

Kotschetkova N.H. 1980. *New late Tournaisian Ostracods of Southern Urals. Stratigraphy and Paleontology of the Paleozoic of the Southem Urals, 6046*. Academy of Sciences of the USSR, Bashkirian Branch, Institute of Geology, Moscow. [In Russian.]

Kotschetkova N. & Janbulatova M. 1987. Ostracodes. *In*: Maslov B. (ed.) *Fauna and Biostratigraphy of Boundary Deposits of the Devonian and Carboniferous of Bertchogyra (Mugodzary)*: 76–91. Academy of Sciences of the USSR, Bashkirian Branch, Institute of Geology, Moscow. [In Russian.]

Kummerow E. 1939. Die Ostrakoden und Phyllopoden des deutschen Unterkarbon. *Abhandlungen der Preussischen Geologischen Landesanstalt, NF* 194: 1–107.

Kumpan T., Babek O., Kalvoda J., Fryda J. & Grygar T.M. 2013. A high-resolution, multiproxy stratigraphic analysis of the Devonian–Carboniferous boundary sections in the Moravian Karst (Czech Republic) and a correlation with the Carnic Alps (Austria). *Geological Magazine* 151: 201–215. https://doi.org/10.1017/S0016756812001057

Kumpan T., Babek O., Kalvoda J., Matys Grygar T., Fryda J., Becker R.T. & Hartenfels S. 2015. Petrophysical and geochemical signature of the Hangenberg Events: an integrated stratigraphy of the Devonian–Carboniferous boundary interval in the Northern Rhenish Massif (Avalonia, Germany). *Bulletin of Geosciences* 90: 667–694. https://doi.org/10.3140/bull.geosci.1547

Lakin J.A., Marshall J.E.A., Troth I. & Harding I.C. 2016. Greenhouse to icehouse: a biostratigraphic review of latest Devonian–Mississippian glaciations and their global effects. *In*: Becker R.T., Königshof P. & Brett C.E. (eds) *Devonian Climate, Sea Level and Evolutionary Events*. Geological Society, London, Special Publications 423. https://doi.org/10.1144/SP423.12

Latreille P.A. 1806. *Genera crustaceorum et insectorum: secundum ordinem naturalem in familias disposita, iconibus exemplisque plurimis explicata*. *Tomus 1*. Koenig, Paris. https://doi.org/10.5962/bhl.title.5093

Le Hir G., Donnadieu Y., Goddéris Y., Meyer-Berthaud B., Ramstein G. & Blakey R.C. 2011. The climate change caused by the land plants invasion in the Devonian. *Earth and Planetary Science Letters* 310: 203–212. https://doi.org/10.1016/j.epsl.2011.08.042

Lethiers F. 1981. Ostracodes du Dévonien terminal de l'Ouest du Canada: systématique, biostratigraphie et paléoécologie. *Geobios Mémoire spécial* 5: 1–236.

Lethiers F. 1982. Les ostracodes du Dévonien supérieur (Nord de la France, Belgique, Ouest du Canada). *Thesis of the University of Lille*.

Lethiers F. & Casier J.-G. 1999a. Autopsie d'une extinction biologique. Un exemple : la crise de la limite Frasnien–Famennien (364 Ma). *Comptes Rendus de l'Académie des sciences, Serie IIA* 329: 303–315. https://doi.org/10.1016/S1251-8050(00)88580-8

Lethiers F. & Casier J.-G. 1999b. Les Ostracodes du Famennien inférieur au stratotype de Coumiac (Montagne Noire, France) : la reconquête post-événementielle. *Bulletin de l'Institut royal des Sciences naturelles de Belgique, Sciences de la Terre* 69: 47–66.

Lethiers F. & Crasquin-Soleau S. 1988. Comment extraire des microfossiles à tests calcitiques de roches calcaires dures. *Revue de Micropaléontologie* 31 (1): 56–61.

Lethiers F. & Feist R. 1991. Ostracodes, stratigraphie et bathymétrie du passage Dévonien–Carbonifère au Viséen Inférieur en Montagne Noire (France). *Geobios* 24: 71–104. https://doi.org/10.1016/0016-6995(91)80038-2

Lethiers F. Braun W.K., Crasquin S. & Mansy J.L. 1986. The Strunian event in western Canada with reference to ostracode assemblages. *Annales de la Société géologique de Belgique* 109: 149–157.

Liao W.H. 2003. Devonian biostratigraphy of Dushan, Southern Guizhou and its coral extinction events. *Acta Palaeontologica Sinica*, *Nanjing* 42 (3): 417–427. [In Chinese with English abstract.]

Ma X.P. & Bai S.L. 2002. Biological, depositional, microspherule, and geochemical records of the Frasnian/Famennian boundary beds, South China. *Palaeogeography, Palaeoclimatology, Palaeoecology* 181: 325–346. https://doi.org/10.1016/S0031-0182(01)00484-9

Ma X.P., Gong Y.M., Chen D.Z., Racki G., Chen X.Q. & Lia W.H. 2016. The Late Denovian Frasnian-Famennian Event in South China - patterns and causes of extinctions, sea level changes, and isotope variations. Palaeogeography, Palaeoclimatology, Palaeoecology, 448: 224–244. https://doi.org/10.1016/j.palaeo.2015.10.047

Martinsson A. 1955. Studies on the ostracode family Primitiopsidae. *Bulletin of the Geological Institution of Uppsala* 36 (1): 1–31.

Marynowski L., Záton M., Rakocinski M., Filipiak P., Kurkiewicz S. & Pearce T.J. 2012. Deciphering the upper Famennian Hangenberg Black Shale depositional environments based on multi-proxy record. *Palaeogeography, Palaeoclimatology, Palaeoecology* 346–347: 66–86. https://doi.org/10.1016/j.palaeo.2012.05.020

McCoy F. 1844. *A Synopsis of the Characters of the Carboniferous Limestone Fossils of Ireland*. Dublin University Press, Dublin. https://doi.org/10.5962/bhl.title.11559

Moore R.C. 1961. *Treatise on Invertebrate Paleontology. Arthropoda 3, Crustacea, Ostracoda*. Geological Society of America and University of Kansas Press.

Morey P.S. 1935. Ostracoda from the basal Mississippian sandstone in Central Missouri. *Journal of Paleontology* 9: 316–326.

Müller G.W. 1894. Die Ostracoden des Golfes von Neapel und der angrenzenden Meeres Abschnitte. *Fauna und Flora Neapel* 21: 1–404. https://doi.org/10.5962/bhl.title.7419

Nazik A., Königshof P., Ariuntogos M., Waters J.A. & Carmichael S.K. 2021. Late Devonian ostracods (Crustacea) from the Hushoot Shiveetiin gol section (Baruunhuurai Terrane, Mongolia) and their palaeoenvironmental implication and palaeobiogeographic relationship. *Palaeobiodiversity and Palaeoenvironments*: 101: 689–706. https://doi.org/10.1007/s12549-020-00446-z

Nützel A. & Kaim A. 2014. Diversity, palaeoecology and systematics of a marine fossil assemblage from the Late Triassic Cassian Formation at Settsass Scharte, N Italy. *Paläontologische Zeitschrift* 88 (4): 405–431. https://doi.org/10.1007/s12542-013-0205-1

Oertli H.J. 1971. The aspect of ostracode fauna – a possible new tool in petroleum sedimentology. *In*: Oertli H.J. (ed.) *Paléoécologie des Ostracodes*: 137–151. Bulletin du Centre de Recherches de Pau SNPA Vol. 5 suppl.

Olempska E. 1981. Lower Carboniferous ostracodes of the Holy Cross Mountains, Poland. *Acta Palaeontologica Polonica* 26: 35–53.

Olempska E. 1997. Changes in benthic ostracod assemblages across the Devonian-Carboniferous boundary in the Holy Cross Mountains, Poland. *Acta Palaeontologica Polonica* 42: 291–332.

Olempska E. 1999. Silicified shallow-water ostracodes from the Early Carboniferous of South China. *Acta Palaeontologica Polonica* 44 (4): 383–436.

Olempska E. & Chauffe K.M. 1999. Ostracodes of the Maple Mill Shale Formation (Upper Devonian) of southeastern Iowa, USA. *Micropaleontology* 45: 304–318. https://doi.org/10.2307/1486139

Paschall O., Carmichael S., Königshof P., Waters J., Ta H.P., Komatsu T. & Dombrowski A. 2019. The Devonian-Carboniferous boundary in Vietnam: sustained ocean anoxia with a volcanic trigger

for the Hangenberg Crisis? *Global Planetary Change* 175: 64–81. https://doi.org/10.1016/j.gloplacha.2019.01.021

Pedder A.E.H. 1982. The rugose coral record across the Frasnian/Famennian boundary. *Geological Society of America, Special Paper* 190: 485–489. https://doi.org/10.1130/SPE190-p485

Perrier V., Vannier J. & Siveter D.J. 2011. Silurian bolbozoids and cypridinids (Myodocopa) from Europe: pioneer pelagic ostracods. *Palaeontology* 54: 1361–1391. https://doi.org/10.1111/j.1475-4983.2011.01096.x

Pisarzowska A., Rakociński M., Marynowski L., Szczerba M., Thoby M., Paszkowski M., Perri M.C., Spalletta C., Schönlaub H.-P., Kowalik N. & Gereke M. 2020. Large environmental disturbances caused by magmatic activity during the Late Devonian Hangenberg Crisis. *Global Planetary Change* 188: 1–24. https://doi.org/10.1016/j.gloplacha.2020.103155

Pollard J.E. 1966. A non-marine ostracod fauna from the coal measures of Durham and Northumberland. *Palaeontology* 9: 667–697.

Posner V.M. 1951. Ostracoda of the Lower Carboniferous of the western flank of the Moscow Basin. *All Union Petroleum Science–Research Geology Exploration Institute (VNIGRI) Transactions, Natural Sciences* 56: 1–108.

Puri H. 1966. Ostracods as ecological and palaeoecological indicators. *Publicazion della Stazione Zoologica di Napoli* 33 Supplement.

Qie W.K., Wang X.D., Zhang X.H., Ji W.T., Grossman E.L., Huang X., Liu J.S. & Luo G.M. 2016. Latest Devonian to earliest Carboniferous conodont and carbon isotope stratigraphy of a shallow-water sequence in South China. *Geological Journal* 51: 915–935. https://doi.org/10.1002/gj.2710

Qie W.K., Liu J.S., Chen J.T., Wang X.D., Mii H.S., Zhang X.H., Huang X., Yao L., Algeo T.J. & Luo G.M. 2015. Local overprints on the global carbonate δ13C signal in Devonian-Carboniferous boundary successions of South China. *Palaeogeography, Palaeoclimatology, Palaeoecology* 418: 290–303. https://doi.org/10.1016/j.palaeo.2014.11.022

Qie W., Sun Y., Guo W., Ting N, Chen B., Song J., Liang K., Yin B., Han S., Chang J. & Wang X.D. 2021. The Devonian–Carboniferous boundary in China. *In*: Aretz M. & Corradini C. (eds) Global review of the Devonian–Carboniferous boundary. *Palaeobiodiversity and Palaeoenvironments* 101 (2): 589–611. https://doi.org/10.1007/s12549-021-00494-z

Qin G., Zhao R. & Ji Q. 1988. Late Devonian and Early Carboniferous conodonts from northern Guangdong and their stratigraphic significance. *Acta Micropalaeontologica Sinica* 5: 57–71.

Raup D.M. 1978. Cohort analysis of generic survivorship. *Paleobiology* 4: 1–15. https://doi.org/10.1017/S0094837300005649

Roundy P.V. 1926. The micro-fauna in Mississippian formations of San Saba County, Texas. *US Geological Survey Professional Paper* 146: 1–63. https://doi.org/10.3133/pp146

Salas M. J., Vannier J. & Williams M. 2007. Early Ordovician ostracods from Argentina: their bearing on the origin of binodicope and palaeocope clades. *Journal of Paleontology* 81: 13–95. https://doi.org/10.1666/05-134.1

Sandberg C.A., Morrow J.R. & Ziegler W. 2002. Late Devonian sea-level changes, catastrophic events, and mass extinctions. *Geological Society of America, Special Paper* 356: 473–487. https://doi.org/10.1130/0-8137-2356-6.473

Sars G.O. 1866. Oversigt af marine Ostracoder. *Norske Videnskaps-Akademi, Förhandlingar* 1865: 1–130.

Sars G.O. 1888. Nye Bidrag til Kundskaben om Middelhavets Invertebratfauna. 4. Ostracoda Mediterranea (Sydeuropaeiske Ostracoder). *Archiv for Mathematik og Naturvidenskab* 12: 173–324. https://doi.org/10.5962/bhl.title.10252

Scott H.W. 1959. The type species of *Paraparchites* Ulrich & Bassler. *Journal of Paleontology* 33: 670–674.

Scott H.W. 1961. Suborder Beyrichicopina Scott n. suborder. Suborder Kloedenellocopina Scott n. suborder. *In*: Moore R.C. (ed.) *Treatise of Invertebrate Paleontology. Part Q. Arthropoda 3*: Q.111–Q.180. Geological Society of America, and University of Kansas Press, Boulder and Kansas.

Schraut G. 1996. Die Arthropoden aus dem Unterkarbon von Nötsch (Kärnten/Österreich). *Abhandlungen der Geologischen Bundesanstalt* 51: 1–193.

Shannon C.E. & Weaver W. 1949. The Mathematical Theory of Communication. *University of Illinois Press, Urbana*, 144 p.

Shaver R.H. 1961. Family Bairdiocyprididae Shaver, n. fam. *In*: Moore R.C. (ed.) *Treatise on Invertebrate Paleontology. Part Q. Arthropoda 3*: Q.364. Geological Society of America, and University of Kansas Press, Boulder and Kansas.

Shi C.G. 1964 The Middle and Upper Devonian Ostracoda from Dushan and Douyun, S., Kueichow. *Acta Palaeontologica Sinica* 12 (1): 34–59. [In Chinese with English abstract.]

Simpson E.H. 1949. Measurement of diversity. *Nature* 163: 188. https://doi.org/10.1038/163188a0

Siveter D.J. 2008. Ostracods in the Palaeozoic? *Senckenbergiana Lethaea* 88: 1–9. https://doi.org/10.1007/BF03043973

Siveter D.J., Vannier J.M.C. & Palmer D. 1991. Silurian myodocopes: pioneer pelagic ostracodes and the chronology of an ecological shift. *Journal of Micropalaeontology* 10: 151–173. https://doi.org/10.1144/jm.10.2.151

Sobolev D.B. 2019. A new ostracodes [sic] from the Devonian–Carboniferous boundary deposits of Pechora–Kozhva Uplift. *Russian Academy of Sciences, Ural Branch, Federal Research Center* "*Komi Science Center*", *Institute of Geology, Academician N.P. Yushkin, Syktyvkar palaeontological miscellany* 9: 45–55. [In Russian.] https://doi.org/10.19110/0568-6156-2019-1-8

Sobolev D.B. 2020. Ostracodes from the Devonian-Carboniferous boundary deposits on the reference section Yjid-Kamenka river (Pechora Uplift). *Vestnik of Geosciences*, 12 (312): 4–25. https://doi.org/10.19110/geov.2020.12.1

Sohn I.G. 1960. Paleozoic species of *Bairdia* and related genera. *United States Geological Survey Professional Paper* 330-A: 1–105. https://doi.org/10.3133/pp330a

Sohn I.G. 1961. *Aechminella*, *Amphissites*, *Kirkbyella* and related genera. *United States Geological Survey Professional Paper* 330–B: 107–160. https://doi.org/10.3133/pp330b

Sohn I.G. 1969. Revision of some Girty's invertebrate fossils from the Fayetteville Shale (Mississippian) of Arkansas and Oklahoma. *Geological Survey Professional Paper F* 606: 40–55.

Sohn I.G. 1971. New Late Mississippian Ostracode genera and species from Northern Alaska. A review of the Paraparchitacea. *United States Geological Survey Professional Paper* 711A: 1–24. https://doi.org/10.3133/pp711a.

Sohn I.G. 1975. Mississippian Ostracoda of the Amsden Formation (Mississippian and Pennsylvanian) of Wyoming. *United States Geological Survey Professional Paper G* 848: 1–22. https://doi.org/10.3133/pp848G

Sohn I.G. 1988. Revision of the Late Mississippian New Ostracode Genera in Coryell and Johnson 1939. *Micropaleontology* 34 (1): 52–62. https://doi.org/10.2307/1485610

Song J.J. & Gong Y.M. 2015. Ostracods from the Emuha Section of Devonian–Carboniferous transition in western Junggar. *Earth Science-Journal of China University of Geoscience* 40: 797–809. [In Chinese with English abstract.]

Song J.J. & Gong Y.M. 2019. Ostracods from the Devonian–Carboniferous transition in Dushan of Guizhou, South China. *Palaeobiodivsersity and Palaeoenvironments* 99: 117–127. https://doi.org/10.1007/s12549-018-0322-7

Song J.J., Crasquin S. & Gong Y.M. 2018. Late Devonian benthic ostracods from western Junggar, NW China: Implications for palaeoenvironmental reconstruction. *Geological Journal* 54 (1): 91–100. https://doi.org/10.1002/gj.3156

Stewart G.A. & Hendrix W.E. 1945. Ostracoda of the Olentagy Shale, Franklin and Delaware counties, Ohio. *Journal of Paleontology* 19: 96–115.

Streel M., Caputo M.V., Loboziak S. & Melo J.H.G. 2000. Late Frasnian–Famennian climates based on palynomorph analyses and the question of the Late Devonian glaciations. *Earth Science Reviews* 52: 121–173. https://doi.org/10.1016/S0012-8252(00)00026-X

Swartz F.M. 1936. Revision of the Primitiidae and Beyrichidae with new Ostracoda from the Lower Devonian of Pennsylvania. *Journal of Paleontology* 10: 541–586.

Tschigova V.A. 1960. New Ostracoda from Dankov–Lebedyan, Khovan and Likhvin deposits of the Russian platform. *Trudy Vsesoyuznyy Neftegazovyy Nauchno–Issledovatelskiy Institut* 23: 205–233. [In Russian.]

Tschigova V.A. 1977. *Stratigrafiya i correlyatsiya neftegazonosnykh otlozhenii Devona i Karbona Evropeiskoi chasti SSR zarubezhnykh stran*. Nedra, Moscow.

Ulrich E.O. & Bassler R.S. 1906. New American Palaeozoic Ostracoda. Notes and descriptions of the Upper Carboniferous genera and species. *United States National Museum Paper* 30: 149–164. https://doi.org/10.5479/si.00963801.30-1446.149

Ulrich E.O. & Bassler R.S. 1908. New American Paleozoic Ostracoda. Preliminary revision of the Beyrichiidae, with description of new genera. *United State Natural Museum Paper* 35: 277–340. https://doi.org/10.5479/si.00963801.35-1646.277

Ulrich E.O. & Bassler R.S. 1923. Paleozoic Ostracoda: their morphology, classification and occurrence. *In*: Maryland Geological Survey (ed.) *Silurian*: 271–391. Johns Hopkins Press, Baltimore.

Walliser O.H. 1996. Global events in the Devonian and Carboniferous. *In*: Walliser O.H. (ed.) *Global Events and Event Stratigraphy in the Phanerozoic*: 225–250. Springer, Berlin. https://doi.org/10.1007/978-3-642-79634-0_11

Wang K.L. 1987. On the Devonian–Carboniferous boundary based on foraminiferal fauna from South China. *Acta Palaeontologica Sinica* 4: 161–173. [In Chinese with English abstract.]

Wang S.Q. 1978. Late Permian and Early Triassic ostracods of Western Guizhou and Northeastern Yunnan. *Acta Palaeontologica Sinica* 17 (3): 277–312 [In Chinese.]

Wang S.Q. 1983a. Ostracods from the Devonian Sipai Formation of Guangxi. *Memoir of the Nanjing Institute of Geology and Palaeontology* 18: 111–154. [In Chinese with English abstract.]

Wang S.Q. 1983b. Ostracods from the early Devonian Ertang Formation of Guangxi. *Memoirs of Nanjing Institute of Geology & Palaeontology, Academia Sinica* 18: 169–192.

Wang S.Q. 1988a. Late Paleozoic ostracode associations from South China and their paleoecological significance. *Acta Palaeontologica Sinica* 27: 91–102. [In Chinese with English abstract.]

Wang S.Q. 1988b. Ostracodes. *In*: Yu. C. (ed.) *Devonian-Carboniferous Boundary in Nanbiancun, Guilin, China-Aspects and Records*: 209–361. Science Press, Beijing.

Wang Y. & Wang X.L. 1996. Trace fossils near Devonian–Carboniferous boundary section in Dushan, Guizhou. *Journal of Stratigraphy* 20: 285–290. [In Chinese with English abstract.]

Wei M. 1988. Systematic palaeontology–Ostracoda. *In*: Hou H.F. (ed.) *Devonian Stratigraphy, Palaeontology and Sedimentary Facies of Longmenshan, Sichuan*: 277–314. Geological Publishing House, Beijing. [In Chinese with English abstract.]

Wei M., Li Y.W., Jiang Z.W. & Xie L.C. 1983. Subclass Ostracoda. *In*: Chengdu Institute of Geology and Mineral Resources (ed.) *Palaeontological Atlas of Southwest China, Guizhou. Volume of Microfossils*: 23–254. Geological Publishing House, Beijing. [In Chinese.]

Whatley R.C. 1990. Ostracoda and global events. *In*: Whatley R.C. & Maybury C. (eds) *Ostracoda and Global Events*: 3–24. Chapman and Hall, London. https://doi.org/10.1007/978-94-009-1838-2_1

Williams M., Stephenson M.H., Leng M.J., Wilkinson I.P. & Miller C.G. 2005. Early Carboniferous (Late Tournaisian – Early Visean) ostracods from the Ballagan Formation, central Scotland, UK. *Journal of Micropalaeontology* 24: 77–94. https://doi.org/10.1007/BF03043974

Williams M., Siveter D.J., Salas M.J., Vannier J., Popov L.E. & Mansoureh G.P. 2008. The earliest ostracods: the geological evidence. *Senckenbergiana Lethaea* 88: 11–21.

Yang S.P. 1964. Lower Carboniferous Tournaisian brachiopods from southeast of Guizhou. *Acta Palaeontologica Sinica* 12 (1): 82–116. [In Chinese.]

Yang S. P. 1978. Lower Carboniferous brachiopod fauna and its stratigraphic significance in Guizhou. *Memoir of Nanjing Institute of Geology & Palaeontology Academy Sinica* 5: 78–142. [In Chinese.]

Zaspelova V.S. 1959. Ostracoda and their value for the stratigraphy of the Devonian of the north-western regions of the Russian Platform. *Trudy Vsesoyuznyy Neftegazovyy Nauchno–Issledovatelskiy Institut* 136: 5–131. [In Russian.]

Zhang L.J. Gong, Y.M. & Ma H.Z. 2011a. The Devonian trace fossils and ichnofacies from South China. *Journal of Palaeogeography* 13 (4): 397–318. [In Chinese with English abstract.]

Zhang S., Wang X. & Zhu H. 2000. Magnetic susceptibility variations of carbonates controlled by sea–level changes: examples in Devonian to Carboniferous strata in southern Guizhou Province, China. *Science in China, Series D* 43: 266–276. https://doi.org/10.1007/BF02906822

Zhang Y.B., Sun Y.L. & Ma X.P. 2011b. Comprehensive biostratigraphic study of the Devonian–Carboniferous boundary in the shallow marine facies of Dushan, Guizhou. *Memoir of the 26th National Congress of the Palaeontological Society of China*, *Guanling, Guizhou*: 85–86.

Zhao R.X. & Zhang X.Q. 1997. The ostracod fossil criteria for the Devonian–Carboniferous boundary in Lechang, Guangdong. *Guangdong Geology* 12 (3): 67–76. [In Chinese with English abstract.]

Zhuravlev A.V. & Sobolev D.B. 2018. Conodonts and ostracodes from the late Tournaisian bathyal sequence of the Polar Urals. *Contemporary Trends in Geoscience* 7 (1): 48–58. https://doi.org/10.2478/ctg-2018-0003

Zhuravlev A.V. & Sobolev D.B. 2019. Devonian–Carboniferous boundary in the East of the Pechora Plate (Kamenka River and Vangyr River sections). *Vestnik IG Komi SC UB RAS* 10: 16–22. https://doi.org/10.19110/2221-1381-2019-10-16-22

Manuscript received: 24 September 2021
Manuscript accepted: 3 December 2021
Published on: 15 March 2022
Topic editor: Christian de Muizon
Desk editor: Solène Kowalski

Printed versions of all papers are also deposited in the libraries of the institutes that are members of the *EJT* consortium: Muséum national d'histoire naturelle, Paris, France; Meise Botanic Garden, Belgium; Royal Museum for Central Africa, Tervuren, Belgium; Royal Belgian Institute of Natural Sciences, Brussels, Belgium; Natural History Museum of Denmark, Copenhagen, Denmark; Naturalis Biodiversity Center, Leiden, the Netherlands; Museo Nacional de Ciencias Naturales–CSIC, Madrid, Spain; Real Jardín Botánico de Madrid CSIC, Spain; Zoological Research Museum Alexander Koenig, Bonn, Germany; National Museum, Prague, Czech Republic.